Estimate T_m^0. [Data from P. J. Lemstra *et al.*, *J. Polym. Sci. A-2*, **10**, 823 (1972).]

2.11 The relative degree of crystallinity, ϕ_c', of a diblock copolymer containing polyethylene was measured as a function of time following a quench to $T = 95\,^\circ$C (i.e. less than T_m), with the following results:

t/s	24	36	48	60	72	84
ϕ_c'	0.0471	0.165	0.367	0.601	0.806	0.942

Determine the Avrami exponent, n. [Data from A. J. Ryan *et al.*, *macromolecules*, **28**, 3860 (1995).] What mechanism of crystal growth is this consistent with?

2.12 Asymmetric block copolymers can form a body-centred cubic phase (Fig. 2.30) due to microphase separation. Small-angle x-ray scattering was performed on a polystyrene-poly(ethylene-*co*-butylene)–poly(styrene) triblock copolymer in which the polystyrene forms the minority component. The 110 first order reflection was observed at $q^* = 0.024\text{Å}^{-1}$. Determine the spacing of (110) planes, and hence the unit cell length, a.

Transmission electron microscopy was performed on the same sample and the radius of polystyrene spheres was found to be 92Å. Estimate the volume fraction of polystyrene. The molar mass of the triblock $M_w = 90\,\text{kg mol}^{-1}$, and assume the density $\rho = 1.05$ g cm^{-3}.

3
Colloids

3.1 INTRODUCTION

The world around us is full of colloids in porous rocks, clays, mists and smoke. The very stuff we are made of, blood and bones, contains colloidal particles. Many foods also contain colloids; for example milk is an amazing foodstuff, providing all the nutrients required for babies, and is a good example of a colloidal dispersion. Since the dawning of the industrial era, new kinds of colloid-containing materials have been prepared, including synthetic paints, foams, pastes, etc. The technology of preparation and processing of such colloids has been industrially important since Victorian times. It is only in the last 150 years, though, that physical chemists and physicists have begun to probe the physical chemical basis of colloidal stability. Insights into the nature of interparticle interactions have led to profound understanding of the behaviour of colloids. Much has recently been gleaned from the study of model colloidal systems such as dispersions of nearly monodisperse spherical particles. This knowledge is leading to a new era of colloid science, where materials can be designed for specific applications based on an understanding of the underlying interparticle interactions.

It is difficult to arrive at a definition of a colloid that is sufficiently broad to cover all instances where the term is employed. However, for our purposes a colloid can be described as a microscopically heterogeneous system where one component has dimensions in between those of molecules and those of macroscopic particles like sand. A typical component of a colloid has one dimension in the range 1 nm to 1 μm. Because of this small size the surface-to-volume ratio in colloids is large, and many molecules lie close to the interface

between one phase and another. Thus surface chemistry is very important in colloid science. This is manifested, for example, in dispersions of solid colloid particles in a liquid, since these can be stabilized by changing the surface chemistry, either by charging the surface or adsorbing molecules on to it, which modifies the steric interactions between particles. An illustration of the increase in the relative proportion of the number of molecules at the surface of a colloidal particle as the volume decreases is provided by Q.3.1 at the end of the chapter.

Colloid particles in dispersions undergo Brownian motion, as discussed in Section 3.8. When they encounter one another, the balance of attractive and repulsive forces controls whether the dispersion is stable. If the repulsive forces (due, for example, to charge or steric effects) are sufficient to balance the attractive van der Waals interactions, then the colloidal suspension is said to be stable. On the other hand, if there is no potential barrier between interacting colloid particles, due to a balance between repulsive and attractive forces, they can attract each other and aggregate. The process of reversible aggregation is termed *flocculation*. The structure consists of a loose arrangement of aggregates termed flocs. If the aggregation is irreversible, it is termed *coagulation*. A coagulated aggregate separates out by sedimentation if it is denser than the medium or by creaming if it is less dense than the medium. The distinction between reversible and irreversible aggregation is not sharp. The primary means of preventing colloidal aggregation, i.e. of imparting colloidal stability, charge stabilization, steric stabilization and addition of polymers, are detailed in Sections 3.5 to 3.7. The fundamental forces that lead to colloidal stabilization are considered in Section 3.3, whilst Section 3.4 is concerned with the characterization of colloids.

It should be noted that surfactants in solution are usually classed as 'association colloids'. In this book they are considered in a separate chapter (Chapter 4) because a detailed consideration of their phase behaviour, properties and applications is merited by their industrial importance. Biological amphiphiles (lipids) are also considered in Chapter 4.

3.2   TYPES OF COLLOIDS

Many colloids are two-phase dispersions. Systems where a dispersed phase is distributed within a continuous dispersion medium are called *simple colloids* or *colloidal dispersions*. Table 3.1 lists examples of various types of

Table 3.1   Types of colloidal dispersions with examples

Disperse phase	Dispersion medium	Name	Examples
Liquid	Gas	Liquid aerosol	Fog, liquid sprays
Solid	Gas	Solid aerosol	Smoke
Gas	Liquid	Foam	Foams and froths
Liquid	Liquid	Emulsion	Milk, mayonnaise
Solid	Liquid	Sol, colloidal dispersion or suspension, paste (high solid content)	Silver iodide in photographic film, paints, toothpaste
Gas	Solid	Solid foam	Polyurethane foam, expended polystyrene
Liquid	Solid	Solid emulsion	Tarmac, ice cream
Solid	Solid	Solid suspension	Opal, pearl, pigmented plastic

such colloids. Amphiphiles in solution are known as *association colloids*. Amphiphilic solutions are the subject of Chapter 4. Macromolecules in solution can also form particles of 1 nm or larger dispersed in a liquid. These can be classified as *macromolecular colloids*. Polymer solutions, however, are discussed in Chapter 2 and are not considered further here.

In *network colloids* the definition of colloids in terms of dispersed phase and dispersion medium breaks down since the networks consist of interpenetrating continuous channels. Examples include porous solids, where a solid labyrinth contains a continuous gas phase. There are also examples of colloids where three or more phases coexist, two or more of which can be finely divided. These are called *multiple colloids*. An example is an oil-bearing porous rock, since both oil and water will be present within the solid pores.

A particular focus of this chapter is colloidal dispersions of solid particles in a liquid. These are both industrially important but also scientifically interesting since model systems can be prepared with which we can probe the intermolecular interactions responsible for colloidal aggregation. As indicated in Table 3.1, such systems are termed *sols*. Sometimes they are also known as lyophobic solids. This reflects a now-outmoded classification of colloids into those that are 'solvent hating' (lyophobic) and those that are 'solvent loving' (lyophilic). Some examples of sols are described in Section 3.9, whilst the aggregation of model sols is discussed in Section 3.15. Other examples of commonly encountered colloids are described in Sections 3.10 to 3.14.

3.3   FORCES BETWEEN COLLOIDAL PARTICLES

3.3.1   Van der Waals Forces

Van der Waals forces result from attractions between the electric dipoles of molecules, as described in Section 1.2. Attractive van der Waals forces between colloidal particles can be considered to result from dispersion interactions between the molecules on each particle. To calculate the effective interaction, it is assumed that the total potential is given by the sum of potentials between pairs of molecules, i.e. the potential is said to be pairwise additive. In this approximation, interactions between pairs of molecules are assumed to be unaffected by the presence of other molecules; i.e. many-body interactions are neglected. The resulting pairwise summation can be performed analytically by integrating the pair potential for molecules in a microscopic volume dV_1 on particle 1 and in volume dV_2 on particle 2, over the volumes of the particles (Fig. 3.1). The resulting potential depends on the shapes of the colloidal particles and on their separation. In the case of two flat infinite surfaces separated *in vacuo* by a distance h the potential per unit area is

$$V = -\frac{A_H}{12\pi h^2}$$ (3.1)

Here A_H is the *Hamaker constant*, which determines the effective strength of the van der Waals interaction between colloid particles. It is noteworthy that the attractive potential between colloid particles falls off much less steeply than the dispersion interaction between individual molecules (Eq. 1.4). Thus, long-range forces between colloidal particles are important for their stability.
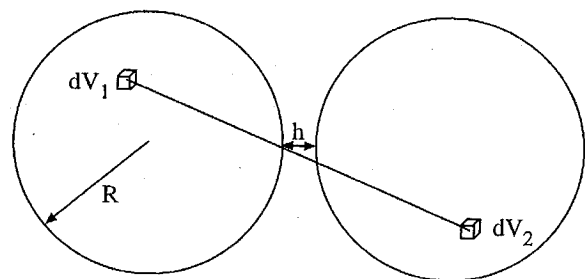

Figure 3.1   Illustrating the method for calculating interparticle forces between colloids. The forces between the volume elements dV of two particles are integrated

For two spherical particles of radius R, where the interparticle separation is small ($h \ll R$), the *Derjaguin approximation* can be used to relate the potential between two curved surfaces to that between two flat surfaces. It is found that Eq. (3.1) is modified to

$$V = -\frac{A_H R}{12h}$$ (3.2)

It is important to note that Eqs. (3.1) and (3.2) apply to colloidal particles in a vacuum. If there is instead a liquid medium between the particles, the van der Waals potential is substantially reduced. The Hamaker constant in these equations is then replaced by an effective value. Consider the interaction between two colloidal particles 1 and 2 in a medium 3. If the particles are far apart, then effectively each interacts with medium 3 independently and the total Hamaker constant is the sum of two particle–medium terms. However, if particle 2 is brought close to particle 1, then particle 2 displaces a particle of type 3. Then particle 1 is interacting with a similar body (particle 2), the only difference being that molecules of particle 2 have been replaced by those of medium 3. Thus the potential energy change associated with bringing particle 2 close to particle 1 in the presence of medium 3 is less than it would be *in vacuo*. The *effective* Hamaker constant is thus a sum of particle–particle plus medium–medium contributions.

The Hamaker approach of pairwise addition of London dispersion forces is approximate because multi-body intermolecular interactions are neglected. In addition, it is implicitly assumed in the London equation that induced dipole–induced dipole interactions are not retarded by the finite time taken for one dipole to reorient in response to instantaneous fluctuations in the other. Because of these approximations an alternative approach was introduced by Lifshitz. This method assumes that the interacting particles and the dispersion medium are all continuous; i.e. it is not a molecular theory. The theory involves quantum mechanical calculations of the dielectric permittivity of the continuous media. These calculations are complex, and are not detailed further here.

3.3.2   Electric Double-Layer Forces

Having in the previous section discussed interactions between uncharged molecules, we now consider the electrical potential around a charged colloidal particle in solution. A particle that is charged at the surface attracts counterions, i.e. an *ionic atmosphere* is formed around it. These tend to
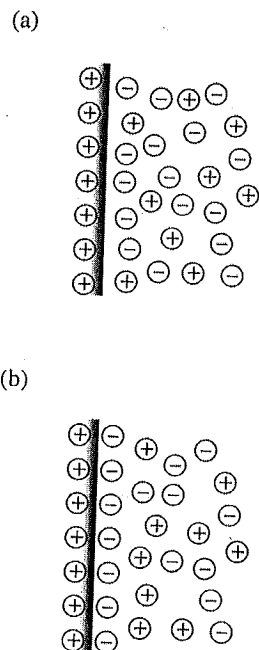
(a)

(b)

Figure 3.2 Models for the electric double layer around a charged colloid particle: (a) diffuse double layer model, (b) Stern model

segregate into a layer adjacent to the layer of surface charges in the colloid particle. Thus an *electric double layer* is created.

In the diffuse double-layer model, the ionic atmosphere is supposed to consist of two regions. Close to the colloid particle, counterions tend to predominate due to strong electrostatic forces. Ions further away from the particle are assumed to be organized more diffusely, according to a balance of electrical forces and those resulting from random thermal motion. In this outer diffuse region (Fig. 3.2a), the concentration of counterions thus decreases gradually away from the surface. In the Stern model, the interface between the inner region and outer diffuse region of the counterion atmosphere is a sharp plane (Stern plane) and the inner region consists of a single layer of counterions termed the Stern layer (Fig. 3.2b).

The diffuse double layer can be described by the Gouy–Chapman equation, which is a solution of the Poisson–Boltzmann equation for a planar diffuse double layer. The Poisson–Boltzmann equation relates the electrical potential to the distribution and concentration of charged species. The distribution of charges in the electrolyte solution is described by Boltzmann distributions.

At a point where the electrical potential is Φ the concentrations of positive and negative ions are given by

$$c_+ = c_0 \exp\left(\frac{-ze\Phi}{k_B T}\right) \tag{3.3}$$

and

$$c_- = c_0 \exp\left(\frac{+ze\Phi}{k_B T}\right) \tag{3.4}$$

where c_0 is the number density (molar concentration = c_0/N_A) of each ionic species of valence z. The excess charge density is then

$$\rho = ze(c_+ - c_-) \tag{3.5}$$

This can be inserted into Poisson's equation to provide an expression for the potential as a function of distance, x, from the charged plane. The Poisson equation is

$$\frac{d^2\Phi}{dx^2} = \frac{\rho}{\varepsilon} \tag{3.6}$$

where ε is the permittivity of the solution ($\varepsilon = \varepsilon_r \varepsilon_0$, where ε_r is the relative permittivity and ε_0 is that of a vacuum). The general solution, using appropriate boundary conditions, is quite complex. In the case that $ze\Phi_0/(k_B T) \ll 1$, i.e. for a system where the surface potential Φ_0 (i.e. that at $x = 0$) is much smaller than $k_B T$ and/or the electrolyte is weakly charged, the potential simplifies to

$$\Phi = \Phi_0 \exp(-\kappa x) \tag{3.7}$$

i.e. it decays exponentially with increasing distance. Here

$$\kappa = \left(\frac{e^2 \sum_i c_i z_i^2}{\varepsilon k_B T}\right)^{1/2} \tag{3.8}$$

The quantity $1/\kappa$ has dimensions of length and is called the Debye screening length.

3.4 CHARACTERIZATION OF COLLOIDS

3.4.1 Rheology

The flow behaviour of colloids is very important to many of their applications. To take an everyday example, margarine should be stiff in the tub but flow under the pressure of the knife as it is spread on bread. The structural and dynamical complexity of colloidal systems leads to a diversity of rheological phenomena. The essential features of many of these effects (shear thinning, shear thickening, viscoelasticity) are common to different soft matter systems. Thus, rheology is discussed in Chapter 1 and is not explicitly considered further here.

3.4.2 Particle Shape and Size

Here we consider colloidal sols, where discrete solid particles are dispersed in a liquid. The sol particles can have three-dimensional (sphere-like), two-dimensional (rod-like) or one-dimensional (plate-like) forms, as exemplified by Fig. 3.3. Examples of these structures include dispersions of highly monodisperse spherical particles that can be obtained by emulsion polymerization of latex particles, dispersions of needle-shaped colloidal particles in cement and asbestos and plate-like particles in aqueous solutions that are the structural basis of clays.

The size of colloidal particles can be measured by a number of methods. Due to the resolution limit, optical microscopy is often unsuitable for the direct observation of colloidal particles, but scanning or transmission electron microscopy are both appropriate. Sedimentation methods can be used for colloid particles that settle under the influence of gravity. The sedimentation rate is proportional to the size of the particles. Particle counting methods such as the Coulter counter (see below) provide the number average distribution of particle volumes, from which a distribution of particle radii can be extracted. Scattering techniques are widely used to determine the size and shape of colloid particles. The angular dependence of the scattered intensity from colloid particles at small angles provides information on particle size and shape (Section 1.9.2). Small-angle light scattering (SALS), small-angle x-ray scattering (SAXS) and small-angle neutron scattering (SANS) have all been exploited in this context.

Electron microscopy methods are outlined in Section 1.9.1. Although colloid particles are usually too small to be directly observed in an optical
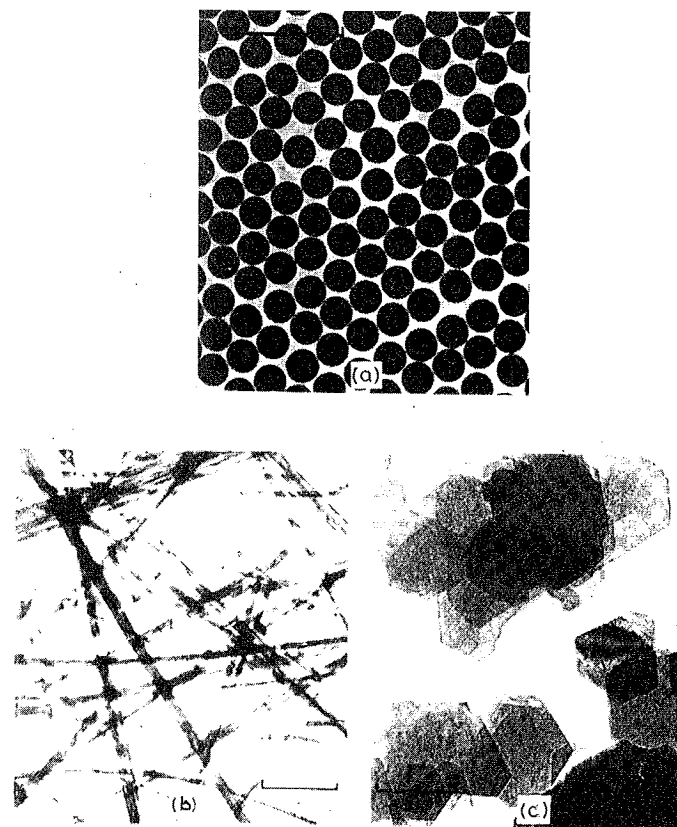
Figure 3.3   Typical shapes of colloid particles: (a) spherical particles of polystyrene latex, (b) fibres of chrysotile asbestos, (c) thin plates of kaolinite. The scale bars indicate 1 μm. [Adapted with permission from D. H. Everett, *Basic Principles of Colloid Science*, Royal Society of Chemistry, 1988]

microscope, it is possible to observe their motions by *ultramicroscopy*. In a suspension of colloidal particles (0.01–1 μm size), Brownian motion is observed due to the uneven forces exerted on them by the molecules of the fluid medium. In ultramicroscopy, a strong beam of horizontal light is directed on to the liquid containing the suspended particles and the vertically mounted microscope is focused on a region just below the surface. The observer sees bright spots of scattered light moving in a dark field, use being made of the fact that the diffraction image around a particle is considerably larger than the particle itself. Confocal microscopy has recently developed as an important technique to directly image (micron size) colloidal particles using a laser

beam focussed in a plane of the sample. It can also be used to probe particle dynamics via maps of their trajectories.

Sedimentation methods rely on observations of the settling of colloid particles under gravity. Sedimentation results from the gravitational force on a particle, which is resisted by the frictional force on the falling body due to the viscosity of the surrounding medium. When these forces are balanced, the particles fall at a constant velocity, termed the sedimentation velocity, v. The frictional force on a spherical particle is given by Stokes' equation (Eq. 1.6 and 1.8). Equating this to the gravitational force we have

$$(\rho_s - \rho_1)\tfrac{4}{3}\pi R^3 g = 6\pi v R \eta \qquad (3.9)$$

Here ρ_s and ρ_1, are the densities of solid particles and liquid respectively, g is the acceleration due to gravity, R is the particle radius (in this context called the Stokes settling radius) and η is the viscosity of the medium. Thus

$$v = \frac{2(\rho_s - \rho_1)g R^2}{9\eta} \qquad (3.10)$$

which can be used to obtain R from measurements of v. In principle, v can be measured from ultramicroscopy measurements, but in practice it is usual to measure the concentration of particles falling a height h. The distribution of particles falling through this distance in time t then gives the particle size distribution. Usually colloidal particles undergo sedimentation very slowly, but a dramatic improvement in rate can be achieved by centrifugation, which if carried out at very high speeds is termed *ultracentrifugation*. In the case where sedimentation is induced by ultracentrifugation (i.e. speeds up to 60 000 rpm), the analysis is similar to that for gravitational sedimentation, but the force acting on the particle now results from centripetal motion rather than gravity. Centrifugation measurements are usually analysed to obtain the molar mass of the particles, but in the case of spherical particles Stokes' law for the frictional resistance can be used to obtain an average radius. It should be noted that Brownian motion of particles still occurs even during centrifugation. If centrifugation is carried out at low speeds (typically 8000 rpm) and/or the Brownian motion is very pronounced, an equilibrium between the two motions can be achieved. This is termed *sedimentation equilibrium*. Measurements of the relative concentrations at different distances from the rotation axis then enable the distribution of particle molar mass to be determined.

Particle sizes can also be measured using a *Coulter counter*, which was originally designed to count the number of particles in a solution flowing through a small orifice. The orifice has an electrode on each side of it, and when a particle passes through the resistance between the electrodes momentarily increases. If this resistance increase exceeds a set threshold level, particles can be counted. By varying the threshold it is possible to detect particles below a certain cut-off size, and in this way a cumulative size distribution is obtained. The method works for particle diameters between about 600 nm and 400 μm; i.e. for colloids it is only applicable at the upper size limit. It is most often used for oil-in-water emulsions, because the droplets are usually quite large. Here the oil droplets produce the electrical pulses due to resistance increases which are the basis of the Coulter counter.

We turn now to small-angle scattering techniques. SANS and SAXS are suitable for particles in the size range 1–100 nm, whereas SALS can be used to obtain particle sizes in the range 10–600 nm. SAXS and SANS are conceptually similar to each other, because in both methods the radiation is scattered by the point scatterers (electrons or atomic nuclei respectively) that make up the colloidal particle. The wavelength of the radiation (typically 0.1 nm) is much smaller than the colloid particle size, so that scattering is observed at small angles. As discussed in Section 1.9.2, SANS can be used to probe the internal structure of colloid particles through contrast variation experiments by deuterium labelling of colloid particles or the use of labelled solvent. SAXS, on the other hand, has the advantage that it can be performed in the laboratory and it is possible to obtain a higher flux of x-rays than of neutrons, which is important when the material is only a weak scatterer.

The hydrodynamic radius of colloidal particles can be obtained from dynamic light scattering (DLS), also known as photon correlation spectroscopy (PCS). Here, the temporal fluctuations of scattered light intensity are measured to provide the autocorrelation function, analysis of which provides the translational diffusion coefficient. Then the Stokes–Einstein equation (Eq. 1.9) is used to determine a hydrodynamic radius. This method is described further in Section 1.9.2.

3.4.3 Electrokinetic Effects

If a colloidal particle is charged, electric fields can have a profound effect on the flow behaviour of the dispersion. This gives rise to a number of electrokinetic phenomena. In *electrophoresis* measurements, the velocity of

a charged colloid particle induced by an electric field in a stationary liquid is measured, from which the mobility

$$u = \frac{v}{E} \qquad (3.11)$$

can be extracted. Here v is the particle velocity and E is the electric field strength. *Sedimentation velocity* measurements involve the reverse effect, i.e. measurement of the electric field strength when charged particles move through a stationary liquid.

Two other electrokinetic effects result from the flow of liquid past a stationary charge. In *electro-osmosis*, the flow of liquid past a stationary charged surface (for example the wall of a capillary tube) is induced by an applied electric field. The pressure necessary to counterbalance this flow is called the electro-osmotic pressure. In the reverse effect, the electric field generated by charged particles flowing relative to a stationary liquid is termed the *sedimentation potential.*

Zeta potential

The zeta potential is the potential at the surface between a stationary solution and a moving charged colloid particle. This surface defines the plane of shear. Its definition is somewhat imprecise because the moving charged particle will have a certain number of counterions attached to it (for example ions in the Stern layer, plus some bound solvent molecules), the combined flowing object being termed the electrokinetic unit. The stability of colloidal suspensions is often interpreted in terms of the zeta potential, because, as we shall see, it is more readily accessible than the surface potential (Eq. 3.7), which describes the repulsive interaction between electric double layers.

Hückel and Smoluchowski equations

These are limiting solutions to the mobility equations for a colloidal dispersion undergoing electrophoresis. In the limit that the charged colloid particle is small enough to be treated as a point charge in an unperturbed electric field ($\kappa R \ll 1$), the Hückel equation can be applied. On the other hand, if the radius of the colloidal particle is large, then it can be approximated as a planar charged surface exposed to a flowing liquid. We also assume that the double layer thickness κ^{-1} is small, so that $\kappa R \gg 1$. In this limit, the Smoluchowski equation provides an expression for the mobility.

The electrical force acting on an isolated colloidal particle of charge q in an electric field of strength E is given by $F = qE$. This expression is valid when the colloid particle is sufficiently small not to modify the applied field. In the Hückel equation, this force is equated to the frictional force resulting from the viscosity of the medium, which is given by Stokes' law (Eq. 1.8), $F = 6\pi\eta v R$, where η is the viscosity of the medium. When the particle is moving steadily, these two forces are balanced and the mobility is

$$u = \frac{q}{6\pi\eta R} \qquad (3.12)$$

The mobility is commonly related to the zeta potential, ζ. The appropriate equation can be derived using the Debye–Hückel theory. The zeta potential is that at the surface between the moving electrokinetic unit (charge $+q$) and that of the mobile part of the double layer (charge $-q$):

$$\zeta = \frac{q}{4\pi\varepsilon R} - \frac{q}{4\pi\varepsilon(R + \kappa^{-1})} \qquad (3.13)$$

(recall that the ionic atmosphere thickness is κ^{-1}). Thus (in the limit that $\kappa R \ll 1$),

$$\zeta = \frac{3\eta u}{2\varepsilon} \qquad (3.14)$$

The Smoluchowski equation applies when the double layer is thin enough or R is large enough such that the motion of the diffuse part of the double layer can be considered to be uniform and parallel to a flat surface. The flow is taken to be laminar; i.e. infinitesimal layers of liquid flow past each other. Within each layer, the electrical and viscous forces are balanced. By balancing these forces and using Poisson's equation (Eq. 3.6) with suitable boundary conditions, it can be shown that the mobility has a form similar to the Hückel equation, although the numerical prefactor is different:

$$u = \frac{\zeta\varepsilon}{\eta} \qquad (3.15)$$

The same expression holds for the mobility in electro-osmosis.

Although the Hückel and Smoluchowski equations are useful limiting laws, they rarely give quantitative predictions for real colloidal sols, since the limits $\kappa R \ll 1$ and $\kappa R \gg 1$ are rarely satisfied in practice.

Henry equation

The Henry equation is a generalization of the Hückel equation for spherical particles with arbitrary double-layer thickness. It is assumed that the charge density is unaffected by the applied field. The result for the electrophoretic mobility of non-conducting particles is

$$u = \frac{2\zeta\varepsilon}{3\eta} f(\kappa R) \tag{3.16}$$

For very small particles in dilute solution, $1/\kappa$ is so large that $\kappa R \to 0$ and in this limit $f(\kappa R) = 1$ and the Hückel equation is recovered. In the limit of large particles, $f(\kappa R) = 1.5$ and the Smoluchowski equation is obtained. The Henry equation allows for values of $f(\kappa R)$ between these limits.

Determination of the Zeta potential

The zeta potential appearing in Eqs. (3.14) to (3.16) is usually obtained by measurements of the streaming potential or via the electro-osmotic effect. An alternative is to directly observe electrophoresis, using, for example, latex dispersions where the particles are sufficiently large to be visible under an optical microscope. The suspension flows through a capillary observation tube, and the velocity of the particles is measured directly by timing individual particles that move over a fixed distance. The electric field strength at the point of investigation can be obtained from the current, cross-sectional area of the tube and the conductivity of the dispersion.

Streaming potential or streaming current measurements are possible when an electrolyte is forced to flow through a capillary by a pressure difference at its ends (Fig. 3.4). The moving electric double layers give rise to a streaming current. The resulting build-up of charge leads to an electric potential that tends to oppose the current, until current due to the pressure gradient is balanced by that from the induced potential. At this point, the induced potential is termed the streaming potential. The streaming potential is given by

$$E = \frac{\varepsilon\Delta p\zeta}{\eta k_0} \tag{3.17}$$

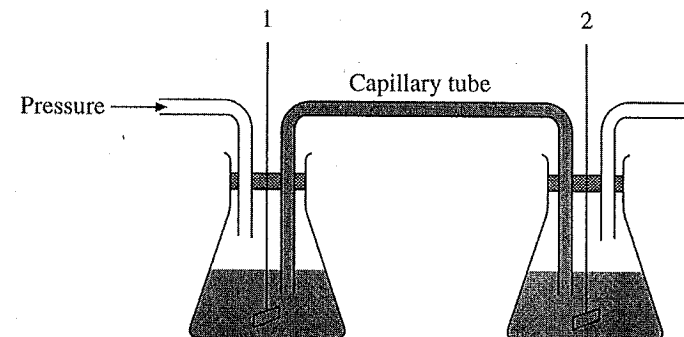where Δp is the pressure difference and k_0 is the conductivity of the electrolyte solution.

Figure 3.4 Schematic of apparatus for measuring streaming potential. A pressure difference applied across the capillary tube causes liquid to flow, which creates a potential difference measured between electrodes 1 and 2

In electro-osmosis, the volume flow rate (dV/dt) is measured through a capillary or a porous plug which can be treated as a series of capillaries. Using the Smoluchowski equation (Eq. 3.15), this is related to the zeta potential. For flow in a capillary of cross-sectional area A, we obtain

$$\frac{dV}{dt} = Av = \frac{AE\varepsilon\zeta}{\eta} \tag{3.18}$$

This equation can also be expressed in terms of current using Ohm's law.

3.5   CHARGE STABILIZATION

3.5.1   Charged Colloids

Electrostatic interactions are important in stabilizing many colloidal systems including clays and sols such as charged latex or silica particles. The surface of a colloidal particle can develop a charge through a number of mechanisms. For example, ionization of surface acid or base groups in aqueous solution can create a charged surface. Preferential ion adsorption or desorption or adsorption/desorption of ionic surfactants similarly leads to the development of an electrical double layer in many colloidal dispersions. Another more subtle effect is selective dissolution. For example, when silver iodide crystals are dissolved in water, the silver ions dissolve preferentially, leaving a negative charge on the crystals (which can be reduced or reversed by addition of Ag^+ ions, for example in the form of silver nitrate). In clays, charge can

be developed by isomorphous substitution of one atom by another, or by cleaving crystals to reveal charged crystal surfaces. The mechanisms by which colloidal clay particles become charged are discussed further in Section 3.11.

The concentration and nature of the electrolyte also has a significant impact on the stability of charged colloid dispersions. This was discussed in Section 3.3.2, where the concept of electric double layers was introduced. The electric double layer results from the atmosphere of counterions around a charged colloid particle. The decay of the potential in an electric double layer is governed by the Debye screening length, which is dependent on electrolyte concentration (Eq. 3.8). In the section that follows, the stability of charged colloids is analysed in terms of the balance between the electrostatic (repulsive) forces between double layers and the (predominantly attractive) van der Waals forces.

The valence of the counterion is the predominant influence in preventing coagulation of a colloidal dispersion. The nature of the counterion, the valence of the co-ion and the concentration of the sol are much less important, and the nature of the sol only has a moderate effect on stability. These empirical observations, made in the late nineteenth century, are known as the Schulze–Hardy rule. We are now able to interpret these effects using a quantitative model known as the Derjaguin–Landau–Verwey–Overbeek theory, discussed in the next section.

Electrostatic interactions are not just important in stabilizing colloidal dispersions, but also influence emulsification, through interactions between head groups of ionic surfactants. The stabilization of emulsions is the subject of Section 3.13.

3.5.2   DLVO Theory

A very useful tool for understanding the stability of colloids is provided by the Derjaguin–Landau–Verwey–Overbeek (DLVO) theory, which was named after the four scientists responsible for its development. The theory allows for both the forces between electrical double layers (repulsive for similarly charged particles) and long-range van der Waals forces that are usually attractive.

In this theory, the total potential energy is expressed as the sum

$$V = V_R + V_A \tag{3.19}$$

where V_R is the repulsive potential energy due to the overlap of electrical double layers on colloid particles and V_A is the attractive van der Waals
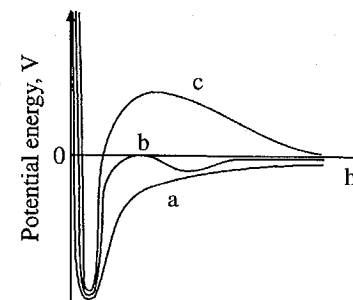
Figure 3.5   Curves of potential energy versus separation between the surfaces of charged colloidal particles. The electrolyte concentration decreases from a to c

energy. Of course, the force can simply be obtained as the negative of the gradient of potential energy with respect to the separation of colloid particles:

$$F = -\frac{dV}{dh} \tag{3.20}$$

By plotting the potential energy as a function of the separation between particle surfaces it is possible to determine whether the colloidal suspension is stable or whether association will occur. If the potential energy curve has a deep attractive minimum at small separations (Fig. 3.5, curve a), the system will be unstable and association can occur. The association will take the form of flocculation if it is reversible or coagulation if it is irreversible. However, sometimes the potential energy curve has a smaller secondary minimum separated from the primary minimum by a barrier. If this barrier is large compared to $k_B T (T = 298K)$ but the secondary minimum is comparable to $k_B T$, then reversible flocculation can occur and a kinetic equilibrium is set up between particles and weakly bound aggregates called flocs (Fig. 3.5, curve b). It is important to note, however, that this is a kinetic barrier, because the potential is lowest in the primary minimum. If there is no secondary minimum and the potential energy barrier is sufficiently large compared to thermal energy ($k_B T$), then very few particles will be able to 'fall into' the primary minimum and so the dispersion is kinetically stable (Fig. 3.5, curve c) and there is no flocculation or coagulation.

We now consider interactions between two spherical colloid particles of radius R in an electrolyte of bulk concentration c_0. The expression for the repulsive potential can, to a good approximation, be derived from the electrical potential as a function of distance from a charged plane, if the radius of the particles is sufficiently large. When the electrical double layers are far

apart, the interaction between them is weak and $\kappa h > 1$. In this limit, the total potential can be written as

$$V = \frac{64\pi R k_B T c_0 \Gamma_0^2}{\kappa^2} \exp(-\kappa h) - \frac{A_H R}{12h} \qquad (3.21)$$

Here A_H is the Hamaker constant and

$$\Gamma_0 = \frac{\exp[ze\Phi_0/(2k_B T)] - 1}{\exp[ze\Phi_0/(2k_B T)] + 1} = \tanh\left(\frac{ze\Phi_0}{4k_B T}\right) \qquad (3.22)$$

A full derivation of Eq. (3.21) is beyond the scope of this chapter (further details can be found in the books by Fennell Evans and Wennerström, 1994, Hunter, 1987, or Shaw, 1992). The repulsive contribution is obtained by a generalization of the Gouy–Chapman equation discussed above. The van der Waals term is identical to Eq. (3.2) and arises from a summation of the dispersion forces, i.e. induced dipole–induced dipole interactions, between all points on each of the colloidal particles.

The DLVO theory can account for the stability of colloidal suspensions, or whether coagulation or flocculation occur. This is illustrated by Fig. 3.5, in which potential energy curves are drawn for three different electrolyte concentrations, decreasing from a to c. If the attractive contribution from van der Waals forces, V_A, dominates the total potential energy curve (Fig. 3.5, curve a), then the colloidal suspension will not be stable, the system will minimize its potential energy by coagulation and the average interparticle separation corresponds to the position of the primary minimum or potential 'well'. If the contribution from repulsive double-layer forces is significant, then a positive potential energy barrier can exist in the total potential energy curve (curve c in Fig. 3.5). If this barrier is large compared to $k_B T$, then the colloidal dispersion is kinetically stable. If the relative contribution of attractive and repulsive forces is such that a secondary minimum develops in the total potential energy curve, then reversible flocculation can occur if this minimum is comparable to $k_B T$. Curve b in Fig. 3.5 illustrates this situation for the case where the maximum of the potential energy curve (force $F = 0$) occurs at $V = 0$. This defines the *critical coagulation concentration* (c.c.c).

3.5.3   Critical Coagulation Concentration

As electrolyte is added to a colloidal suspension, the diffuse double-layer thickness around a particle is compressed so that the range of double-layer

forces is reduced. Coagulation can occur at an electrolyte concentration such that the repulsive double-layer interaction is reduced sufficiently to enable attractive interactions to predominate. This occurs at a critical coagulation concentration (c.c.c.). Using the potential defined in Eq. (3.21), it is straightforward to show (see Q. 3.9) that at the c.c.c. ($V = 0$ and $F = 0$) the interparticle separation is

$$h = \frac{1}{\kappa} \qquad (3.23)$$

The critical coagulation concentration can then be estimated by substituting $\kappa h = 1$ into Eq. (3.21) and determining κ (Q. 3.9). This can be equated to the Debye length κ defined in Eq. (3.8) to determine the c.c.c. The approximate concentration (moles/unit volume) is

$$\text{c.c.c.} = \frac{9.85 \times 10^4 \varepsilon^3 (k_B T)^5 \Gamma_0^4}{N_A e^6 A_H^2 z^6} \qquad (3.24)$$

or, for an aqueous dispersion at 25°C,

$$\text{c.c.c.} = \frac{3.84 \times 10^{-39} \Gamma_0^4}{(A_H/\text{J})^2 z^6} \text{ mol dm}^{-3} \qquad (3.25)$$

The striking feature of this result is the strong dependence on the valence of the electrolyte (i.e. sixth-power dependence) at high potentials where Γ_0 tends to unity. This strong dependence on electrolyte charge is in agreement with the Schulze–Hardy rule. In contrast, the c.c.c. is essentially independent of the specific nature of the ions.

3.6   STERIC STABILIZATION

Steric stabilization of a colloidal dispersion is achieved by attaching long-chain molecules to colloidal particles (Fig. 3.6). Then when colloidal particles approach one another (for example due to Brownian motion), the limited interpenetration of the polymer chains leads to an effective repulsion which stabilizes the dispersion against flocculation. Steric stabilization has several advantages compared to charge stabilization. First, the interparticle repulsion does not depend on electrolyte concentration, in contrast to charge-stabilized colloids where the electric double-layer thickness is very sensitive to ionic strength. Second, steric stabilization is effective in both
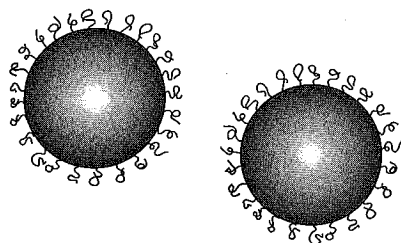
Figure 3.6 In steric stabilization, the contact of colloidal particles is prevented by attached long-chain molecules, often copolymers

non-aqueous and aqueous media, whereas charge stabilization is usually exploited in aqueous solutions. Finally, steric stabilization operates over a wide range of colloid concentrations, in contrast to charge stabilization which is most effective at low concentrations. The most effective steric stabilizers are block or graft copolymers (Section 2.3.4), where one type of block is soluble in the dispersion medium and the other is insoluble so that it attaches to the colloid particles.

The interactions between sterically stabilized colloid particles can be mapped on to those of the bare particles when the adsorbed polymer layer is matched to the dispersion medium or to the core of the particle. A steric stabilization layer of thickness δ surrounding a particle of radius R prevents the particle surfaces coming closer than 2δ. If the properties of the adsorbed layer are matched to those of the dispersion medium, then for a given interparticle separation the attractive potential will be unchanged by the coating layer. However, at contact, the attraction will be weaker than it would be for contact of bare particles since the 'cores' are effectively separated. On the other hand, if the properties of the adsorbed layer are close to those of the core, the coated particle will simply behave as though it was larger, and thus (by Eq. 3.2) the attraction at contact will be stronger than for uncoated particles. Thus, by matching the properties of the adsorbed polymer to those of the dispersion medium, attractive interactions between particles can be reduced, reducing the tendency for association. In the limit where the attractive potential well is reduced to a few $k_B T$ ($T = 298$K), Brownian motion can overcome the interparticle attractions and the dispersion is stabilized.

In principle, if sterically stabilized colloid particles collide and the adsorbed layers do not interpenetrate, the stability of the colloidal dispersion will be increased by an 'elastic' effect. This arises because the compression of one layer of polymers by another will restrict the number of conformations available to each polymer chain. This decreases the entropy and so increases
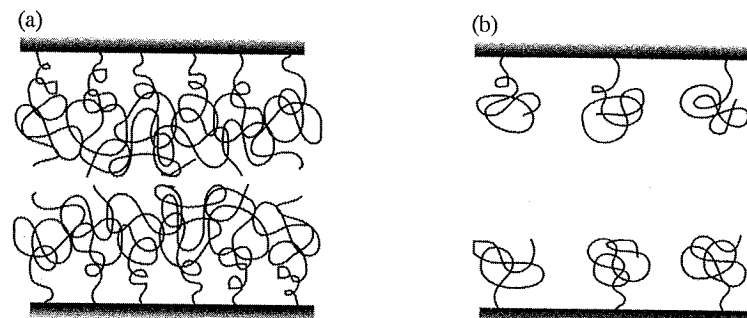
Figure 3.7 Polymer chains grafted at a planar interface: (a) brushes, at high grafting density, (b) mushrooms, at low grafting density

the free energy, and thus association is disfavoured. However, in practice, interpenetration of polymer layers is always important. Polymer chains adsorbed at a planar interface are sketched in Fig. 3.7. When the polymer chains are densely grafted (i.e. the distance between graft points is smaller than the polymer radius of gyration), they tend to adopt a conformation which is stretched away from the grafting point, a so-called *polymer brush*. When the polymer chains are less densely grafted, there is room for them to adopt a less stretched conformation, termed a *polymer mushroom*.

Consider the compression of brushes in a good solvent. As polymer brushes are compressed in a good solvent, the local density of polymer segments increases. This leads to the osmotic tendency for molecules of the dispersion medium to diffuse into the interlayer region to reduce the segment concentration. This tends to force the surfaces apart. The same effect is driven by a second tendency. The increase in concentration of polymer segments upon compression reduces the number of conformations available to the polymer chains, so that the entropy of the system is reduced. It is thus favourable for the surfaces to be well separated. As the grafting density is decreased, the magnitude of the repulsive interaction decreases, as shown by the free energy curves in Fig. 3.8a. The total free energy is sketched in Fig. 3.8b. This shows that if the grafting density becomes too low (well-separated polymer mushrooms), as in curve iv, the repulsive interaction is not large enough to overcome the attractive forces at small interparticle separations. Aggregation can then occur at an interparticle separation corresponding to the free energy minimum.

The behaviour in a poor solvent is more complex. A polymer chain avoids contact with such a solvent. When a second polymer layer is brought close, a polymer coil at one surface can approach the other surface through the
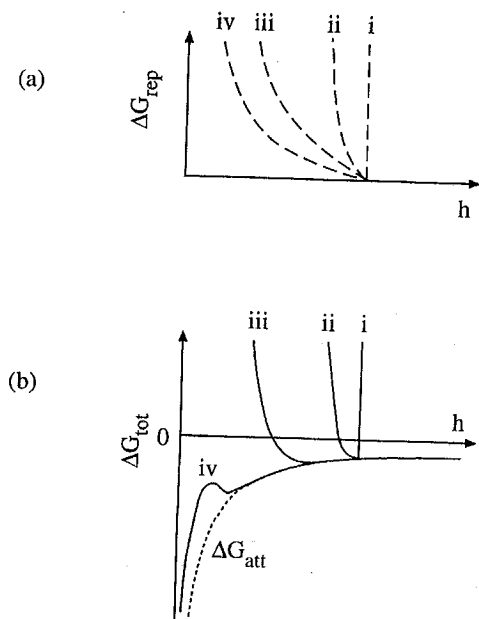
Figure 3.8   Potential energy curves for a pair of sterically stabilized colloid particles, separated by a distance h. (a) Repulsive contribution to the free energy, (b) attractive contribution and total free energy. The grafting density decreases from i to iv

intervening polymer layer without too much exposure to solvent. This leads to an increased configurational entropy and thus an attractive force between the plates or colloid particles. This attractive force only operates at intermediate length-scales; at short separations repulsion is dominant. It is thus evident that solvent quality is very important in steric stabilization. In a good solvent, repulsive interactions between colloidal particles occur if the grafting density is high enough, but if the solvent quality is poor, then attractive interactions between particles can lead to flocculation. The crossover from one behaviour to the other occurs at the theta point of the solvent. The transition from a stable colloidal dispersion to a flocculated system occurs at a *critical flocculation point* (CFPT), which can be attained by variation of temperature (CFT) or pressure (CFP). Flocculation can also be induced by adding a miscible liquid that is a non-solvent for the polymers, this leading to a volume change which defines a critical flocculation volume (CFV).

The preceding descriptions of steric stabilization mechanisms assume that the time-scale for the particle encounter is much shorter than that for
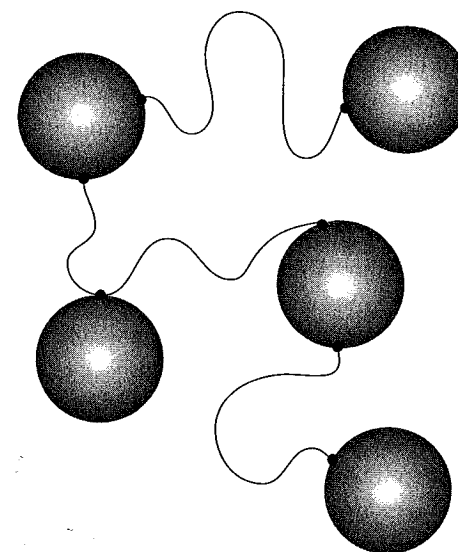
Figure 3.9   Illustrating bridging of polymer chains between colloid particles

adsorption or desorption of the polymer chains. Effective steric stabilization also requires that the adsorbed layers are sufficiently thick and that the surface coverage is complete.

3.7   EFFECT OF POLYMERS ON COLLOID STABILITY

Just as polymer chains can adsorb on to single colloid particles, at low concentrations different sections of one polymer chain can adsorb on to two different colloid particles (Fig. 3.9). This leads to so-called *bridging flocculation*. The polymer bridges force the colloid particles together, and thus lead to flocculation. For bridging flocculation to occur, two important conditions must be met. First, the polymer flocculant must have sufficient molar mass such that the chains are at least long enough to span the range of interparticle separations. The polymer molar mass required for bridging will be dependent on electrolyte concentration because the higher this is, the thinner the electric double layers and hence the shorter the polymer required to induce bridging flocculation. Second, the surface coverage of adsorbed polymer chains must not be complete, to allow for adsorption of segments

from one or more chains attached to other particles when Brownian collisions occur. This implies that bridging flocculation is an active mechanism at low polymer concentrations. Thus, bridging leads to a rather loose flocculated structure. Examples of systems where bridging flocculation occurs include colloid solutions to which gelatin is added. Bridging flocculation is also exploited in the final stages of water purification, where addition of a few parts per million of a high molar mass polyacrylamide leads to the flocculation of the remaining particulates in the water. In this case the polymer, which forms a polyelectrolyte in solution, also enhances the sensitivity of colloidal sols to flocculation via charge neutralization. Indeed, in water and effluent treatment it is found that the only effective polymeric flocculants are those bearing the opposite charge to the colloid particles, although bridging flocculation can still also occur.

Flocculation can also be induced or prevented via free polymer in a good solvent. *Depletion flocculation* occurs when polymer chains are excluded from the region between the particles. This occurs when the polymer size (r.m.s. end-to-end distance) is greater than the interparticle separation. It is then unfavourable for the polymer to 'squeeze into' the interparticle gap, because of the cost in configurational entropy. On the other hand, it is energetically favourable for the solvent to be expelled from this gap to solvate the polymers in the bulk solution. Thus the colloid particles tend to be brought into association, leading to flocculation. This can be viewed as an osmotic process, i.e. the net flow of polymer from regions between colloid particles into the bulk solution. This leads to an osmotic compression, i.e. the closer approach of colloid particles. Use is made of depletion flocculation to fuse biological cells, using poly(ethylene glycol) in aqueous solution.

3.8   KINETIC PROPERTIES

Colloidal particles undergo Brownian motion (Section 1.4). There is an interplay between the kinetic energy associated with this motion and their stability, since if the collision energy of particles is of the order of a few $k_B T$ ($T = 298$K) they will be able to overcome the typical repulsive potential barrier that leads to the stability of charged colloids (see Section 3.5.2). The energies of the particles are given by a Boltzmann distribution, and at room temperature this means that very few will be able to overcome the energy barrier. The kinetics of association of colloidal particles are determined by

the presence of this potential barrier and its magnitude, although we do not consider the details here.

3.9   SOLS

Sols are dispersions of solid particles in a liquid. Sols that are incompatible with the liquid are said to be lyophobic, i.e. solvent-hating, whereas 'solvent-loving' sols are lyophilic, although, as mentioned in Section 3.2, these terms are not used rigorously. If the sol is dispersed in an aqueous medium, it is said to be a hydrosol. Sols can, in principle, be prepared by dispersion methods, in which a bulk sample is broken up into colloidal particles by mechanical means. This can be achieved by milling or using ultrasound. However, the method is not suitable for preparing finely divided particles. To prepare finely dispersed colloidal sols it is necessary to turn to aggregation or condensation methods. Condensation methods include dissolution and reprecipitation or condensation from a vapour or chemical methods. The latter are the most generally applicable, and this is the technique used to prepare metal sols by precipitation from a supersaturated solution. Particles are formed by a nucleation and growth mechanism; i.e. crystal centres are formed first and then grow by deposition of additional material. For example, gold sol can be made by reduction of chlorauric acid, $HAuCl_4$, or silver iodide sol from silver nitrate and potassium iodide. Sulphur sols can be made by oxidation of hydrogen sulphide or thiosulphate solutions. Sols are most easily formed from insoluble substances because in those that are more soluble, small particles can redissolve or attach themselves to growing particles.

Unfortunately, these methods lead to rather polydisperse sols. This is because the nucleation step is not controlled. Therefore new particles are being nucleated at the same time as existing ones are growing, a process termed heterogeneous nucleation. Furthermore, early nucleated particles can join or attach themselves to younger particles, and thus perturb the growth process. Several procedures are available to ensure more homogeneous nucleation, including self-seeding and controlled hydrolysis methods. In the self-seeding method, small seed crystals are added to a supersaturated solution and act as sites for subsequent growth. This method is used to prepare monodisperse gold sols, for example.

Controlled hydrolysis is another method for preparing relatively monodisperse sols. It is achieved by confining the nucleation process to a 'short burst' by suitable control of the reaction rate or conditions of concentration or temperature. It is necessary to ensure that the concentration for nucleation of

new crystals is only achieved for a short time. The concentration for nucleation can exceed the supersaturation concentration if the system is perturbed from equilibrium (the supersaturation concentration is a maximum at equilibrium). When it is possible to prepare a supersaturated solution and then concentrate it, a concentration will be reached where nucleation occurs rapidly. This immediately reduces the degree of supersaturation as molecules are depleted from solution and thus the conditions for nucleation are 'automatically' removed. An example of controlled hydrolysis is the preparation of sulphur sols by oxidation of very dilute solutions of sodium thiosulphate ($Na_2S_2O_3$) in HCl. Silver bromide and silver iodide sols can also be made highly monodisperse by controlled hydrolysis. Control of the dispersity of these particles is important in photographic film. More industrially relevant, the same method is used to make monodisperse silica (silicon dioxide) sols from silicic acid or orthosilicates. Silica particles are widely used as fillers for paints and rubber reinforcing agents.

Monodisperse latex sols are made by emulsion polymerization from a seed sol. The seed sol is an emulsion, stabilized by a surfactant above the critical micelle concentration (Section 4.6). When the concentration is reduced below the critical micelle concentration, the seed sol particles can grow but no new ones are nucleated. The properties of the resulting monodisperse sols are discussed in more detail in Section 3.15.

Clays are an important class of sols and are considered separately in Section 3.11.

3.10   GELS

A colloidal gel is formed by association of colloid particles or molecules in a liquid such that the solvent is immobile. In rheological terms, a gel is a Bingham fluid; i.e. it has a finite yield stress below which it does not flow. This definition is deliberately broad in order to include gels formed in concentrated polymer solutions due to network formation (an example is gelatin in water, Section 3.14.7) as well as gels formed by association of sol particles. Examples of the latter include greases formed from inorganic sols or clays at high mineral concentration.

Association of sol particles can occur through bridging flocculation, if the bridges are extensive enough to produce a continuous network extending throughout the sample. In fact, it is not always necessary for the particles to form a chemical network, as shown by the formation of gels in concentrated surfactant solutions, when they form cubic phases (see Section 4.10.2). There are no chemical links or bridging chains between the micelles in cubic micellar

structures. Cubic phases are by definition solids in a rheological sense, and the gels formed by such structures behave as model 'soft solids'.

Gels formed by polymers in aqueous solutions can often be swollen to a substantial extent. In contact with water such gels will imbibe water, because of an osmotic effect. The water can diffuse into the polymer network, but the polymer chains in the network cannot diffuse out. Thus, the network behaves as a kind of semi-permeable membrane. If the gel is strong enough, swelling stops when the internal pressure in the gel caused by the stretched network is equal to the osmotic pressure. On the other hand, if the gel is weak the internal pressure will cause the gel to break up, and the polymer will dissolve in solution.

The process of *syneresis* in gels results from the kinetics of gel formation. The initially formed gel structure may not be the most stable. The diffusion of polymer chains, which is greatly retarded in the gel, may slowly lead to the formation of a more stable compact structure. An increased pressure may then be exerted on the water in the gel, leading to its slow expulsion, a process termed syneresis.

3.11   CLAYS

In addition to their widespread use in bricks and ceramics, clays are widely exploited as fillers in making paper and paints. Another important application is their use as drilling muds in oil-wells, where they serve several purposes, including removal of cuttings from the drill-hole, sealing of the borehole with an impermeable barrier and as coolants.

Clays are colloidal suspensions of plate-like mineral particles (Fig. 3.10). These platelets have typical aspect ratios of 10:1 and can be micrometres
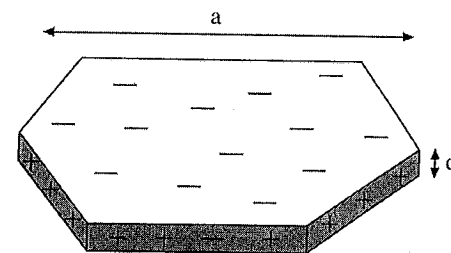

Figure 3.10   A clay particle, typical of kaolinite. The aspect ratio a/c is typically about 10. [Reproduced with permission from R. J. Hunter, *Foundations of Colloid Science*, Vol. I, Oxford University Press, Oxford (1989)]

long. They stack into layered structures where the layers are held together by van der Waals forces or sometimes by hydrogen bonding. In many clays, there are water layers in between the mineral platelets and the clays can be swollen, this being typical of the behaviour of clays in ordinary soil. In other types of clay, the bonding between plates is stronger so that they do not swell in water, an example being mica.

The basic structural unit of clays consists of one or two layers consisting of silicon tetrahedrally bonded with oxygen atoms combined with one layer of octahedrally coordinated aluminium or magnesium atoms. The silica and alumina/magnesia groups are packed such that they form layers. The aluminium or magnesium is coordinated with some oxygen and some hydroxyl groups. The simplest structure is called kaolinite, sketched in Fig. 3.11. In this structure there is a 1:1 sequence of silica and alumina layers. Some oxygen atoms in the silica layer are shared with the alumina layer. The presence of hydroxyl and oxygen groups on the surfaces of the layers means that the layers are hydrogen bonded to each other and so the planes are hard to separate. The ideal kaolinite structure is electrically neutral. However, in practice the plates formed by real crystals have negative charge on their basal planes. This results from the substitution of tetravalent silicon by trivalent aluminium. This negative charge is balanced by counterions, such as Na^+ and Ca^{2+} sandwiched between the layers.

In the ideal 2:1 clay structure there are two layers of silica to one of alumina (pyrophillite) or two layers of silica to one of magnesia (talc). The absence of hydroxyl groups at the surfaces of the triple layer prevents hydrogen bonding. In this case, the layered structure is held together by van der Waals interactions between the platelets. These are weak, so that the crystals can readily be cleaved along the basal planes. A good example of a system showing easy cleaving is mica, the structure of which is related to

$(OH)_3$
Al_2
$O_2, (OH)$
Si_2
O_3
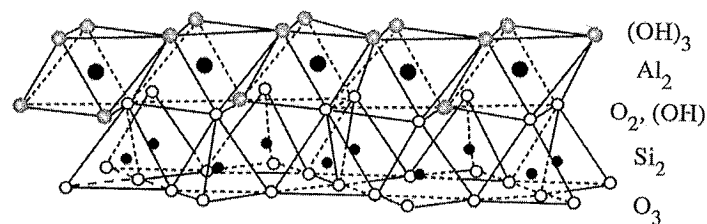
Figure 3.11 Structure of one layer of the ideal kaolin structure, $(Al(OH)_2)_2$ $.O.(SiO_2)_2$. [Reproduced with permission from R. J. Hunter, *Foundations of Colloid Science*, Vol. I, Oxford University Press, Oxford (1989)]

pyrophillite by replacing one quarter of silicon atoms by aluminium atoms. This leads to an imbalance of charge, which again is balanced by counterions, in this case K^+. These fit into the silica lattice and result in strong electrostatic forces between the triple layer structures, so that mica is similar to kaolinite in that it does not swell in water. In contrast, montmorillonite is a clay related to the pyrophillite structure which does swell in water. The structure is obtained by substitution of approximately one in six of the aluminium ions in the pyrophillite structure by magnesium or other divalent ions. Bentonite is a related material, consisting of a mixture of montmorillonite with beidellite in which the silicon atoms in the pyrophillite structure are replaced by aluminium. Bentonite is widely used in oil-well drilling muds. Montmorillonite-type clays swell in water. When hydrating these materials, it is observed that the initial swelling process occurs by the formation of a few discrete water layers (up to four). Impure clays such as those found in soil, on the other hand, can swell to many times their original size.

At the edges of clay platelets, covalent bonds are broken, leading to a net positive charge, as indicated in Fig. 3.10. This has been demonstrated by mixing charged colloidal gold with clay. The negatively charged gold sol particles decorate the positively charged edges of the clay platelets. The development of charge on clay particles can lead to the formation of gels, because association of edges and faces of platelets can lead to aggregates of these particles. However, for oil-well drilling applications a concentrated clay suspension with a low viscosity is required. This can be achieved by *peptization* using a polyphosphate. Peptization is simply a process whereby the composition of the dispersion medium is changed, in this case by addition of polyvalent counterions (it is nothing to do with peptides!). This reverses the charge on the platelet edges, so that there is a repulsive barrier between them, the dispersion is stable and flows freely as required.

Mica is a unique colloid in that it is possible to cleave atomically flat sheets from this clay mineral. These have been exploited in so-called surface forces experiments (Section 1.9.6), where the force between two mica sheets sandwiching a liquid of interest is measured as a function of distance between them. The method has allowed a direct determination of the Hamaker constant for mica plates separated by different liquids. Recent extensions of the method have enabled the measurement of the forces between polymer layers adsorbed on to the mica, for various polymer architectures at different grafting densities and in the presence of different solvents (or none).

3.12 FOAMS

A foam is defined as a coarse dispersion of a gas in a liquid, where the volume fraction of gas is greater than that of the liquid. Solid foams (for example foam rubber or polystyrene foam) are also possible, but here we focus on more common liquid foams. These are always formed by mixtures of liquids (usually containing a soap or surfactant) and never by a pure liquid. If the volume fraction of gas is not too high, the bubbles in the foam are spherical, but at higher gas volume fractions the domains are deformed into polyhedral cells, separated by thin films of liquid (Fig. 3.12). Typically the gas bubbles are between 0.1 and 3 mm in diameter.

Foams are not thermodynamically stable due to their large interfacial area and thus surface free energy. However, some foams, particularly those formed by addition of small amounts of foaming agents such as soaps or surfactants, can be metastable. These foaming agents act to a certain extent to retard drainage of liquid from the foam and to prevent its rupture. Foams formed by other liquids such as alcohols or short chain fatty acids are unstable, and the foam collapses rapidly.

Foams formed by surfactants or soaps are not indefinitely stable because of two main effects. The first is *drainage* of liquid due to gravity, which leads to thinning of the liquid film. The second is *rupture*, which results from random disturbances (mechanical, thermal, evaporation, impurities). A foam that initially contains bubbles can develop into a foam containing polyhedral cells as a result of drainage, or the latter can develop rapidly from liquids of low viscosity if the volume fraction of gas is high. The development of a foam structure is a dynamic process involving several stages. Initially drainage of liquid occurs throughout the liquid film, leading to a polyhedral cellular structure. The vertices of the polyhedra are called *plateau borders*. Due to the curvature of the liquid film in this region, the liquid pressure is lower than in the surrounding channels because the gas pressure is uniform
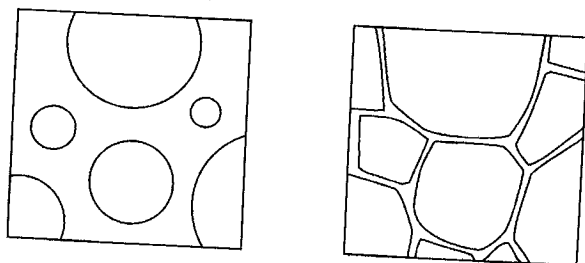
Figure 3.12   Foam structure. Left: spherical bubbles. Right: polyhedral cells
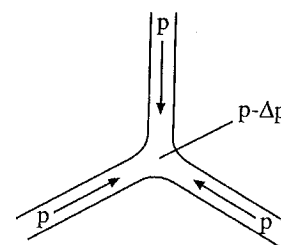
Figure 3.13   Plateau border between three cells in a foam. Due to the curvature of the liquid–gas interface, the pressure is lower by Δp at the point of intersection of the channels, leading to capillary flow

and the liquid interface area is larger where it is more curved (Fig. 3.13). This pressure drop leads to liquid flow at the plateau borders, and if the resulting forces overwhelm the surface tension supporting the liquid channels the film will rupture and the foam will collapse. Alternatively, if there is a balance of forces the film may achieve a pseudo-equilibrium thickness. Addition of too much surfactant can cause a foam to collapse, since the interfacial tension can become too low. Foams can also be destabilized by creaming, i.e. the tendency for regions of high gas content to rise to the top of the foam, leaving denser regions close to the bulk liquid. Another important effect is the selective growth of large bubbles at the expense of small ones, a process termed *Ostwald ripening*.

In foams formed by liquids containing surfactants the molecules tend to form lamellae parallel to the liquid film surface, at which there is an excess of surfactant. When draining occurs in such films, the Gibbs and Marangoni effects tend to oppose the destabilizing influence. If a film is subject to strong thinning forces, the surface area will increase and so the surface excess concentration of surfactant will decrease, which leads to an increase in surface tension. This increase in surface tension is termed the Gibbs effect and tends to oppose thinning. A related effect results from the difference in the static surface tension in the draining film and the dynamic surface tension. Surfactant molecules tend to flow into the region of temporarily reduced surface excess in order to restore the original surface tension (usually lower), which is termed the Marangoni effect. The opposite effect occurs if the surface area of the film is decreased. Whenever there is a change of surface area and thus surface excess, the resultant diffusion of surfactant molecules takes a finite time and there is a transient difference in surface tension. Other processes have been suggested to accompany the Gibbs–Marangoni effect, in particular it has been proposed that diffusing surfactant molecules at the liquid surface drag underlying liquid along with them, thus opposing the thinning process.

The Gibbs–Marangoni effect results from the surface excess of surfactant and so does not occur in pure liquids.

3.13 EMULSIONS

Emulsions are dispersions of immiscible or partially miscible liquids. Usually intimate mixing of the two phases is ensured by homogenization (for example by stirring) or ultrasonication. Sometimes chemical energy is liberated when the liquids come into contact, and this can also be used to prepare emulsions. The free energy required to disperse a liquid of volume V into drops of radius R is approximately

$$\Delta G = \gamma \frac{3V}{R} \qquad (3.26)$$

where γ is the interfacial tension. We can see from this equation that lowering the interfacial tension leads to a reduction in free energy and hence a relative stabilization of the emulsion.

Emulsions are a very important type of colloid, being found in foodstuffs, pharmaceutical products, cosmetics and agricultural products, for example. Emulsions in food colloids are so important that we defer a full discussion to the next section. Here we consider both *emulsions* and *microemulsions*. The two are distinguished by the fact that emulsions (macroemulsions) are thermodynamically unstable, whereas microemulsions are stable. In addition, the dynamics are distinct, the kinetics of exchange of molecules in and out of the stabilizing film being much greater in microemulsions than in emulsions. As suggested by the name, the dispersed phase in microemulsions is characterized by a smaller droplet size than in emulsions, and this historically was used to define them. Microemulsions are discussed more fully below.

Emulsions and microemulsions can also be formed in polymer blends. Here a surfactant such as a block copolymer is used to reduce the interfacial tension since it will selectively adsorb at a polymer–polymer interface. In favourable cases, the interfacial tension can be reduced to zero and a microemulsion is formed that is thermodynamically stable.

3.13.1 Emulsions

In the most common examples of emulsions, one phase is aqueous and the other is an oil (used in the sense of an insoluble organic species). Two types

of emulsion can be distinguished, water-in-oil (w/o) and oil-in-water (o/w), in which water or oil are the dispersed phase respectively. Milk contains fat droplets in a continuous aqueous phase, and so is an example of an oil-in-water emulsion. Another example is mayonnaise, which is a dispersion of vegetable oil in vinegar or lemon juice, stabilized by natural lecithin surfactant molecules. Margarine, on the other hand, is a water-in-oil emulsion. The two types of emulsion can be distinguished by simply adding water or oil. An oil-in-water emulsion can take up water (for example milk can be diluted) whereas oil can be added to a water-in-oil emulsion. Other identification methods exploit the selective solubilization of a dye in the dispersion medium, or differences in electrical conductivity (usually water has a higher conductivity than the oil).

Typically, droplets in emulsions contain dispersed particles in the size range 0.1–10 μm, which covers the wavelengths of visible light. Thus emulsions can often appear cloudy because they scatter light. In contrast, the particles in microemulsions are smaller (1–100 nm) and the sample appears clear and is optically isotropic.

Emulsions are not thermodynamically stable and tend to break up due to a number of processes. These include flocculation due to net attractive forces between dispersed droplets, coagulation where the droplets are irreversibly aggregated, creaming or sedimentation (which can occur for unaggregated droplets) and coalesence, where droplets merge. The latter usually involves large droplets growing at the expense of small ones, this being another example of Ostwald ripening (Section 2.5.7).

The spontaneous formation of emulsions is rather uncommon but can result from transient fluctuations in an oil–water interface due to thermal gradients (the Marangoni effect, see the preceding section) or in the case where the interfacial tension is negative. This unusual situation can be achieved in a blend of two liquids exhibiting an upper critical solution temperature (also known as the upper consolute temperature) (see Fig. 2.18), when the system is cooled below this transition. However, almost always emulsions are stabilized using emulsifiers or emulsifying agents. These are surface-active agents, proteins or finely divided solids. They reduce the interfacial tension, which is the most important factor in controlling the long-term kinetic stability of emulsions. The activity of surfactant emulsifiers is often quantified through the *hydrophile–lipophile balance* (HLB) scale, which is an empirical range of numbers between 1 and 20. The more hydrophilic the amphiphile, the higher its HLB. The action of surfactants is discussed more fully in Section 4.3.2. Proteins contain hydrophilic and hydrophobic sequences and thus undergo weak preferential adsorption at the oil–water interface. Naturally occurring proteins are essential to the emulsification of many foods. In addition
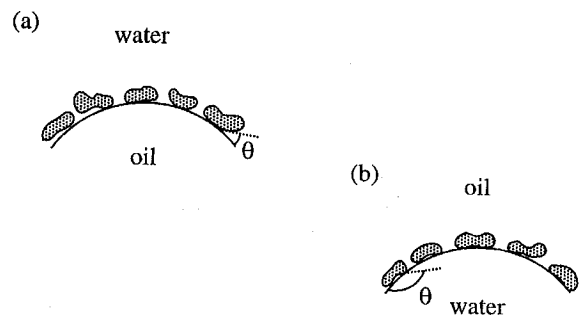
Figure 3.14 Stabilization of emulsions by finely divided solids. Preferential wetting of (a) water in an oil-in-water emulsion, (b) oil in a water-in-oil emulsion

to lowering interfacial tension, the adsorbed film of protein or surfactant forms a membrane that is strong and elastic enough to support the emulsion and prevent the coalescence of dispersed droplets. This can also be achieved very effectively using dispersed solids, which provide a steric mechanism (Pickering stabilization) of coalescence prevention by eliminating droplet contact. Finely divided solids act to stabilize emulsions by aggregating at the oil–water interface due to preferential wetting by one phase or the other (Fig. 3.14). For example, if the solid particles are preferentially wetted by water they will act to stabilize oil-in-water emulsions.

Emulsion stability is also favoured if the volume fraction of the dispersed phase is small. Usually, but not always, the liquid with the lower volume fraction forms the dispersed phase. However, this is not the case if the dispersed phase forms a close-packed structure of droplets, because by definition this occupies a volume fraction $\phi = 0.74$. Emulsions are also more stable if the droplet size distribution is narrow. If there is a large disparity in droplet sizes, Ostwald ripening is enhanced and small droplets are 'swallowed' up when they come into contact with larger ones (because the net result of this process is to reduce the interfacial curvature per unit volume). High viscosity of the dispersion medium also favours emulsification, simply by retarding break-up mechanisms such as creaming and coalescence. Electrostatic interactions can enhance the stability of oil-in-water emulsions through the use of ionic surfactants. Even simple inorganic electrolytes can preferentially adsorb at the interface, and the resulting electric double-layer repulsion will reduce droplet coalescence. Creaming or sedimentation can be reduced if the density difference between dispersion medium and dispersed phase is small. One way of achieving this that is exploited in paint technology is to disperse water droplets into oil drops which are dispersed in water, i.e. a water-in-oil-in-water emulsion.
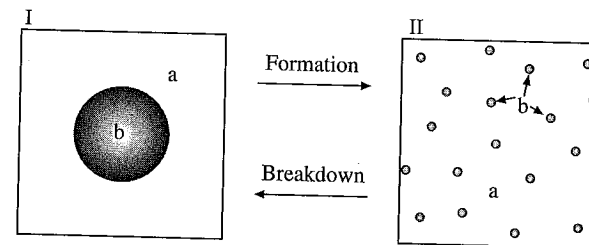
Figure 3.15 Formation and breakdown of an emulsion of liquid b in liquid a

Emulsions can be destabilized by agitation, which leads to droplet coalescence, centrifuging which leads to creaming or by adding salt to electrostatically stabilized systems. Temperature changes (that cause freezing, for example) or filtration can also be used to break up emulsions.

The thermodynamic stability of emulsions can readily be assessed by comparing the free energy to that of an undispersed system (Fig. 3.15). The total free energy in the undispersed system (I), excluding surface terms, is given by

$$G^I = G_a^I + G_b^I + G_{ab}^I \tag{3.27}$$

Here G_a^I and G_b^I are the bulk free energies of liquids a and b, and G_{ab}^I is the excess free energy associated with the liquid–liquid interface. This takes the form

$$G_{ab}^I = \gamma_{ab} A^I \tag{3.28}$$

for an interface of area A^I, where γ_{ab} is the interfacial tension.

When liquid b is dispersed in liquid a by mechanical work to form an emulsion (II), it is necessary to include a term in the free energy that reflects the decrease in order of the system due to the formation of droplets:

$$G^{II} = G_a^{II} + G_b^{II} + G_{ab}^{II} - TS^{II}(\text{config}) \tag{3.29}$$

The entropic term $-TS^{II}(\text{config})$ partly offsets the increase in free energy required to create more interfacial area. The configurational entropy has the form

$$S^{II}(\text{config}) = -Nk_B\left[\ln\phi_b + \left(\frac{1-\phi_b}{\phi_b}\right)\ln(1-\phi_b)\right] \tag{3.30}$$

where ϕ_b is the volume fraction of liquid b and N is the number of droplets. Note that the form of Eq. (3.30) is similar to that for the configurational entropy of mixing of two liquids (or of polymer segments, Eq. 2.20). Since the bulk free energies G_a and G_b are unchanged by the dispersion process, the change in free energy upon formation of an emulsion is

$$\begin{aligned} \Delta G(\text{dispersion}) &= G_{ab}^{II} - G_{ab}^{I} - T\Delta S \\ &= \gamma_{ab}\Delta A - TS^{II}(\text{config}) \\ &\approx \gamma_{ab}A^{II} - TS^{II}(\text{config}) \end{aligned} \qquad (3.31)$$

where ΔA is the increase in surface area in the emulsion with respect to the undispersed system. The free energy change ΔG is usually positive for pure liquids, implying that an emulsion, once formed, is not thermodynamically stable although it may be kinetically stabilized.

The limiting value of γ_{ab} for which emulsification occurs is defined by $\Delta G = 0$, or

$$\gamma_{ab}(\text{crit}) = -\frac{k_B T}{4\pi r^2}\left[\ln\phi_b + \left(\frac{1-\phi_b}{\phi_b}\right)\ln(1-\phi_b)\right] \qquad (3.32)$$

where we have made use of the relationship $A^{II} = 4\pi r^2 N$, with r the average drop radius. In emulsions stabilized by surfactant, the interfacial tension is reduced compared to that between pure liquids. This then leads to a reduction in the free energy required to break up the emulsion. In many cases, the emulsion can form spontaneously since $\Delta G(\text{dispersion}) \leq 0$.

3.13.2 Microemulsions

Microemulsions are classified into two types: dispersed and bicontinuous (Fig. 3.16). Dispersed microemulsions consist of droplets stabilized by surfactant. Bicontinuous phases consist of continuous networks of water and oil, separated by amphiphilic membranes. Cosurfactant is usually, but not always, required to form a microemulsion. This cosurfactant is often an alcohol. When microemulsions are formed without cosurfactant, the resulting ternary system is a simple model for phase behaviour. Usually ternary phase diagrams (oil + water + surfactant) are plotted in a triangular representation as shown in Fig. 3.17. At each point in the phase diagram, the concentration of each species is determined by drawing a line parallel to the corresponding axis, lying along one edge of the triangle.
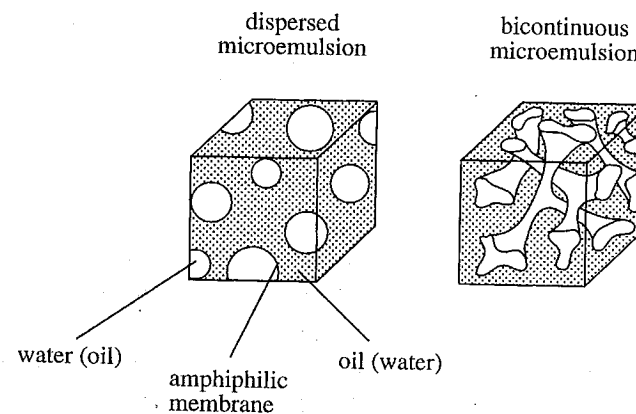
Figure 3.16 Dispersed and bicontinuous microemulsions

The stability of microemulsions is often described in terms of the spontaneous curvature of the surfactant interface. Spontaneous curvature of a surfactant monolayer results from the difference in area per head group compared to the area of the tail group. Bicontinuous microemulsions possess a spontaneous curvature, H_0, close to zero. In droplet microemulsions, in contrast $H_0 \neq 0$, being positive or negative depending on whether the interface is curved towards oil (o/w microemulsion) or towards water (w/o microemulsion) respectively. Because the spontaneous curvature is close to
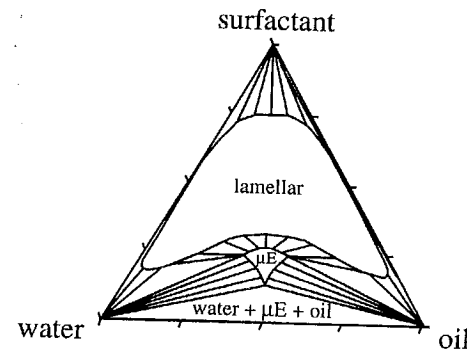

Figure 3.17 Schematic phase diagram of a ternary oil/water/surfactant system in which a microemulsion (μE) is formed at equal volume fractions of oil and water. A similar phase diagram is exhibited, for example, by the non-ionic surfactant $C_{12}E_5$ in water and tetradecane at $47.8°C$. The tie lines indicate the compositions of the equilibrium phases of the two-phase regions

zero, the formation of a bicontinuous microemulsion competes with the formation of a lamellar (layered) phase (Section 4.10.2).

Droplet microemulsions are widely used to solubilize compounds that are otherwise insoluble. They are usually of the oil-in-water type. The droplets can often be swollen with the 'oil', but only to a limited extent, without perturbing the microemulsion structure or leading to its break-up. If a large amount of oil is added to a spherical droplet, transformation to a phase of rod-like droplets or even planar lamellae is possible. Droplet microemulsions are the basis of floor and car waxes, hand cleaning gels for grease removal, flavour-release liquids and pesticide dispersions. Another important application is in tertiary oil recovery. Improved oil recovery compared to primary methods can be achieved by pumping water down an oil-well to displace oil, this being secondary oil recovery. In tertiary oil recovery, a surfactant microemulsion is driven via the injection well into the oil reservoir, where it can solubilize oil by lowering the water–oil interfacial tension. This surfactant 'slug' is backed up by a layer of polymer solution, to prevent backflow. Both polymer and surfactant are driven into the oil-well using water, and then recovered at the surface through a second bore-hole.

Microemulsions in equilibrium with excess oil or water are classified according to the scheme introduced by Winsor. These two-phase regions are sketched in Fig. 3.18. A Winsor I microemulsion is an oil-in-water system with excess oil, a Winsor II microemulsion is a water-in-oil system with excess water and a Winsor III microemulsion is a 'middle phase' system, with an excess of both water and oil. Winsor III microemulsions are thus used in tertiary oil recovery. Transitions between these phases formed using non-ionic surfactants can be controlled by variation of the HLB through temperature, whereas for ionic surfactants transitions can be driven by changing salt concentration. The temperature at which a microemulsion contains equal amounts of water and oil is termed the *phase inversion temperature* (PIT).
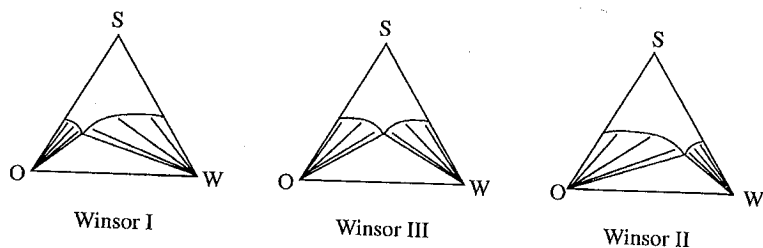
Figure 3.18 Schematic of ternary phase diagrams for Winsor microemulsions. In the left-hand shaded area, the microemulsion is in equilibrium with excess water, and in the right-hand shaded area, the microemulsion is in equilibrium with excess oil

3.14   FOOD COLLOIDS

Colloids in one form or another are constituents of many foods. Obviously we cannot consider comprehensively every kind of food colloid here, so instead we limit ourselves to a few important examples that illustrate the principal types of behaviour.

3.14.1   Milk

Milk is a classic food colloid, the constituents and structure having been extensively investigated. It is also an important foodstuff, being a complete nutrition provider for young mammals. It is basically an oil-in-water emulsion, stabilized by protein particles. Fresh unskimmed cow's milk typically contains 86 % water, 5 % lactose, 4 % fat, 4 % protein and 1 % salts. The milky appearance of milk is due to the presence of large colloidal particles called *casein micelles*. These have typical dimensions of about 100 nm, and so scatter light. Casein micelles are polydisperse associates of proteins bound together with 'colloidal' calcium phosphate. Casein 'micelles' are really misnamed. Whereas in surfactant micelles there is a dynamic equilibrium between molecules and closed micelles (Section 4.6.5), casein micelles are based on a structure that is practically irreversibly associated due to bridging by colloidal calcium phosphate. It is thought that these bridges link together smaller (10–20 nm) submicelles formed from casein proteins, as illustrated in Fig. 3.19. Evidence for this is provided by electron microscopy, which shows 'raspberry' particles, indicating an agglomerated structure within casein micelles. Casein micelles are very stable and can survive high temperatures
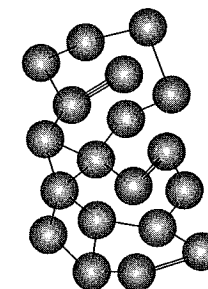

Figure 3.19 Model for the structure of a casein micelle. Casein protein subunits are linked by colloidal calcium phosphate to produce a raspberry-like structure

during pasteurization or the high shear rates experienced during homogenization. Thus it is possible to dry milk, and when rehydrated the particles are redispersed. The dispersion of casein micelles is thought to be stabilized by a combination of steric forces due to a layer of casein protein at the surface and electrostatic repulsive forces from negatively charged surface layers.

Casein micelles are dispersed in an aqueous phase that contains lactose, small ions and whey proteins. The fat in milk is present in globules (0.2–15 μm diameter) dispersed in the aqueous matrix and stabilized by a membrane of proteins and phospholipids at the oil–water interface. Milk fat is partially crystallized below 40°C.

Whipped cream is stabilized by interactions between aggregates of milk fat globules and air bubbles. It is an emulsion as well as a foam. Liquid fat that leaks out of broken globules forms a membrane holding together the remaining globules and hence the bubbles. However, this process must not be carried too far because if the membrane is disrupted or the liquid fat content is too high, churning into butter results. Usually 30–40 % fat is required to produce butter. The butter initially takes the form of dispersed buttermilk droplets but these 'grains' can be drained and then kneaded to form a butter pat. The structure of butter is quite complex. However, it is known that the fat phase is continuous and that this is comprised of a continuous structure of liquid fat containing domains of both fat crystals and solid fat globules (stabilized by adsorbed protein layers), many of the fat crystals being within the fat globules. Interdispersed in the continuous fat phase are water droplets and air cells.

Yoghurt and cheese are examples of colloidal gels formed from a network of aggregated casein micelles. Cheese is prepared by the addition of rennet, an enzyme that acts on the casein micelles and leads to clotting, i.e. to sedimentation into curds and whey. Yoghurt is made from milk coagulated by the addition of bacteria. Variation of pH or exposure to high temperature for prolonged periods can also cause the aggregation of casein micelles.

3.14.2   Proteins in Foods

Denaturation of a protein (by heating or variation in pH, for example) leads to the break-up of its secondary or tertiary structure (Section 2.5.4). Because secondary and tertiary structures are held together by weak forces from hydrogen bonds, ionic bonding or hydrophobic forces, unfolding of proteins can occur during denaturation. The proteins adopt a disorganized conformation instead of a compact one. Provided this is not achieved chemically, the native structure can usually be reformed from the denatured protein.

Denaturing of proteins is readily observed when an egg is cooked, as both the egg white and yolk change in consistency and colour. However, in this case, the denaturing is not reversible!

3.14.3   Surfactants in Foods

Surfactants are used in foods because of their surface-active properties. For example, they are used as emulsifiers because they can stabilize a liquid film by adsorbing at the air–liquid or oil–liquid interface. The partitioning is governed by the hydrophile–lipophile balance (HLB). For example, fatty acids are more soluble in oil phases and so have a low HLB whereas salts of fatty acids are more water soluble and have a high HLB.

3.14.4   Emulsifiers and Stabilizers

Many foods are complex emulsions; i.e. they contain dispersions of one liquid in another although other phases (such as air bubbles or ice crystals) may be present as well. As with surfactants, emulsions can be of the oil-in-water or water-in-oil type. A good example of an oil-in-water emulsion is mayonnaise, whereas margarine and low-fat spreads are water-in-oil emulsions (in these examples the emulsion is stabilized by additional components in the mixture, see below).

Many emulsions formed by mixing two liquids are unstable and liquid droplets can eventually coalesce together. Food emulsifiers are surface-active molecules that counteract this process. Foaming agents work in a similar way to prevent the collapse of a foam by coalescence of bubbles in it. Emulsifiers may be added surfactants or they may be proteins that are naturally present in the food. Typical examples of 'natural' emulsifiers include lecithin and monoglycerides. Lecithin, obtained from soybean or egg yolks, is primarily formed from phosphatidylcholine lipids (see Fig. 4.4). It has long been used as an emulsifier in margarine. Common man-made emulsifiers include sorbitan fatty acid esters ('Spans') and polyoxyethylene sorbitan esters ('Tweens') (see Fig. 4.3). The former have a low HLB and are oil soluble whereas the latter have a high HLB and are water soluble.

Emulsifiers and foaming agents act in two ways. First, they lower the surface tension and hence favour the formation of interfaces. Second, they stabilize droplets or bubbles mechanically by formation of a 'membrane' at the surface. In a similar manner, particulate matter can stabilize emulsions

and foams by selective accumulation at oil–water or air–water interfaces, as illustrated in Fig. 3.14 and discussed in the preceding section.

The term *emulsifier* is often used ambiguously or incorrectly in the food industry. In addition to its definition as a substance that promotes emulsion formation by interfacial action, it is also used to describe materials that promote the shelf-life of foods in other ways, or that simply change the texture or 'mouth-feel' of some foods.

Stabilizers impart long-term stability to food colloids. They can be distinguished from emulsifiers, because by definition they can only stabilize an emulsion that has already been formed. The most common stabilization mechanism in food colloids is the adsorption of proteins at the oil–water or air–water interface. Polysaccharides such as carrageenan or xanthan are common additives to foods that impart stability. Proteins are surface active due to hydrophobic amino acid residues distributed along the polypeptide chain. Thus a protein can act as an emulsifier as well as a stabilizer. In contrast, polysaccharides are not very surface active and so do not act as emulsifiers. The adsorbed layer (for example between oil and water) in food colloids contains both proteins and small-molecule surfactants, which may have been added as emulsifiers. In addition, polysaccharides may also be present if they have been added as stabilizers, although the interfacial concentration will be similar to that in bulk since they exhibit little preferential adsorption. An example of natural stabilization in a familiar food is provided by mayonnaise, in which particles of lipoprotein from egg yolks acts as a stabilizer by adsorbing at the oil–water interface, both as an adsorbed layer and in discrete droplets. The latter mechanism is an example of so-called Pickering stabilization, i.e. the selective adsorption of particulate material at the oil–water and air–water interfaces. Another example is in margarine which is stabilized by fat crystals.

3.14.5 Foams

Foams formed by liquids such as beer are very familiar. Although there are differences between countries, a stable head on beer is generally considered desirable, the optimal foam consisting of small, tight white bubbles. Beer foam has a high air content, so that the bubbles in freshly poured beer are polyhedral. A dry polyhedral foam can be deposited on the side of the glass as it is emptied, a process termed 'lacing' or 'cling'. The ethanol in beer is important to foam formation because it reduces the surface tension at the air–liquid interface, which leads to the formation of smaller air bubbles. However, too much ethanol is not good because the adsorption of ethanol

at the interface can compete with those of stabilizers such as proteins. This can cause the protein to aggregate in the bulk solution and ultimately to precipitate out.

Beer foam is not stable over long times due to liquid drainage and, ultimately, rupture (Section 3.12). The problem of stabilizing beer foam has attracted a lot of attention from the brewing industry. Natural glycoproteins and polypeptides formed from malt in beer act as stabilizers by adsorbing at the air–liquid interface. It is believed that the higher the molecular weight of the protein, the better it acts as a foaming agent. Artificial additives such as propylene glycol alginate are sometimes added because they can prevent foam collapse caused by lipids or surfactants. Lipids can be selectively adsorbed at the air–liquid interface but they do not act as stabilizers. In fact, some lipids from malt and yeast may be present in sufficient quantities to impair foam stability by reducing the surface tension. In addition, surfactants and lipids can be deposited in a beer glass as a result of incomplete cleaning, i.e. from lack of removal of washing-up liquid, or from bar snacks consumed by the drinker, or from lipstick marks left on the glass. It has recently been shown that use of nitrogen rather than carbon dioxide to form bubbles in beers leads to smaller bubble size and enhanced stability.

Foams are formed by whipping air into, for example, egg whites. The whites of hens' eggs are formed by a mixture of proteins that constitute albumen. Whipped egg whites on their own can be baked to form a meringue or can form a component of cake mixtures. A cake mixture is a complex multi-component system, being simultaneously a foam, an emulsion and a complex colloidal dispersion. Of the main components of a cake batter— egg, fat, flour and sugar—only the sugar is non-colloidal. The process of transformation of these ingredients into a cake (i.e. a solid foam) is not completely understood, although it is known that it is vital to retain the air bubbles, and the mechanisms associated with air bubble size and distribution have been investigated.

3.14.6 Ice-cream

Ice-cream deserves a special place in food colloids due to the range of colloidal phenomena that are involved in developing a satisfying, smooth texture. Ice-cream can be classified as an emulsion or as a colloidal dispersion (suspension) but also as a foam, since it is a soft solid containing air bubbles. Despite the best efforts of the manufacturers, the air content is usually not more than 50 % of the total volume, and the bubbles are spherical in contrast to those in beer. The fat in ice-cream is dispersed in an oil-in-water
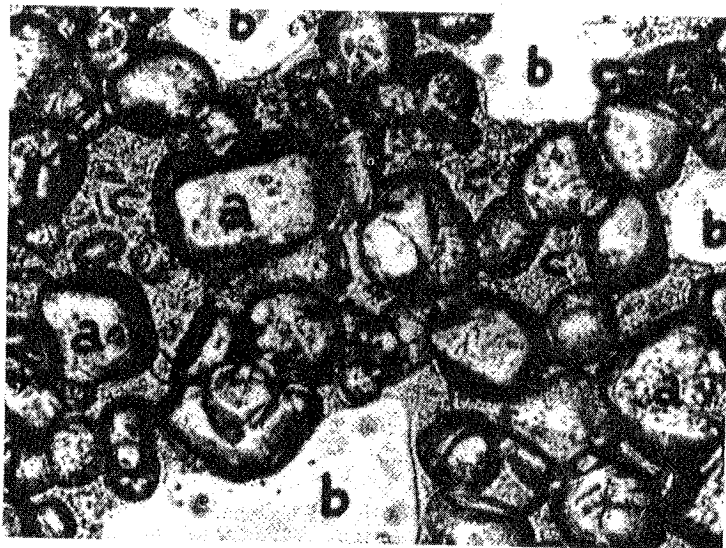
Figure 3.20 Typical structure of ice-cream revealed in an electron micrograph. (a) Ice crystals, average size 50 μm, (b) air cells, average size 100–200 μm, (c) unfrozen material. [From W. S. Arbuckle, *Ice Cream*, 2nd Edition, Avi Publishing Company (1972) with kind permission of Springer Science and Business Media]

emulsion, although the oil content is usually low. The fat content varies from country to country, and in some countries can be vegetable fat as well as, or instead of, milk fat. Ice-cream is prepared by mixing the ingredients, followed by pasteurization, homogenization, cooling, ageing, flavouring and hard freezing. The resulting structure is shown in Fig. 3.20. It contains small ice crystals (50 μm size) and air cells (about 100–200 μm) within a continuous matrix of unfrozen emulsion that is primarily sugared water. To produce ice-cream with a smooth texture, it is necessary to carefully control the size and aggregation of the ice crystals, the amount of air, the state of aggregation of fat globules and the viscosity of the aqueous phase. The desired size of fat globules (2 μm) is achieved during the homogenization process. The development of small ice crystals, which are small enough not to produce a 'gritty' texture, is achieved by careful control of the freezing process, during which mixing and aeration is also carried out. The freezing process is accompanied by an increase in concentration of sugar in the aqueous phase, as water is crystallized as ice. Stabilizers are sometimes added to inhibit the crystallization process and to impart a creamy texture. Ice–cream fat globules are naturally stabilized by adsorption of proteins or lipids to the oil–water interface. The proteins include casein in the form of molecules,

and also as complete micelles or micellar subunits. 'Emulsifiers' in ice-cream are not, then, primarily involved in stabilizing the emulsion, since this role is performed by the milk proteins. Instead, emulsifiers help to prevent the complete destabilization of the emulsion. This takes place during the aeration and freezing stage, when the emulsion is partly broken up to form a stable foam. The final process in ice-cream production is to freeze it at about −30°C for handling and packaging. Further ice crystallization occurs at this stage.

3.14.7 Gelatin

Gelatin is a good example of a network colloid. It is formed from denatured collagen in water. The triple-helix collagen biopolymers are crosslinked into a network. The crosslinking is non-covalent hydrogen bonding and ionic bonding. Thus the gelation process is thermoreversible, i.e. the network can be broken up by heating. In contrast, typical polysaccharide gels such as pectin are not thermoreversible. Gelatin can act as a protective colloid to prevent flocculation and coagulation by reinforcing an emulsion structure, and is used as such for example in ice-cream to reduce the formation of large ice crystals.

3.15 CONCENTRATED COLLOIDAL DISPERSIONS

Latex dispersions have attracted a great deal of interest as model colloid systems in addition to their industrial relevance in paints and adhesives. A latex dispersion is a colloidal sol formed by polymeric particles. They are easy to prepare by emulsion polymerization, and the result is a nearly monodisperse suspension of colloidal spheres. These particles usually comprise poly(methyl methacrylate) or poly(styrene) (Table 2.1). They can be modified in a controlled manner to produce charge-stabilized colloids or by grafting polymer chains on to the particles to create a sterically stabilized dispersion. Charge-stabilized latex particles obviously interact through Coulombic forces. However, sterically stabilized systems can effectively behave as hard spheres (Section 1.2). Despite its simplicity, the hard sphere model is found to work surprisingly well for sterically stabilized latexes.

Model hard sphere systems can be prepared from sterically stabilized latexes. One system that has been extensively studied is PMMA spheres, grafted with poly(12-hydroxystearic acid). Typically the cores are several hundred nm in diameter, whereas the grafted polymer layer is about 10 nm

thick. The PMMA spheres are prepared to be as monodisperse as possible, by careful control of the emulsion polymerization process. It is possible to achieve a polydispersity (standard deviation of the particle size distribution divided by the mean size) as low as 0.05 in this way. Care is taken to remove ions by dialysis so that Coulombic double-layer forces are minimized. In addition, the refractive index of the solvent is selected to match that of the PMMA. This reduces the effective Hamaker constant and hence long-range attractive van der Waals forces (Section 3.3.1). In addition, this index matching facilitates light scattering experiments (eliminating refraction effects), which along with neutron diffraction has been used to probe the structure of the dispersions. The hard sphere model had been studied through computer simulations before experiments on model sterically stabilized colloidal dispersions were performed. The hard sphere model is athermal; i.e. phase transitions as a function of temperature are not possible. There is no enthalpy associated with any of the transitions observed on increasing concentration; they are all driven by molecular packing entropy. The phase behaviour depends on the volume fraction of spheres, ϕ. At low volume fractions, the system is fluid (Fig. 3.21a). However, at $\phi = 0.494$, freezing to a crystalline solid (Fig. 3.21b) starts to occur. On the other hand, melting occurs when the volume fraction $\phi < 0.545$, so that in the range $0.494 < \phi < 0.545$, there is a coexistence of fluid and crystal. At larger volume fractions there is a tendency for glass formation because the viscosity of the system is so high that diffusion is restricted and particles cannot arrange into a crystal lattice. The transition between crystal and glass is kinetically controlled. The glass transition occurs at $\phi \approx 0.58$. This sequence of transitions obtained from computer simulations of the hard sphere model agrees well with those observed for sterically stabilized PMMA latex particles. To quantitatively map the experimental observations on to those for hard spheres, it is necessary

(a)   (b)
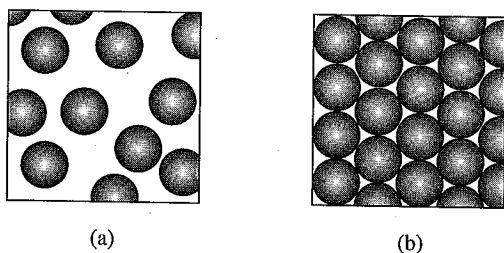
Figure 3.21 Order in latex sols: (a) fluid, at low particle volume fractions, (b) close-packed crystalline solid, at high particle volume fractions

to treat the colloid particles as effective hard spheres, by allowing for the volume occupied by the grafted chains as well as the core volume fraction. Using the core volume fraction alone, the transitions are observed at smaller values of the volume fraction than those for hard spheres.

The structure of model latex dispersions has been investigated using small-angle neutron scattering. From these measurements on the liquid phase it is possible to obtain the structure factor as a function of the wavenumber q (Eq. 1.25). The structure factor $S(q)$ can be inverted to obtain the radial distribution function, $g(r)$ (Eq. 1.29). The radial distribution function shows that long-range order develops in sterically stabilized colloidal dispersions as the volume fraction is increased, consistent with the approach towards crystalline order. In other words, $g(r)$ goes from a form characteristic of a liquid (see Fig. 5.9c) to that of a solid (see Fig. 5.9a). Crystalline order above the critical volume fraction $\phi = 0.494$ is manifested by the development of Bragg peaks in the small-angle neutron scattering pattern. The location of observed reflections indicates that the crystalline structure is usually close-packed cubic, specifically face-centred cubic or hexagonal close-packed. Colloidal dispersions can also be studied using small-angle light scattering. Whether this is more suitable than SANS depends on the size of the particles, the scattering contrast in the system as well as access to an appropriate instrument.

FURTHER READING

Dickinson, E., *An Introduction to Food Colloids*, Oxford University Press, Oxford (1992).
Everett, D. H., *Basic Principles of Colloid Science*, Royal Society of Chemistry, Cambridge (1988).
Fennell Evans, D. and H. Wennerström, *The Colloidal Domain. Where Physics, Chemistry, Biology and Technology Meet*, VCH, New York (1994).
Hunter, R. J., *Foundations of Colloid Science*, Oxford University Press, Oxford, Vol. I (1987) and Vol. II (1989).
Shaw, D. J., *Introduction to Colloid and Surface Chemistry*, 4th Edition, Butterworth–Heinemann, Oxford (1992).

QUESTIONS

3.1 Give an approximate expression for the fraction of molecules of length l in the surface layer of a cube of side d. Using this equation, determine

the fraction of silver bromide molecules (molar volume 30 cm^3 mol^{-1}) in a cube of length (a) 1 cm and (b) 10 nm.

3.2 Calculate the Debye screening length κ^{-1} at 25°C for (a) 0.01 M NaCl, (b) 10^{-4} M NaCl and (c) 0.01 M K$_2$SO$_4$. How does the Debye screening length depend on temperature?

3.3 The Hückel equation requires that $\kappa R \ll 1$. Calculate the concentration of monovalent electrolyte in water at 25°C required to satisfy $\kappa R = 0.1$, given that $R = 20$ nm.

3.4 Calculate the sedimentation velocity due to gravitational falling for colloidal particles of density 1.5 g dm^{-3} in water at 20°C when the particle size is (a) 1 nm and (b) 1 μm.

3.5 Colloids are often sedimented by centrifugation. The centripetal force experienced by a colloidal particle is $m(1 - v_0\rho)\omega^2 x$, where v_0 is the partial specific volume of the medium, ρ is the density and ω is the angular velocity. The opposing frictional force is given by Eq. (1.6) with $v = dx/dt$ the velocity at a distance x from the rotation axis. Use these relationships to derive an expression for the molar mass of the particle as a function of temperature, sedimentation coefficient $s = dx/dt/(\omega^2 x)$, diffusion coefficient, velocity and density.

3.6 The electrophoretic mobility of colloid particles was measured in a 0.01 M 1:1 salt solution and found to be $u = 4 \times 10^8$ m^2 s^{-1} V^{-1}. Calculate the zeta potential for particles of radius (a) 100 nm and (b) 1 nm.

3.7 Mica has a charge density of 0.32 C m^{-2}. According to the Gouy–Chapman equation, the charge density, σ, at a planar surface is related to surface potential via

$$\sigma = (8k_B T c_0 \varepsilon_r \varepsilon_0)^{1/2} \sinh\left(\frac{ze\Phi_0}{2k_B T}\right)$$

Calculate the surface potentials on mica for 1:1 aqueous salt solutions at concentrations of 10^{-2} M and 10^{-4} M (at 25°C).

3.8 The surface forces apparatus was used to measure the force between mica sheets when the gap was filled with the two salt solutions of Q. 3.7. Using the DLVO theory, plot the force versus separation curves in the form F/R versus h, assuming that the mica sheets are spherical charged surfaces of radius R. Use the Hamaker constant $A_H = 2.2 \times 10^{-20}$ J for the mica–water system.

3.9 The critical coagulation concentration (c.c.c.) for a suspension of colloidal particles in an electrolyte can be estimated from the DLVO theory. It is defined by the conditions $V = 0$ and $dV/dh = 0$, where

V is the total potential and h is the separation between particle surfaces. Use these conditions to obtain an expression for κ. By equating this to κ from the Debye–Hückel theory, derive Eq. (3.24) for the c.c.c.

3.10 A colloidal latex dispersion was sterically stabilized using polyoxyethylene. Calculate the molecular weight needed to achieve a steric stabilization layer of thickness equal to the Debye screening lengths in Q. 3.2(a) and (b). Assume a Gaussian chain conformation and a segment length $l = 0.56$ nm. How realistic is the assumption of a Gaussian conformation at low and high grafting densities?

3.11 (a) Show that in a diffusion process following Fick's law, the concentration of particles increases linearly with distance along the direction of diffusion. [Hint: rearrange Eq. (1.10) and integrate].
(b) Show that the concentration profile for a process obeying Fick's second law varies with time and distance according to the exponential function

$$c(x, t) = c_0 \left(\frac{1}{4\pi Dt}\right)^{1/2} \exp\left(\frac{-x^2}{4Dt}\right)$$

where c_0 is a constant.

3.12 The interfacial tension between water and hexane is 50 mN m^{-1} at 20°C. Show that it is not possible to prepare an emulsion for a 50:50 binary mixture. What critical surface tension would be required to form an emulsion of droplet size $r = 10$ nm? How could you achieve this surface tension in practice?

4

Amphiphiles

4.1 INTRODUCTION

Amphiphiles have a Jekyll and Hyde character. They are molecules with two sides to their nature. One part likes a solvent (i.e. is soluble in it) and the other does not. Although amphiphiles can self-assemble into ordered structures in organic solvents, here we consider aqueous solutions, unless explicitly stated otherwise. Amphiphilic molecules contain both a *hydrophilic* (water-loving) part and a *hydrophobic* (water-hating) part (usually a hydrocarbon chain).

The terms amphiphile and surfactant are often used interchangeably. The word *surfactant* originates from *surface-acti*ve agent. This points to a key property of surfactants: their tendency to segregate to an air-water interface and consequently to lower the surface tension compared to pure water. This is an important aspect of the use of surfactants in detergents. Surfactants belong to two broad classes. Ionic surfactants have an ionic hydrophilic head group attached to a hydrophobic tail, both cationic and anionic surfactants being widely used. In nonionic surfactants, the hydrophilic group is usually a short poly(oxyethylene) chain, attached to a hydrocarbon tail.

Natural amphiphiles are often lipids. In this chapter, we focus on polar lipids with an amphiphilic character, such as phospholipids (see the next section for examples). The latter, together with proteins, make up cell membranes that are formed from self-assembled bilayer structures. A key feature of amphiphilic membranes in biological systems is that they are ordered and yet fluid, allowing the transport of material across them. The properties of membranes are considered in Section 4.11 of this chapter.

The thermodynamic properties of amphiphiles in solution are controlled *by the tendency for the hydrophobic region to avoid contact with the water, which has been termed the hydrophobic effect.* This leads to the association of molecules into *micelles,* which are spherical or elongated structures in which the hydrophobic inner core is shielded from water by the surrounding *corona* formed from the hydrophilic ends of the molecules. These aggregates form by spontaneous self-assembly at sufficiently high concentrations of amphiphile, above a *critical micelle concentration.* The formation of micelles is predominantly an entropic effect, as deduced from comparisons of the contributions of the enthalpy and entropy to the Gibbs free energy of micellization. The enthalpic contribution results partly from the energetically favourable enhancement of interactions between the hydrocarbon chains. The entropic contribution arises from the local structuring of water due to hydrogen bonding (which results in a loose tetrahedral arrangement of H_2O molecules). Unassociated hydrocarbon chains break up the hydrogen bonds between water molecules and impose a locally more ordered structure that is entropically unfavourable. Because this disruption of water structure is reduced when micelles are formed, they are entropically favoured compared to unassociated molecules.

At high concentrations, amphiphiles can self-assemble into *lyotropic liquid crystalline* phases. As discussed in Chapter 5, a liquid crystalline phase is one that lacks the full three-dimensional translational order of molecules on a crystal lattice. Lyotropic refers to the fact that such phases are formed by amphiphiles as a function of concentration (as well as temperature). Lyotropic phases with one-dimensional translational order consisting of bilayers of amphiphiles separated by solvent are called lamellar phases. A two-dimensional structure is formed by the hexagonal packing of rod-like micelles. Cubic phases are formed by packing micelles into body-centred cubic or face-centred cubic arrays, for example. The bicontinuous cubic phases are more complex structures, where space is partitioned into two continuous labyrinths (usually a surfactant bilayer separating two congruent subvolumes of water).

The lamellar lyotropic liquid crystal phase is often formed in detergent solutions. When subjected to shear lamellae can, under certain conditions, curve into closed shell structures called vesicles (Section 4.11.4). These are used in pharmaceutical and cosmetic products to deliver molecules packed into the core. Selective solubilization in micelles finds similar applications, although micelles tend to break down more rapidly than vesicles when diluted. Applications for hexagonal and cubic structures may stem from the recent discovery that they can act as templates for inorganic materials such as silica, which can be patterned into an ordered structure with a regular array of nm-sized pores. This is useful for catalysis and molecular separation technologies.

This chapter is organized as follows. Examples of different types of amphiphiles are introduced in Section 4.2. Because surfactants are the basis of the enormous detergent industry, their surface activity is considered in some detail in Section 4.3. The structural properties of adsorbed surfactant films are considered in Section 4.4. In Section 4.5, we proceed to a discussion of the adsorption of surfactants on to a solid. Micellization and the definition of the critical micelle concentration are considered in depth in Section 4.6. This leads on to the technologically important subjects of detergency in Section 4.7 and solubilization in micelles in Section 4.8. The tendency for amphiphiles to aggregate into structures with distinct packings and interfacial curvatures at high concentrations is analysed quantitatively in Section 4.9. This leads to a discussion of lyotropic liquid crystal phase formation in Section 4.10. Membrane phases and vesicles are biologically important structures resulting from bilayer formation, and are the subject of Section 4.11. Finally, Section 4.12 focuses on a direct application for lyotropic liquid crystal phases: the templating of inorganic minerals.

4.2 TYPES OF AMPHIPHILE

Much of the early work on amphiphiles was undertaken on soaps and lipids based on fatty acids, and the corresponding non-systematic chemical names of these parent compounds and their derivatives are still commonly encountered. For convenience, Table 4.1 lists the systematic and trivial names of fatty acids, along with their structures. The names of derivatives are based on these; for example sodium dodecyl sulphate is (still!) sometimes referred to as sodium lauryl sulphate. Other non-systematic names also exist to cause further confusion! For example, hexadecyl (C_{16} chain) compounds are often termed 'cetyl' derivatives. The use of the term 'fatty' here and elsewhere is used to indicate an alkyl chain with 12 or more carbon atoms, i.e. a hydrocarbon that forms fats.

In the following, we give examples of typical amphiphiles. The term surfactant is used somewhat interchangeably with amphiphile, although surfactant is usually implied in this book to mean a man-made substance, as opposed to a biological lipid. This convention is not, however, universal.

Ionic surfactants may be of two types: *anionic* having a negatively charged head group and *cationic* having a positively charged head group. Common types of anionic surfactants are shown in Fig. 4.1. A good example is sodium dodecyl sulphate (SDS) (based on Fig. 4.1, top). The chemical formulae of

Table 4.1 Fatty acid nomenclature

Number of C atoms	Common name of acid	Systematic name of acid	Structure
Saturated fatty acids			
12	Lauric	Dodecanoic	$CH_3(CH_2)_{10}COOH$
14	Myristic	Tetradecanoic	$CH_3(CH_2)_{12}COOH$
16	Palmitic	Hexadecanoic	$CH_3(CH_2)_{14}COOH$
18	Stearic	Octadecanoic	$CH_3(CH_2)_{16}COOH$
20	Arachidic	Eicosanoic	$CH_3(CH_2)_{18}COOH$
22	Behenic	Docosanoic	$CH_3(CH_2)_{20}COOH$
24	Lignoceric	Tetracosanoic	$CH_3(CH_2)_{22}COOH$
Unsaturated fatty acids			
16	Palmitoleic	9-Hexadecenoic	$CH_3(CH_2)_5CH=CH(CH_2)_7COOH$
18	Oleic	9-Octadecenoic	$CH_3(CH_2)_7CH=(CH_2)_7COOH$
18	Linoleic	9,12-Octadecadienoic	$CH_3(CH_2)_4CH=(CH_2)_2(CH_2)_6COOH$
18	α-Linolelic	9,12,15-Octadecatrienoic	$CH_3CH_2(CH=CHCH_2)_3(CH_2)_6COOH$
18	γ-Linoleic	6,9,12-Octadecatrienoic	$CH_3(CH_2)_4(CH=CHCH_2)_3(CH_2)_3COOH$
20	Arachidonic	5,8,11,14-Eicosatetraenoic	$CH_3(CH_2)_4(CH=CHCH_2)_4(CH_2)_3COOH$
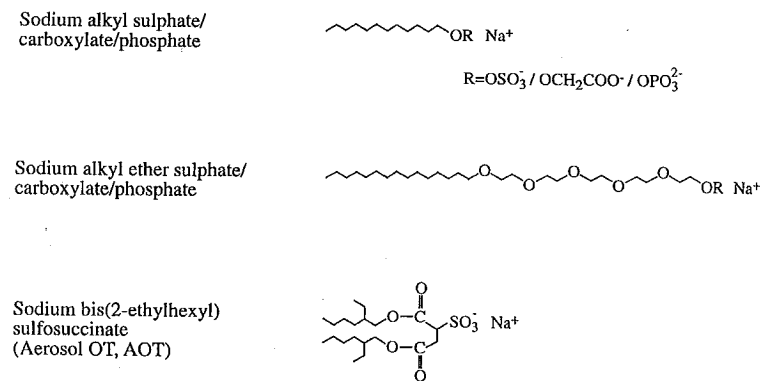
Figure 4.1 Typical anionic surfactants

typical cationic surfactants are shown in Fig. 4.2. As can be seen, the head group is often based around a quaternary ammonium ion—hence the common name of 'quat'. A good example of a cationic surfactant is the 'quat' didecyldimethylammonium bromide (often abbreviated DDAB). Cationics based on amines are also common. Among synthetic surfactants, anionics are the most widely produced, cationics being made in much smaller quantities. One reason for the lower usage of cationics is their higher aquatic toxicity compared to other types. Generally, ionic surfactants are sensitive
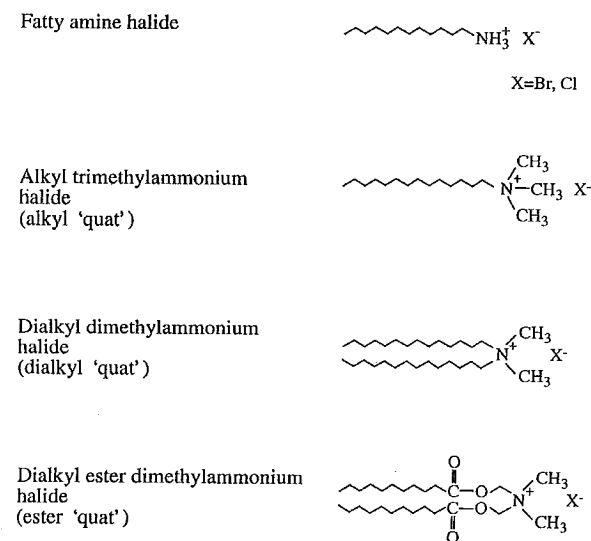
Figure 4.2 Typical cationic surfactants

to the presence of ions in hard water. In addition, cationic and ionic surfactants are generally not mutually compatible, although there are important exceptions.

Zwitterionic surfactants contain both positive and negative charges in the head group. Usually the positive charge is associated with an ammonium group and the negative charge is often a carboxylate. Zwitterionic surfactants are used in cosmetic products, since they have been found to be non-irritants for skin and eyes. The sphingomyelin lipid shown later in Fig. 4.4 is an example of a zwitterionic surfactant. *Amphoteric* surfactants can be either cationic, zwitterionic or anionic, depending on pH. They can be distinguished from zwitterionic surfactants because they pass from cationic to anionic form on increasing pH, with the zwitterionic form only being stable in a certain pH range.

Typical *nonionic* surfactant structures are shown in Fig. 4.3, along with some common names. The hydrophilic group of nonionic surfactants is usually a polyether chain, and more rarely a polyhydroxyl chain. The hydrophobic tail is often simply an alkyl chain. The fatty alcohol ethoxylates (also known as polyoxyethylene glycol monoethers) are a particularly important class that is widely used and extensively studied. They are abbreviated to C_mE_n, where C stands for methyl and E for oxyethylene and the subscripts
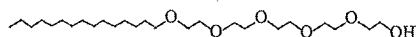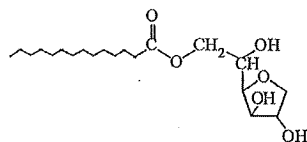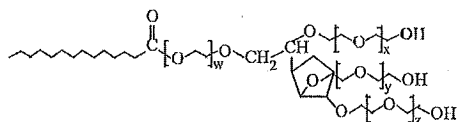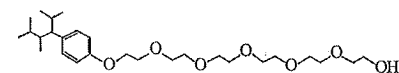
Figure 4.3   Typical nonionic surfactants

denote the number of repeats. The term polyoxyethylene needs to be used cautiously, since usually n is not much more than 12, i.e. they are oligomeric chains rather than polymeric ones. Nonionic surfactant production is approaching that of anionic surfactants, with a growth curve that is increasing faster. Nonionic surfactants are not sensitive to hard water and are usually compatible with other types of surfactant.

Lipids are defined as substances of biological origin that are soluble in organic solvents but only sparingly soluble or insoluble in water. They exhibit amphiphilic behaviour. Examples of lipid structures are shown in Fig. 4.4. Fatty acid salts (which are rarely encountered in pure form in nature) have only a single alkyl chain, but it is common for lipids to contain two or more hydrocarbon tails. For example, phospholipids are built from a phosphate head group and a double tail of hydrophobic alkyl chains. These structural units are linked by a glycerol group which provides two arms for attachment of the hydrocarbon chains. This class of amphiphile is thus more accurately a class of the hydrocarbon chains.

Figure 4.4   Typical lipids

termed glycerophospholipids. These are the major lipid component of cell membranes, the group of phosphatidylcholine (Fig. 4.4) found in cells also being known as lecithins.
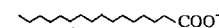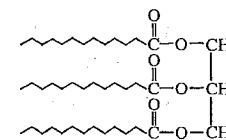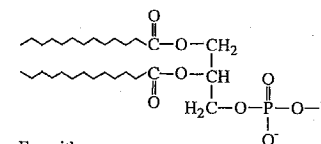
Sphingolipids are derivatives of amino alcohols with hydrocarbon chains containing 16–20 carbon atoms. An example of the most common type of sphingolipid, termed a sphingomyelin, is shown in Fig. 4.4. This type of sphingolipid contains a phosphatidylcholine or phosphatidylethanolamine head group, similar to the phospholipids shown in Fig. 4.4. The sheath-like membrane surrounding nerve cells is rich in sphingomyelin lipids. Other types of sphingolipid such as cerebrosides and gangliosides are important components of brain cell membranes.

4.3   SURFACE ACTIVITY

4.3.1   Surface Tension

The defining characteristic of surfactants is their ability to lower surface tension at the air-water interface. Surface tension results from an imbalance in intermolecular forces at the surface of a liquid. There are fewer molecules on the vapour side than on the liquid side of molecules near the surface, leading to a net repulsive force and hence a gradual decrease in density (Fig. 4.5). Surface tension, γ, can be defined in two equivalent ways. First, in terms of
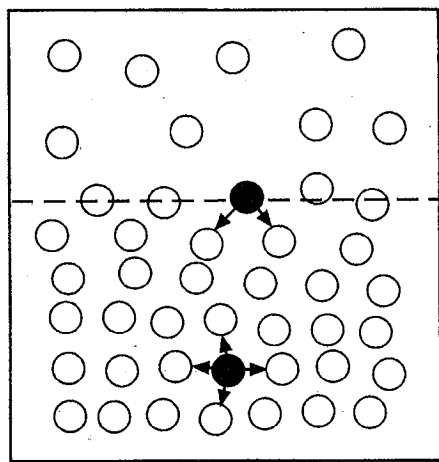
Figure 4.5   Surface tension arises from the imbalance of forces on molecules at the liquid–gas interface
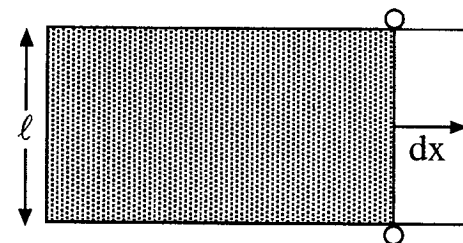
Figure 4.6   Stretching a soap film suspended on a wire frame by moving a slider through a distance dx

the work done to create an area ΔA of surface:

$$w = \gamma \Delta A \qquad (4.1)$$

Alternatively, surface tension is given by the force per unit length associated with this process. The equivalence of these two definitions can be readily confirmed by a simple example. Consider a liquid film (such as soap film) suspended on a wire frame, which is stretched by moving a slider (Fig. 4.6). The surface tension is the force per unit length, $\gamma = F/(2l)$, where the factor of two arises because the film has two sides. Then the work done for an infinitesimal extension dx is

$$dw = F\,dx = \gamma 2l\,dx = \gamma\,dA \qquad (4.2)$$

These equivalent definitions imply that surface tension can be expressed either in units of $mJ\,m^{-2}$, or more commonly in $mN\,m^{-1}$. The latter convention will be adopted in the remainder of this chapter.

Surface tension can be measured in many ways. One of the most accurate and conceptually simple methods is to measure the rise of a liquid in a capillary (Fig. 4.7a). The surface tension is related to the height of liquid supported by gravity, the tube radius, the contact angle of the liquid meniscus and the density difference between liquid and vapour. The determination of surface tension using this *capillary rise* method is easiest when the liquid completely wets the capillary wall, i.e. when the contact angle (Section 4.5.1) is near zero.

Another conceptually simple method is to weigh falling drops of a liquid. The surface tension of drops at the point of detachment from a vertically mounted tube is proportional to their weight. Care has to be taken to make

(a)   (b)

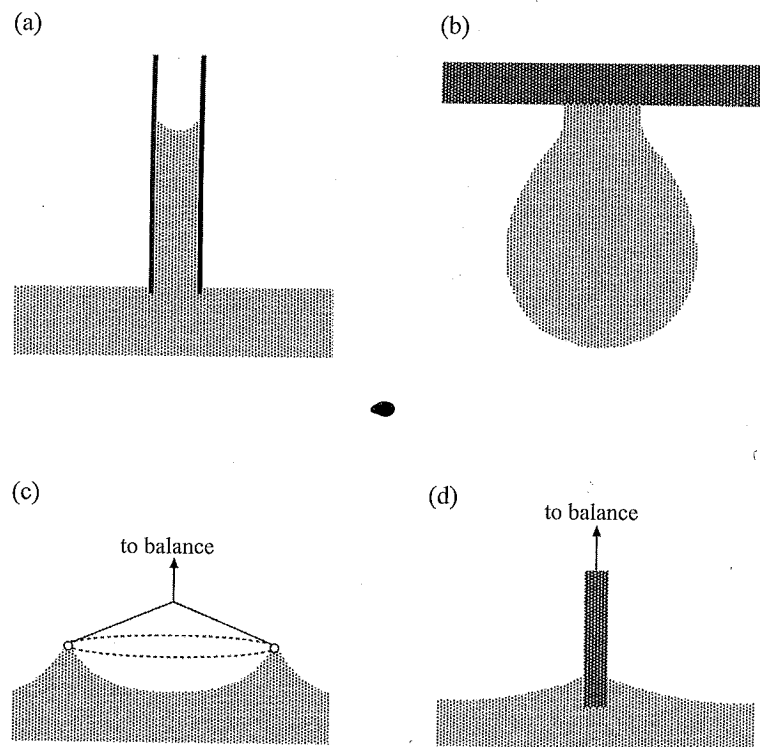(c)   (d)

Figure 4.7   Methods for measuring surface tension: (a) capillary rise, (b) pendant drop, (c) du Noüy ring, (d) Wilhelmy plate

sure that the tip of the tube is smooth and free of nicks; otherwise the shape of the falling droplet is distorted. A method related to this, but involving a more complex analysis, is to measure the shape of a *pendant droplet* (Fig. 4.7b). This is suitable for determining the surface tension of a system that is slow to reach its equilibrium value; for example a viscous polymer solution can take hours to reach its equilibrium surface tension. In the pendant drop method the shape of the suspended droplet is compared to theoretical profiles, which can be calculated by balancing the hydrostatic (gravitational) force and the surface tension. The symmetrical situation of sessile droplets (created by deposition on to a horizontal solid) can be analysed in a similar way. Pendant or sessile bubbles can obviously also be treated in an analogous fashion.

The most common methods used to measure surface tension of surfactant solutions using commercial instruments are the *du Noüy ring* and *Wilhelmy plate* techniques (Fig. 4.7c and d). In the former, the force necessary to detach a ring or wire loop from a liquid surface is measured (for example using

a balance). This detachment force is proportional to surface tension. The Wilhelmy plate method works similarly, in the detachment mode. Here, a glass plate or slide is pulled from the surface. The weight of the meniscus formed is measured with a force balance, and is equal to the vertical component of the surface tension. In practice, the Wilhelmy plate method usually works in reverse, i.e. the slide is immersed in the liquid by raising the liquid and the corresponding change in weight due to the meniscus is measured. Both Du Noüy and Wilhelmy plate methods work best when the liquid wets the immersed solid (i.e. ring or plate).

All of the above methods involve measurements of the essentially equilibrium surface tension. Often it is desirable to measure a dynamic surface tension, to probe changes in surface tension at short times (for example during a mixing process). It is possible to measure surface tensions on time-scales down to a few milliseconds in several ways. One example is the oscillating jet method. A jet of liquid emerging from a non-circular nozzle is unstable and oscillates about its preferred circular cross-section. The wavelength of the oscillations in the liquid stream and the flow rate can be used to obtain the surface tension. The dynamic surface tension can also be obtained using the maximum bubble pressure method. Here, air is continuously blown through two capillaries with different diameters dipped into a liquid. The pressure required to form a bubble is inversely proportional to the capillary diameter and directly proportional to the surface tension of the liquid. The use of two capillaries means that the dependence on capillary diameter can be eliminated.

4.3.2   Interfacial Tension

Interfacial tension is defined as the surface free energy for the interface between two immiscible liquids. As with surface tension, it results from an imbalance in intermolecular forces across the interface. It has the same units as surface tension, conventionally mN m^{-1}. Surfactants are very effective at reducing the interfacial tension between water and organic solvents, and this is one of the mechanisms by which they act as detergents (see Section 4.7). The difference between the surface tensions of the two liquids (γ_α, γ_β) and the interfacial tension between them ($\gamma_{\alpha\beta}$) defines the work of adhesion (Fig. 4.8a):

$$w_{\alpha\beta} = \gamma_\alpha + \gamma_\beta - \gamma_{\alpha\beta} \qquad (4.3)$$

Note that the surface tensions refer to the liquid–vapour interface. For pure liquids, the work of cohesion is defined as the work required to pull apart
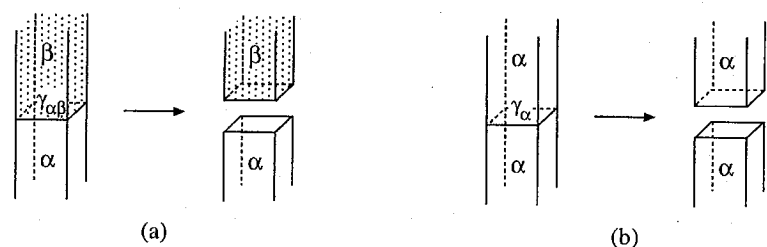
Figure 4.8 (a) Work of adhesion is associated with the creation of surfaces for two different liquids and the destruction of the interface between them (b) Work of cohesion is associated with the creation of two surfaces of the same liquid

a volume of unit cross-sectional area (Fig. 4.8b):

$$w_{\alpha\alpha} = 2\gamma_\alpha \qquad (4.4)$$

The work of cohesion and the work of adhesion are both defined for a reversible process. Surface tension can be interpreted as half of the work of cohesion.

Several of the methods used to measure surface tension can also be exploited to measure interfacial tension. Both du Noüy ring and Wilhelmy plate surface tensiometers can be used with the ring or plate placed at the liquid–liquid interface. The drop weight method can also be applied with drops of one liquid falling into another. If the density of the two liquids is equal and the drops are small enough, then they will usually be spherical. For large droplets, gravitational effects proportional to volume can outweigh surface tension forces proportional to area, and the droplet shape can then be analysed by pendant or sessile drop methods. The spinning drop tensiometer is an extension of this method which can be used to measure very low interfacial tensions. Here a capillary filled with droplets of one liquid in another is positioned horizontally and rotated around its axis. The surface tension can be obtained by analysing the shape and radius of the distorted droplets as a function of rotation speed.

When a drop of liquid is placed on another with which it is immiscible, its wetting is quantified by a *spreading coefficient*. Consider, for example, the wetting of an oil on water. The oil can form a lens that does not spread. Alternatively, it can spread into a thin film, the thickness of which is uniform over the surface, this being termed a 'duplex' film if it has two independent interfaces with well-defined surface tensions. Finally, it can form a thin film coexisting with excess liquid in droplets. Which process occurs depends on the spreading coefficient, which is the difference between the work of

adhesion of oil on water (w_{ow}) and the work of cohesion of the oil (w_{oo}):

$$S = w_{ow} - w_{oo} \qquad (4.5)$$

Here, S is termed the spreading coefficient. A more convenient definition of S is in terms of measurable interfacial tensions:

$$S = \gamma_{wa} - (\gamma_{oa} + \gamma_{ow}) \qquad (4.6)$$

i.e. S is the difference in the surface tension of the air–water interface, γ_{wa}, and that of oil at the air–water interface, with contributions from the oil–air and oil–water interfacial tensions, γ_{oa} and γ_{ow} respectively. For the initial spreading of one liquid on another, S must be greater than or equal to zero. We have been careful here to specify an initial spreading coefficient, because this may change due to the mutual saturation of one liquid with another that may occur after the initial spreading, due to a finite solubility. For example, the initial spreading coefficient for benzene on water is

$$S = 72.8 - (28.9 + 35.0) = 8.9\,\mathrm{mNm^{-1}}$$

where $\gamma_{wa} = 72.8$ mN m^{-1} is the surface tension of pure water. Because $S > 0$, spreading occurs. However, benzene is partially soluble in water and acts to measurably reduce the surface tension, so that the equilibrium spreading coefficient is

$$S = 62.4 - (28.9 + 35.0) = -1.5\,\mathrm{mNm^{-1}}$$

Because $S < 0$, the initial spreading stops and the benzene film retracts to form lenses.

4.4   SURFACTANT MONOLAYERS AND LANGMUIR–BLODGETT FILMS

Many insoluble substances such as long chain fatty acids, alcohols and surfactants can be spread from a solvent on to water to form a film that is one molecule thick, called a *monolayer*. The hydrophilic groups (for example —COOH or —OH) point into the water, whereas the hydrophobic tails avoid it.

The molecules in a monolayer can be arranged in a number of ways, especially when they are closely packed, depending on the lateral forces between them. This can be probed using a variety of physical methods. A
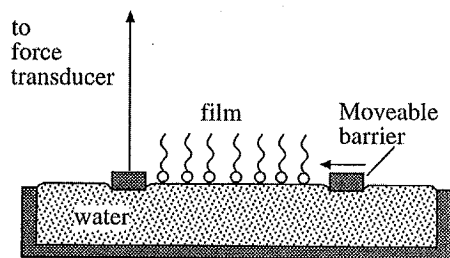
Figure 4.9 Schematic of a Langmuir trough

number of two-dimensional phases exist analogous to three-dimensional phases in bulk solids.

One of the main methods used to study monolayers is surface pressure–area isotherms. Surface pressure is the reduction in surface tension due to the presence of the monolayer:

$$\pi = \gamma_0 - \gamma \qquad (4.7)$$

i.e. it is the pressure that opposes the normal contracting tension of the bare interface. Surface pressure–area isotherms are often measured for films compressed using a Langmuir trough (Fig. 4.9). The insoluble substance is spread from a volatile solvent to ensure a uniform monolayer and the area of the monolayer is controlled through a moveable barrier. The horizontal force necessary to maintain the float at a fixed position is measured using a torsion balance and this provides the surface tension. Since only micrograms of material are present in monolayers, it is necessary to ensure that the water is as pure as possible, such that impurities are kept below the p.p.b. level. It is also important to clean the water surface prior to deposition of a monolayer to remove any airborne particles.

A commonly used alternative to the Langmuir film balance method of determining surface pressure is to measure surface tension using a Wilhelmy plate (Section 4.3.1), dipped into the monolayer at different stages of compression.

The shape of the surface pressure–area isotherm depends on the lateral interactions between molecules. This in turn depends on molecular packing which is influenced by factors such as the size of head group, the presence of polar groups, the number of hydrocarbon chains and their conformation (straight or bent). Here we focus on two fatty acids with different chain lengths and consider the structures formed in monolayers at different surface pressures as a function of the area per molecule.
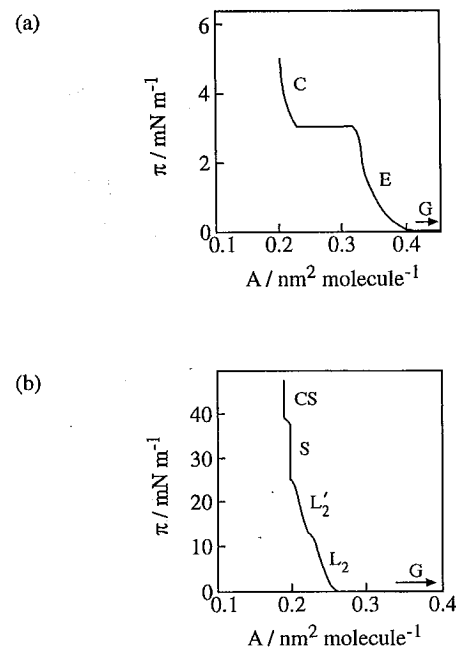
Figure 4.10 Surface pressure–area isotherms: (a) n-hexadecanoic acid on a subphase of 0.01 M HCl at 30 °C [data from N. R. Pallas and B. A. Pethica, Langmuir, 1, 509 (1985)]; (b) n-docosanoic acid on a subphase of 0.01 M HCl [data from E. Stenhagen in Determination of Organic Structures by Physical Methods, E. A. Braunde and F. C. Nachod (Eds.), Academic Press, New York (1955)]

A surface pressure–area isotherm for a monolayer of n-hexadecanoic acid is shown in Fig. 4.10a. At large film areas, a two-dimensional gaseous (G) phase is formed. The average area per molecule is large, although locally they tend to cluster into small islands or clumps. The isotherm satisfies a two-dimensional version of the ideal gas equation (Eq. 4.33), as discussed further in Section 4.6.3. As the film is compressed, a transition occurs to an expanded (E) phase, across which there is a plateau in surface pressure. In the expanded phase, the area per molecule is smaller than that in the G phase, but still significantly greater than that of a close-packed molecule. Upon further reduction of film area, a transition occurs when the area per molecule is close to 0.2 nm². The surface pressure then rises steeply, signalling the formation of a two-dimensional condensed (C) phase. The transition occurs when the area per molecule is approximately equal to that of a close-packed fatty acid chain.

Considering monolayers on a dilute acid subphase, increasing the chain length of a fatty acid enhances the tendency for formation of condensed
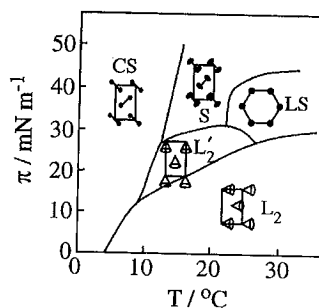
Figure 4.11 Phase diagram in terms of surface pressure versus temperature for *n*-docosanoic acid monolayers [Data from R. M. Kenn *et al.*, *J. Phys. Chem.*, 95, 2092, Copyright (1991) American Chemical Society]. The cones indicate the direction of molecular tilt

phases. Indeed, *n*-docosanoic undergoes a direct transition from the gas phase to a condensed phase (here specifically identified as L_2, Fig. 4.11) without an intermediate expanded phase (Fig. 4.10b). Several further condensed phases (L'_2, S, CS, Fig. 4.11) are formed at lower film areas. The formation of distinct condensed phases (depending on temperature as well as surface pressure) is also characteristic of surfactant and lipid monolayers. Condensed phases have a range of structures that are two-dimensional liquid crystal or crystal phases with different packings (hexagonal or rectangular) and molecular tilts. A representative phase diagram for *n*-docosanoic acid (Fig. 4.11) shows some of the structures. This illustrates the range of temperature over which condensed phases formed at a given surface pressure are stable. Although amphiphiles form lyotropic liquid crystal phases in the bulk, these two-dimensional phases are in fact analogues of thermotropic smectic liquid crystal phases (Section 5.2.2). This is because it is the packing of molecules that determines the symmetry of the structure and not that of molecular aggregates such as micelles or lamellae.

It is possible to build up multilayers by successive deposition of monolayer films on to a solid substrate. This is termed the Langmuir–Blodgett technique and the films are called Langmuir–Blodgett (or LB) films. They are of great interest because it is possible to construct multilayer stacks one layer at a time, with controlled alternation in the molecular orientation. By use of suitable molecules (for example porphyrins, phthalocyanines and charge-transfer complexes), the in-plane electrical conductivity can be made large enough for the multilayer to be an organic semiconductor. These are used in molecular electronic devices such as gas sensors and diodes. Alternatively, LB multilayers of non-conducting molecules such as fatty acids or polymers can be deposited on inorganic

materials to form insulating layers in semiconductor devices such as transistors. Another application exploits the ability to build multilayers of non-centrosymmetric molecules to produce films exhibiting non-linear optical behaviour.

To be deposited successfully on a solid substrate in an LB film, a monolayer should be in a condensed phase. The most common deposition mode is termed Y-type. Here a monolayer is picked up on a hydrophilic substrate (often glass) as it is pulled from the monolayer. The hydrophilic head groups attach on to the substrate, leaving a surface that is now covered by hydrophobic chains. The substrate plus monolayer is then dipped back into the film, picking up a monolayer in the reverse orientation. The resulting LB film is thus a stack of bilayers (Fig. 4.12). It is sometimes observed that deposition only occurs on the upstroke. Then monolayers are deposited with the same orientation each time, leading to a Z-type film (Fig. 4.12). In contrast, if monolayers are only deposited on the downstroke, the result is an X-type film (Fig. 4.12). Of course, it is possible to build up multilayers of different molecules by alternating the deposition sequence, for example by Z-type deposition on the upstroke through a monolayer of A followed by a downstroke through a monolayer of B (X-type deposition).

4.5   ADSORPTION AT SOLID INTERFACES

Adsorption of surfactants on to solid surfaces is important in many of their applications, for example in detergency, when a dirt particle is surrounded by adsorbed surfactant molecules. It is also crucial to the solubilization of solid materials, for example latex and pigment particles in paints.

4.5.1   Wetting and the Contact Angle

If a liquid is placed on a solid, it may either spread so as to completely wet the substrate or de-wet to form droplets with a finite contact angle. The contact angle is the angle between the substrate surface and a tangent drawn to the liquid surface at the point of contact with the solid (Fig. 4.13). The equilibrium state results from a balance of three interfacial tensions. The solid/vapour surface tension γ_{sv} is balanced by the sum of the solid/liquid interfacial tension and a component of the liquid/vapour surface tension resolved parallel to the substrate, $\gamma_{lv} \cos \theta$:

$$\gamma_{sv} = \gamma_{sl} + \gamma_{lv} \cos \theta \qquad (4.8)$$
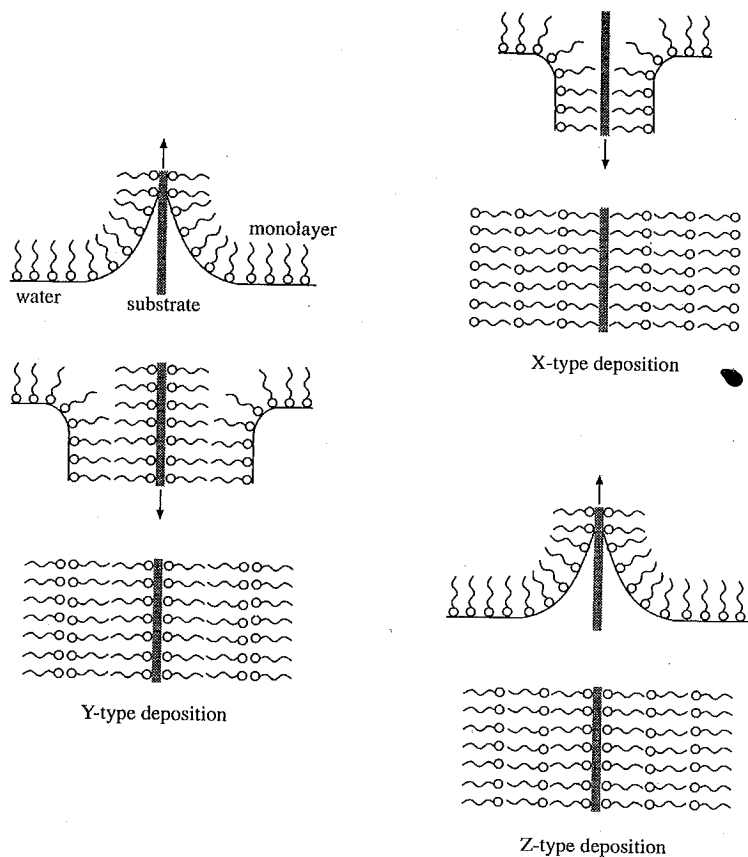
Figure 4.12   Deposition on to a hydrophilic substrate to form Langmuir–Blodgett films. Y-type deposition: a monolayer is deposited on the upstroke and downstroke. X-type deposition: a monolayer is only deposited on the downstroke. Z-type deposition: a monolayer is only deposited on the upstroke
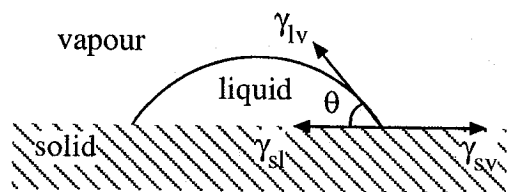

Figure 4.13   The contact angle, θ, of a liquid on a solid results from a balance of interfacial tensions

This is known as the Young equation, which can be used to determine the interfacial tension γ_{sl} from contact angle measurements, if γ_{sv} and γ_{lv} are measured separately. A liquid with a zero contact angle on a given solid will spread to completely wet that substrate. Liquids with contact angles $0 < \theta < 90°$ de-wet the solid surface to form droplets. Droplets of a liquid with a contact angle $\theta > 90°$ on a given solid will move easily about on the surface. An example is mercury droplets on most solid substrates. Another important consequence of a large contact angle is that such a liquid cannot enter a capillary made of the solid.

4.5.2   Langmuir Adsorption Equation

The adsorption of amphiphiles from solution on to a solid surface is described by the Langmuir adsorption equation. It is sometimes known as the Langmuir isotherm, since it refers to adsorption as a function of concentration (or pressure, when dealing with gases) at constant temperature. The Langmuir adsorption equation assumes that the surface is homogeneous, adsorption cannot occur beyond monolayer coverage, and all adsorption sites are equivalent. In addition, the equation applies to dilute solutions where there are no surfactant–surfactant or surfactant–solvent interactions.

The Langmuir adsorption equation provides an expression for the fractional adsorbed amount (surface coverage), Θ, as a function of surfactant concentration, c. It can be derived from the rates of adsorption and desorption, which are equal at equilibrium. The adsorption rate is

$$\frac{d\Theta}{dt} = k_a c (1 - \Theta) \qquad (4.9)$$

where k_a is the rate constant for adsorption. Similarly, the rate of desorption is given by

$$\frac{d\Theta}{dt} = k_d \Theta \qquad (4.10)$$

where k_d is the rate constant for desorption. At equilibrium, the adsorption and desorption rates are the same, and the surface coverage is

$$\Theta = \frac{Kc}{1 + Kc} \qquad (4.11)$$

where $K = k_a/k_d$ is the equilibrium constant. In the limit of large K or c, $\Theta \approx 1$, and the surface is saturated with surfactant. In the other limit, at very low solution concentrations, $\Theta = Kc$, i.e. the coverage is proportional to concentration. Writing the coverage as

$$\Theta = \frac{\Gamma}{\Gamma_{max}} \qquad (4.12)$$

where Γ is the adsorbed amount and Γ_{max} is the adsorption at full coverage (obtained above the critical micelle concentration, Section 4.6.1), we obtain

$$\frac{1}{\Gamma} = \frac{1}{\Gamma_{max}} + \frac{1}{Kc\,\Gamma_{max}} \qquad (4.13)$$

Thus, a plot of $1/\Gamma$ versus $1/c$ provides Γ_{max} and K. This is therefore the most convenient representation of the Langmuir isotherm. From the value of K obtained, it is possible to determine the Gibbs energy of adsorption, ΔG_{ads}, via

$$\Delta G_{ads} = -RT \ln K \qquad (4.14)$$

4.6 MICELLIZATION AND THE CRITICAL MICELLE CONCENTRATION

4.6.1 Definition of the Critical Micelle Concentration

The hydrophilic–hydrophobic nature of amphiphilic molecules leads to their self-assembly into a variety of structures in aqueous solution, as will be discussed further in Section 4.10.2. Micelles are one of the main types of structure formed by the association of amphiphiles. They consist of a core of hydrophobic chains (often alkyl chains) shielded from contact with water by hydrophilic head groups, which may be ionic or nonionic. The hydrophilic units of surfactants form a micellar corona. Micelles can either be spherical or extended into an ellipsoidal or rod-like shape. This depends on the packing of the molecules, as discussed further in Section 4.10.1. In this section we consider spherical micelles, since these are usually the type formed at the critical micelle concentration. A spherical micelle is sketched in Fig. 4.14. Unassociated molecules coexisting with micelles are often called unimers, and this nomenclature is used here.
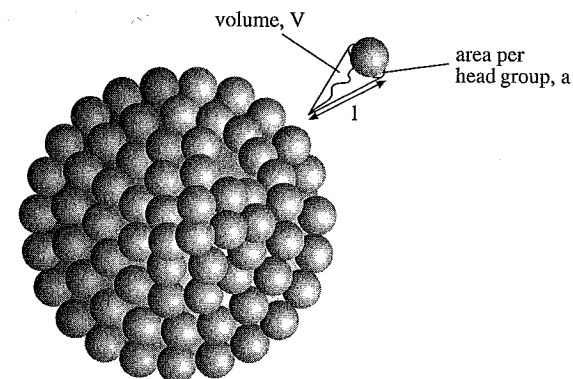
Figure 4.14   A spherical micelle. The packing of amphiphilic molecules is controlled by the effective cross-sectional area of the head group, a, and the hydrophobic chain of length l and volume V. These quantities define a surfactant packing parameter (see Eq. 4.53)

The *critical micelle concentration* (CMC) occurs at a fixed temperature as amphiphile concentration increases. The CMC is not a thermodynamic phase transition. It is defined phenomenologically from a sharp increase in the number of molecules associated into micelles. The precise location of the CMC thus depends on the technique used to measure it. Many physical properties exhibit abrupt changes at the CMC, as illustrated in Fig. 4.15. Some of these are colligative properties such as osmotic pressure or ionic conductivity. Other techniques are sensitive to changes in the dynamics of molecules at the CMC. For example, the self-diffusion coefficient measured by dynamic light scattering decreases discontinuously
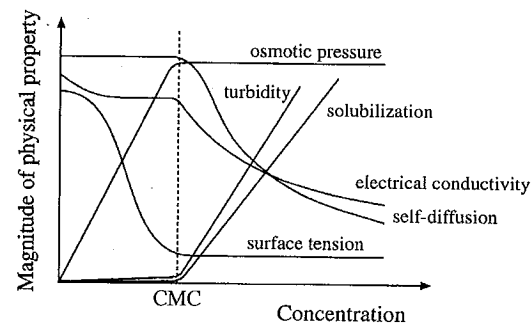

Figure 4.15   Many physical properties exhibit a discontinuity near to the critical micelle concentration (CMC). The CMC is not a thermodynamic quantity but is defined by sharp changes in measurable quantities, which occur in a concentration range close to the CMC

when micelles are formed, since these move more slowly than molecules. The most widely used technique to obtain the CMC is, however, surface tension measurement.

Micellization can also occur upon varying temperature at fixed concentration above or below a *critical micelle temperature* (CMT), depending on whether the self-assembly process is endothermic or exothermic. However, it is most common to determine the CMC rather than the CMT, since this enables comparison of CMC values at a fixed temperature (often 25 °C).

4.6.2   Surface Tension and the CMC

Addition of many organic molecules such as alcohols causes a decrease in the surface tension of an aqueous solution, because they are adsorbed preferentially at the air–water interface as they are, to some extent, hydrophobic. In contrast, the surface tension of most electrolyte solutions increases with concentration, because ions are depleted from the surface due to attractive interactions in the bulk solution. The same behaviour is observed for hydrophilic solutes such as sugars.

The concentration dependence of surface tension for a surfactant solution is distinctive because it is sensitive to the formation of micelles. Unlike non-amphiphilic molecules, the decrease of surface tension with increasing concentration is non-monotonic. Upon increasing the concentration of a pure amphiphile, the surface tension decreases rapidly from the value $\gamma = 72$ mN m^{-1} for pure water until a point at which it levels off and becomes almost independent of concentration (Fig. 4.16). This point is the CMC. Note that the concentration is plotted on a logarithmic scale in Fig. 4.16. The reason for this will become apparent when we consider Eq. (4.27). The limiting value of surface tension above the CMC is typically around 35 mN m^{-1}. That the surface tension is independent of concentration above the CMC is sometimes ascribed to saturation of the surfactant in the surface monolayer. However, it is actually due to a chemical potential that is almost independent of concentration above the CMC, as discussed in the following section.

Measurements of surface tension are very sensitive to any impurities present in the surfactant. As little as 0.01% of an impurity such as an alcohol will lead to a pronounced minimum in the curve of γ versus $\ln c$, close to the CMC (Fig. 4.16). This is because alcohols also selectively segregate to the surface, but their surface tension is usually lower than that of surfactants. Thus, the alcohol will induce micellization below the CMC for the pure surfactant. However, as concentration is increased
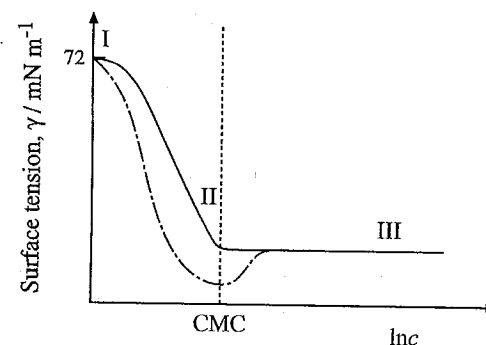
Figure 4.16   Variation of surface tension with concentration (on a logarithmic scale) for a pure aqueous surfactant solution (solid line) and a solution containing surface-active impurities such as alcohols (broken line)

above the CMC, the surfactant replaces alcohol in the micelles so that the surface tension increases.

4.6.3   Gibbs Adsorption Equation

We consider the partitioning of one species to the interface between two phases (α and β) containing several species j in different amounts n_j. This procedure will lead to a relationship between the surface tension and concentration for a surfactant, i.e. in this particular case we consider the excess of nonionic surfactant at the air–water interface. It is assumed that the interface can be described by a plane, which is only an approximation because the accumulation of a component (for example surfactant) at the interface leads to a layer of finite thickness. Furthermore, such a layer can alter the structure of the adjacent phases due, for example, to dipole–dipole interactions. There is thus some arbitrariness in the definition of the interfacial plane, but nonetheless we shall see shortly that a convenient choice presents itself.

The excess of a component j at the interface σ is

$$n_j^\sigma = n_j - \left\{ n_j^\alpha + n_j^\beta \right\} \tag{4.15}$$

where n_j^α and n_j^α are the amounts of component j in pure phases α and β. The excess per unit area defines the surface excess Γ_j:

$$\Gamma_j = \frac{n_j^\sigma}{A} \tag{4.16}$$

where n_j^σ denotes the number of moles of j in excess at the surface and A is the surface area.

Thermodynamics provides us with an expression for the internal energy, U, of a one-phase system of several components:

$$U = TS - pV + \sum_j \mu_j n_j \qquad (4.17)$$

where the symbols have the following meanings: T = temperature, S = entropy, p = pressure, V = volume and μ = chemical potential. Equation (4.17) becomes, for a surface phase,

$$U^\sigma = TS^\sigma - pV^\sigma + \gamma A + \sum_j \mu_j n_j^\sigma \qquad (4.18)$$

where we have not placed a superscript σ on the chemical potentials since in equilibrium $\mu_j^\sigma = \mu_j^\alpha = \mu_j^\beta$. A generalization of the Gibbs–Duhem equation (see a physical chemistry or thermodynamics textbook for a discussion of this) to the case of a surface leads to the relationship

$$dU^\sigma = TdS^\sigma + \gamma\, dA + \sum_j n_j^\sigma\, d\mu_j \qquad (4.19)$$

Differentiating Eq. (4.18) and comparing it with Eq. (4.19) leads to the Gibbs adsorption equation:

$$S^\sigma dT + A d\gamma + \sum_j n_j^\sigma\, d\mu_j = 0 \qquad (4.20)$$

At constant temperature, we obtain the Gibbs adsorption isotherm

$$A d\gamma + \sum_j n_j^\sigma d\mu_j = 0 \qquad (4.21)$$

Dividing through by A, and recalling the definition of surface excess (Eq. 4.16) leads to

$$d\gamma = -\sum_j \Gamma_j\, d\mu_j \qquad (4.22)$$

Now we turn to the particular case of a surfactant adsorbed at the air–water interface. For an arbitrary interface, Eq. (4.22) becomes

$$d\gamma = -\Gamma_1\, d\mu_1 - \Gamma_s\, d\mu_s \qquad (4.23)$$

where l denotes the liquid solvent and s denotes the single, non-ionized, surfactant solute. The most convenient choice of dividing surface between air and water is that for which the surface excess of solvent $\Gamma_1 = 0$. Then

$$d\gamma = -\Gamma_s\, d\mu_s \qquad (4.24)$$

The chemical potential of the surfactant can be written as

$$d\mu_s = RT\, d\ln a \qquad (4.25)$$

where a is the activity of the surfactant (in water). In the limit of an ideally dilute solution this can be replaced by

$$d\mu_s = RT\, d\ln c \qquad (4.26)$$

where c is the concentration (in mol dm^{-3}) of surfactant. Thus, from Eq. (4.24), the surface excess is given by

$$\Gamma_s = -\frac{1}{RT}\left(\frac{\partial\gamma}{\partial\ln c}\right)_T \qquad (4.27)$$

where the subscript T emphasizes that the gradient is calculated from an isotherm, i.e. measurements of surface tension as a function of concentration at constant temperature. The relationship

$$\Gamma_s = -\frac{c}{RT}\left(\frac{\partial\gamma}{\partial c}\right)_T \qquad (4.28)$$

is equivalent to Eq. (4.27), although plots of γ versus $\ln c$ are more convenient. Since the surface excess here is the number of surfactant molecules per unit area at the air–water interface, the inverse of Γ_s can be used to calculate the average area per molecule from the limiting slope of $\partial\gamma/\partial \ln c$ just below the CMC. Here the gradient of γ plotted against $\ln c$ is constant.

The preceding derivation has been for the interfacial excess of a non-ionic surfactant. For a 1:1 ionic surfactant, it is necessary to account for the fact that both surfactant and counterion adsorb at the interface (creating two molecules of ions per mole of surfactant) and Eq. (4.27) is modified to give

$$\Gamma_s = -\frac{1}{2RT}\left(\frac{\partial\gamma}{\partial\ln c}\right)_T \qquad (4.29)$$

(with a similar modification to Eq. 4.28).

A typical plot of γ versus $\ln c$ is shown in Fig. 4.16. We will now discuss three regimes of behaviour, indicated in this figure, and relate the variation of surface tension to the adsorbed structure at the water surface, and to micellization in the bulk. Surface adsorption and micelle formation are clearly correlated, since the CMC is most often determined from surface tension measurements. It might be supposed that the observed concentration independence of γ above the CMC arises because the surface excess is saturated due to formation of a complete monolayer at the CMC. According to this picture, above the CMC, surfactant molecules are unable to adsorb at the air–water interface, and so form micelles in bulk. However, we shall see that this interpretation is an oversimplification of the subtle physical chemistry involved.

In regime I, the surface tension decreases linearly with increasing concentration, i.e.

$$\gamma = \gamma_0 - kc \qquad (4.30)$$

where k is a constant. Thus, from the definition of surface pressure, Eq. (4.7),

$$\pi = kc \qquad (4.31)$$

Differentiating Eq. (4.30), we find that $d\gamma/dc = -k$. Inserting this into the Gibbs equation in the form of Eq. (4.28) leads to

$$\pi = \Gamma_s RT \qquad (4.32)$$

or from the definition of surface excess (Eq. 4.16),

$$\pi A = n_s RT \qquad (4.33)$$

This shows that in dilute solution the surfactant behaves like an ideal gas in two dimensions, since the equation has the same form as the ideal gas equation $pV = nRT$ in three dimensions.

In regime II, the decrease of γ with $\ln c$ becomes approximately linear. This occurs just below the inflection point that indicates the CMC. This linear proportionality means that Γ_s is constant. It may seem paradoxical that the surface excess saturates even below the CMC; however, an explanation for this has been proposed. The total concentration of surfactant in the surface layer has a contribution from the bulk surfactant concentration plus the surface excess. The bulk surfactant concentration continues

to increase slightly with $\ln c$, even though the surface excess is saturated. This creates an increase in packing density in the adsorbed monolayer up to the CMC. In this region, the average area per molecule can be calculated using the Gibbs adsorption equation (Eq. 4.27 or Eq. 4.28).

In regime III, above the CMC the surface tension is nearly constant. This is due to the very weak dependence of chemical potential on concentration, and not because of saturation of the adsorbed layer, since this already occurs in regime II. To see this, we note that the chemical potential of the surfactant, in dilute solution, is given by Eq. (4.26). Below the CMC, the total surfactant concentration is equal to the unimer concentration, $c = c_s$, so chemical potential increases logarithmically with concentration as for any dilute solution. However, above the CMC, Eq. (4.37) in the limit $c \gg c_s$ gives

$$c_s = c^{1/p}(Kp)^{-1/p} \qquad (4.34)$$

where p is the *association number* (average number of molecules per micelle). Thus, the chemical potential is given by

$$\mu_s = \mu_s^\theta + \frac{RT}{p} \ln c - \frac{RT}{p} \ln[KP] \qquad (4.35)$$

This equation indicates that chemical potential is very weakly dependent on surfactant concentration above the CMC. To achieve the same change in μ_s caused by doubling the concentration below the CMC requires that c be increased by 2^p above the CMC. For typical association numbers ($p \approx 20$–100), this is too large to be achieved, indicating that chemical potential is nearly constant above the CMC.

4.6.4   The Krafft Temperature

The solubility of ionic surfactants is strongly dependent on temperature. The solubility is often very low at low temperatures but increases rapidly in a narrow range as the temperature increases. The point at which the solubility curve meets the critical micelle concentration curve is termed the Krafft point, which defines the Krafft temperature (Fig. 4.17). The dramatic increase in solubility on increasing temperature above the Krafft temperature is due to an interplay between the temperature-dependent solubility of amphiphilic molecules and the temperature dependence of the CMC. The latter is generally very weak. If the amphiphile solution is below the CMC then the
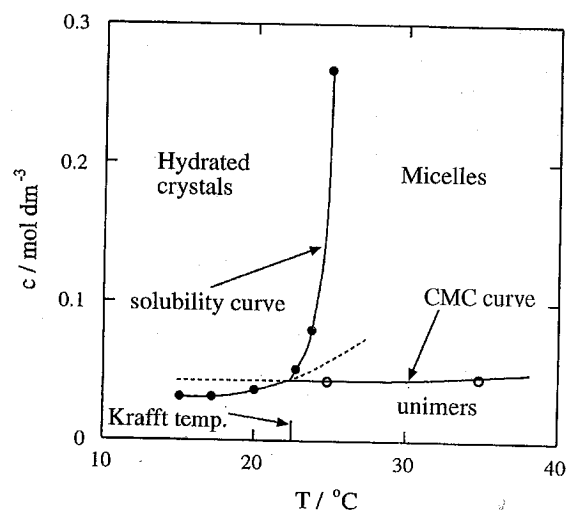
Figure 4.17 Phase diagram near the Krafft point of sodium decyl sulphonate. [From K. Shonda and E. Hutchinson, *J. Phys. Chem.*, **66**, 577, Copyright (1962) American Chemical Society]

surfactant solubility is limited by the low solubility of the molecules. In contrast, if the concentration is above the CMC, then as the temperature increases, the total solubility of the surfactant is increased dramatically as the molecules form (soluble) micelles. Thus only a small increase in unimer solubility leads to a sharp increase in amphiphile solubility.

The Krafft point increases strongly as the alkyl chain length increases. This is largely due to the dependence of the CMC on alkyl chain length (Section 4.6.6), but also reflects differences in the packing of surfactant molecules in the crystal. The Krafft point depends on the crystal structure of the amphiphilic molecules, because at low solvent concentrations the surfactant–solvent mixture comprises hydrated crystals. The variation in crystal structure explains the observed odd–even variation in Krafft temperature with chain length in the amphiphile, because there is a difference in packing of the molecules which alternates with the number of carbons in the hydrophobic tail. Likewise, strong interactions between head groups stabilize the crystal and so strongly increase the Krafft temperature, as generally does the addition of salt. Insertion of a double bond into the hydrophobic chain often reduces the stability of the crystal phase, and so leads to a reduction in the Krafft temperature.

4.6.5   Models for Micellization

Open association model

A number of models have been developed to describe micellization in surfactants. In the model of *open association*, there is a continuous distribution of micelles containing 1.2.3 . . . . . *n* molecules. However, the open association model does not lead to a critical micelle concentration and so is generally inapplicable to amphiphiles in solution.

Closed association model

The *closed association* model can account for the observation of a critical micelle concentration. It is also known as the mass action model. It is assumed that there is a dynamic equilibrium between molecules and micelles containing p molecules. In practice, micelles are not monodisperse (Section 1.8), i.e. there is a range of values of association number. Usually, the dispersity in p amounts to about 20–30 % of its value, which is not large enough to change the behaviour captured by models for monodisperse micelles. In the following, we consider the equilibrium between nonionic surfactant molecules and monodisperse micelles in dilute solution:

$$pS \rightleftharpoons S_p \qquad (4.36)$$

The Gibbs energy change of micellization per mole of micelles is then
  At equilibrium

$$K = \frac{c_p}{c_s^p} \qquad (4.37)$$

where c_p is the concentration (in mol dm^{-3}) of micelles of association number p, and c_s is the concentration of unassociated surfactant molecules.
  Then the Gibbs energy change of micellization per mole of micelles is

$$\Delta_{mic} G^\ominus = -RT \ln K = -RT \ln \frac{c_p}{c_s^p} \qquad (4.38)$$

Per mole of surfactant molecules this becomes

$$\Delta_{mic} G^\ominus = -\frac{RT}{p} \ln K = -\frac{RT}{p} \ln c_p + RT \ln c_s \qquad (4.39)$$

Assuming p is large (which it typically is), the first term on the right hand side can be neglected and at the CMC we have

$$\Delta_{\mathrm{mic}} G^{\ominus} = RT \ln c_{\mathrm{CMC}} \qquad (4.40)$$

For an ionic surfactant, the equilibrium involves in addition the counterions (denoted C). Equilibrium (4.36) is instead

$$pS^{x} + (p - n)C^{y} \rightleftharpoons S_{p}^{\alpha} \qquad (4.41)$$

Here $\alpha = n/p$ is the degree of dissociation of the surfactant and x and y are the charges of surfactant and counterion respectively. Following the same method used to obtain Δ_{mic} above, i.e. writing an expression for K, and calculating $\Delta_{\mathrm{mic}} G^{\ominus} = -RT \ln K$ in the case of large association numbers, we obtain

$$\Delta_{\mathrm{mic}} G^{\ominus} = RT \left(2 - \frac{n}{p} \right) \ln c_{\mathrm{CMC}} \qquad (4.42)$$

where we have, in addition, used the fact that for a fully ionized surfactant the concentration of surfactant and counterions is equal and equal to the CMC at this concentration.

The closed association model means that above the CMC, added molecules go into micelles. The fraction of unassociated molecules and of micelles are plotted together in Fig. 4.18. Further information on calculating the fraction of associated molecules can be found in Section 6.4.5, where the one-dimensional self-assembly (of cylindrical micelles for example) is considered.
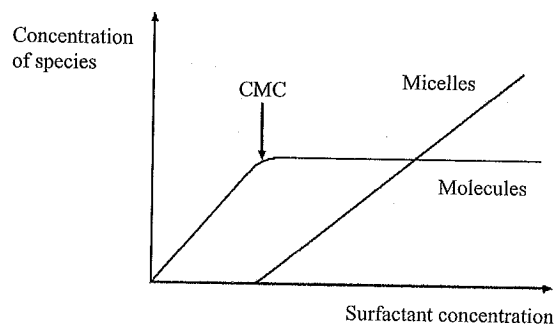
Figure 4.18   Mole fraction of unassociated molecules and micelles as a function of total surfactant concentration [Reprinted from J.N. Israelachvili, *Intermolecular and Surface Forces*, Academic Press, London, Copyright (1991) with permission from Elsevier].

Considering again the case of a nonionic surfactant, the standard molar enthalpy of micelle formation is then

$$\Delta_{\mathrm{mic}} H^{\ominus} = R \frac{d \ln c_{\mathrm{CMC}}}{d(1/T)} \qquad (4.43)$$

However, $\Delta_{\mathrm{mic}} H^{\ominus}$ and $T\Delta_{\mathrm{mic}} S^{\ominus}$, determined from the temperature dependence of the Gibbs energy, are less sensitive to the association number than is $\Delta_{\mathrm{mic}} G^{\ominus}$ itself. Assuming that $\Delta_{\mathrm{mic}} H^{\ominus}$ is approximately constant within a certain temperature range, Eq. (4.43) can be integrated to yield

$$\ln c_{\mathrm{CMC}} = \frac{\Delta_{\mathrm{mic}} H^{\ominus}}{RT} + const. \qquad (4.44)$$

Thus the logarithm of the CMC can be plotted against inverse temperature to extract the micellization enthalpy. Equivalently, the logarithmic concentration can be plotted against the inverse critical micelle temperature.

Micellization is predominantly driven by an increase in entropy of the system of molecules in micelles compared to unassociated molecules. This is because unassociated molecules lead to an ordering of the surrounding water, i.e. a reduction in entropy, due to the hydrophobic effect. This ordering effect is reduced when molecules associate into micelles. The gain in entropy of the water upon micelle formation outweighs the enthalpy penalty (caused by the 'demixing' of water and surfactant) and the loss of configurational entropy of the molecules due to the constraints imposed by the micellar structure. Thus for the overall process $\Delta_{\mathrm{mic}} G_{\mathrm{m}}^{\ominus}$ is negative, because the $T\Delta_{\mathrm{mic}} S_{\mathrm{m}}^{\ominus}$ term is larger than the positive $\Delta_{\mathrm{mic}} H_{\mathrm{m}}^{\ominus}$ term (see, for example, Q. 4.4).

Phase separation model

The transition between molecules and micelles upon increasing amphiphile concentration becomes sharper for larger association numbers. In the limit of very large association numbers, the amphiphile solution above the CMC can be modelled as a pseudo-phase-separated system of micelles and unimers. The CMC then corresponds to the saturation concentration of surfactant in the unimer state. In equilibrium, the molar chemical potentials of unimer in the aqueous phase and of associated amphiphile in the micellar phase are equal. From this, it can be shown that (Q. 4.10) the molar Gibbs energy of micellization is given by Eq. (4.40).

The phase separation model is restricted to micellization which produces micelles with a very large association number, p. In addition, it can only describe the association process into micelles and not the association and dissociation described by the equilibria, upon which closed association models are based. However, the main problem with the model is that micelles cannot rigorously be considered to constitute a separate phase, since they are not uniform and homogeneous throughout. However, it is a simple model which works quite well for micelles with large association numbers. As with the closed association model, the phase separation model can be applied to ionic surfactants, provided that allowance is made for the association of counterions with the micelle.

4.6.6 Variation of the CMC and Association Number with Temperature, Surfactant Type, Chain Length and Addition of Salt

Effect of temperature

For most surfactants, the CMC is essentially independent of temperature. An exception is nonionic surfactants based on oxyethylene units as the hydrophilic group, for which the CMC decreases strongly with increasing temperature. In addition, the decrease in the CMC is monotonic, whereas for ionic surfactants, the CMC first decreases slightly with increasing temperature, but then increases a little.

Increasing temperature for ionic surfactants usually opposes micellization due to enhanced molecular motion that reduces p. For oxyethylene-containing nonionics, temperature causes the association number to increase up to the cloud point, when phase separation occurs because polyoxyethylene becomes insoluble in water. The cloud point decreases with decreasing oxyethylene (E) chain length; indeed, surfactants of the type C_mE_n (Section 4.2) with $n < 4$ are insoluble in water and so the system is always phase separated. As the association number increases with temperature, the solvent quality for oxyethylene becomes worse, causing the corona to shrink. A compensation between the increase in p and a decrease in corona size results in an approximately constant overall micellar radius.

Effect of surfactant type

The CMC is usually much lower for nonionic surfactants than for ionic ones, when the comparison is made for equal hydrophobic chain lengths.

This is because electrostatic repulsions between head groups have to be overcome to form micelles from ionic surfactants, but not for nonionic amphiphiles. It follows from this argument that the CMC is higher the larger the head group charge in ionic surfactants. The chemical nature of the hydrophobic chain also influences the CMC. For example, fluorination of an alkyl chain increases the hydrophobicity dramatically compared to a hydrocarbon chain, and the CMC decreases sharply.

Effect of hydrophobe chain length

Increasing the length of the hydrophobic part of an amphiphile favours micellization. Thus an increase in the chain length leads to a reduction in the CMC. This is often described by an empirical relationship of the form

$$\log c_{\text{CMC}} = A - B n_{\text{C}} \qquad (4.45)$$

where n_{C} is the number of carbon atoms in the chain (see Q. 4.4 for an example). For a wide range of surfactants $1.2 < A < 1.9$ and $0.26 < B < 0.33$. This behaviour holds for chains containing up to about 16 carbon atoms. Increasing the chain length beyond this does not lead to significant decreases in the CMC, possibly due to coiling of long hydrocarbon chains in the unimers to minimize hydrophobic interactions of unassociated molecules. For ionic surfactants, it is found that the CMC decreases by approximately a factor of two for each additional $-CH_2$ unit, whereas for nonionic surfactants the increase is larger, typically a factor of three. Making comparisons for chains with the same number of carbon atoms, the reduction in CMC with n_{C} is greater for linear alkyl chains than for branched chains because linear chains can pack together better in micelles.

The decrease in the CMC can be accounted for using thermodynamics, via Eq. (4.40). Making comparisons for a homologous series, the contribution to the Gibbs energy per methylene unit, $\Delta_{\text{mic}} G_{\text{m}}^{\ominus} (CH_2)$, is approximately -3 kJ mol^{-1} for a wide range of amphiphile types and the corresponding decrease in $\Delta_{\text{mic}} G_{\text{m}}^{\ominus}$ with increasing n_{C} largely accounts for the decrease in the CMC.

As expected, adding $-CH_2$ units to an alkyl chain increases the size of the micelle, and hence the association number, p. Indeed, the association number of nonionic surfactants increases roughly linearly with the number of $-CH_2$ units.

In oxyethylene-based nonionic surfactants, the hydrophilic group is much larger relative to the core than it is for most ionic surfactants. This

means that the structure changes more gradually from the hydrophobic interior of the micelle to the surrounding water for the former. Another consequence is that micellar properties depend also on the length of the oxyethylene chain. Increasing the length of this chain causes the CMC to increase slightly because the molecules become more hydrophilic. The association number decreases with increasing size of the hydrophilic group because otherwise it is not possible to cover the hydrophobic micellar core with large hydrophilic groups. However, the micelle size stays approximately constant due to a compensation between the reduction in association number and the increase in micellar corona size, i.e. the same explanation as for the temperature dependence.

Effect of salt and cosolutes

For ionic surfactants, addition of salt decreases the CMC and increases p. This is because the added electrolyte reduces the repulsion between charged head groups. The effect is larger for longer chain surfactants, since the reduction in head group repulsion has a proportionally greater effect on molecular packing than for amphiphiles containing short hydrophobic chains. Addition of salt also increases the sensitivity of the CMC to alkyl chain number, i.e. the decrease in CMC with increasing chain length is larger at higher salt concentrations and can approach that of nonionic surfactants. The effect of salt also depends on the valency of the electrolyte ion, in particular of the added counterions. Salt has little effect on the CMC or association number of nonionic surfactants.

Addition of cosolute can either increase or decrease the CMC, depending on the polarity of the molecules. Highly water soluble cosolutes tend to increase the CMC, since the solubility of surfactant molecules is enhanced. On the other hand, alcohols are less polar than water and are distributed between the aqueous phase and micelles. The water solubility of alcohols determines whether they are predominantly solubilized in micelles or in the aqueous phase. Medium chain length alcohols tend to be solubilized within micelles and thus increase p and lower the CMC for both ionic and nonionic surfactants. In contrast, short chain alcohols are water soluble and can either increase or decrease the CMC.

4.7 DETERGENCY

A detergent is an agent for the removal of soil from fabric. For many centuries, soap was the pre-eminent detergent as well as the king of personal

care products. Traditional soaps are sodium and potassium salts of fatty acids, made by saponification of triglycerides (Fig. 4.4). However, soaps have a number of disadvantages. For example, they form scum in hard water which contains Ca^{2+} or Mg^{2+} ions, and in addition they do not function well in acid solutions due to the formation of insoluble fatty acids. In the last few decades, a large array of synthetic surfactants has been prepared to avoid these problems. Considering laundry detergents, the surfactants have carefully tailored characteristics so that their detergent action is maximized for the wash conditions, i.e. temperature, solution conditions (pH, salt content, etc.) or dirt type (oily or other). Because of the range of conditions encountered, commercial detergents contain a mixture of surfactants, usually nonionic and anionic. The most commonly encountered types are alcohol ethoxylate nonionic surfactants (Fig. 4.3) and alkyl sulphonate and/or alkyl aryl sulphonate anionic surfactants (Fig. 4.1). The surfactants are the most important component for removing oily soil, but enzymes in 'biological' detergents play an important role in hydrolysis of particles in stains such as tea or blood, or in food stains containing proteins, starch or triglycerides. In addition to surfactant and enzymes, modern detergent formulations also include builders such as zeolites or phosphates, which help to reduce surfactant precipitation due to the presence of calcium or magnesium salts in areas of hard water. Anionic polyelectrolytes are included in detergent formulations to remove particulate soil, which may contain clay and other charged mineral particles. Other common ingredients include bleaching agents, perfumes and fluorescing agents (to whiten laundry).

To be effective as a detergent, a surfactant has to fulfil a number of functions. First, it must effectively wet the fabric, so that the detergent will come into contact with the surface to be cleaned. Second, it should facilitate the removal of dirt from the fabric surface. Third, it should solubilize or disperse dirt, and help to prevent its redeposition. Figure 4.19 summarizes the action of detergent through these processes.

In regard to wetting, surfactants readily lower the surface tension of fabrics compared to water, so this is not a critical consideration in formulation. However, the rate of diffusion of surfactant molecules to the fabric surface is important, and here it is usual to reach a balance between the highly surface active properties of molecules with long hydrophobic chains and the faster diffusion rate of small molecules. A 12-carbon chain represents a good compromise.

The mechanism of removal of dirt depends on whether it is particulate or oily/fluid. In the former case, the surfactant must lower the work of adhesion of the dirt particle to the solid fabric surface. If the dirt is a
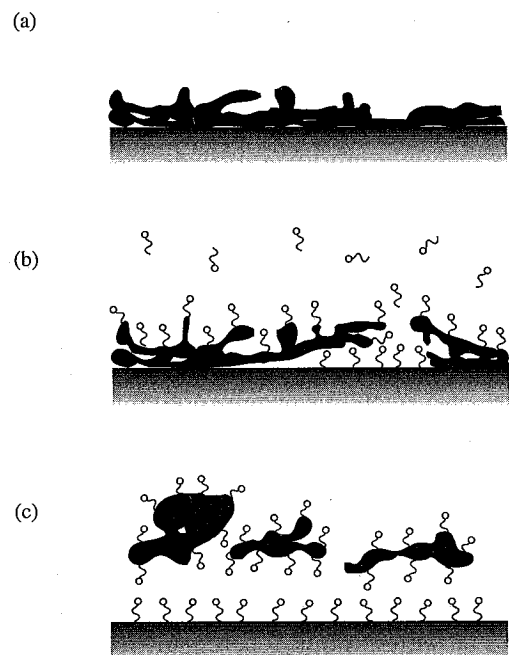
(a)

(b)

(c)

Figure 4.19 Illustrating detergent action. (a) Surface covered with greasy dirt. (b) Detergent is added to the solution. The surfactant molecules reduce adhesion of dirt to the surface when they are deposited with their hydrophobic tails on the solid surface or dirt particle. The dirt particles are thus more readily removed by mechanical action. (c) Dirt particles are held as a suspension by an adsorbed layer of surfactant. [Reproduce with permission of the estate of Irving Geis]

liquid, the surfactant must reduce the contact angle at the fabric surface. If the contact angle is initially less than $90°$, which is usually the case for oily dirt on polar textiles such as cotton, the surfactant acts to remove the oily dirt globule via a 'roll-up' mechanism (Fig. 4.20a). When the contact angle is larger ($90° < \theta < 180°$), the roll-up mechanism is not completely effective, and some material is left on the fabric surface. This can be removed by a solubilization or emulsification mechanism (Fig. 4.20b,c).

These considerations mean that for removal of dirt, surfactants must effectively adsorb at solid–liquid or liquid–liquid interfaces. This is not always directly correlated to the surface activity at the air–water interface, which characterizes surfactants, and very effective nonionic surfactants are not always sufficiently surface active to form good foams, which is psychologically important in the washing process. Thus, surfactants that tend to form good foams are also added. All of the mechanisms of dirt removal are enhanced by mechanical action, for example due to rotation of the washing machine drum.

(a)

(b)

(c)
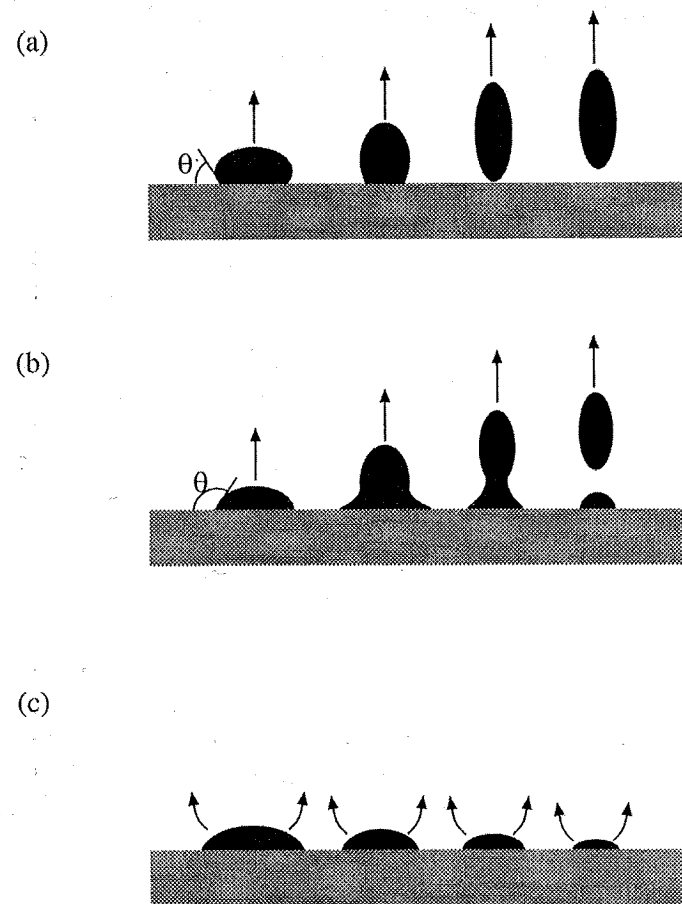
Figure 4.20 Detailed mechanisms for greasy dirt removal from a solid surface: (a) roll-up, (b) emulsification and (c) solubilization

To prevent redeposition of dirt, the surfactant molecules should adsorb on to dirt particles in solution, with the hydrophobic tail dissolved in the dirt and the head group in contact with water (Fig. 4.19c). Charged head groups in the anionic surfactant component of detergent formulations lead to electrostatic repulsions between solubilized dirt particles, preventing precipitation. For nonionic surfactants, the head group leads to a hydration barrier, i.e. a depletion of water close to the head group, which reduces contact between surfactant-solubilized dirt particles. The surfactant left adsorbed on the fabric surface will also prevent redeposition due to electrostatic or steric repulsions. Although the solubilized dirt particles resemble micelles containing solubilized material, they are

too large and irregular to be micelles as defined by equilibrium thermo-dynamics in Section 4.6.5. Builders are also important in preventing dirt redeposition and scum formation in hard water.

It is believed that the formation of a microemulsion can enhance deter-gent action since the oil–water interfacial tension can be lowered consid-erably, which facilitates solubilization of oily dirt particles by surfactant. The microemulsion is of Winsor type III (Section 3.13.2), with small amounts of surfactant forming a 'middle phase' microemulsion in equi-librium with excess oil and water. The oil–water interfacial tension is a minimum at the phase inversion temperature (PIT) of an oil–water-surfactant system, so it is desirable to optimize the properties of the detergent mixture so that the system is close to the PIT at the washing temperature. Microemulsions made from mixtures of nonionic surfac-tants are used in hard surface cleaning products. Usually they are sold in concentrated form and diluted prior to use.

4.8 SOLUBILIZATION IN MICELLES

Micelles are important in a number of industrial and biological pro-cesses because they are able to solubilize otherwise insoluble organic compounds. In particular, micelles with a hydrocarbon core can solu-bilize organic compounds that are insoluble in water, such as drug or dye molecules or flavour compounds. This is relevant to pharmaceutical preparations where water-insoluble drug compounds need to be deliv-ered, and likewise in the incorporation of fragrance and colouring into personal care products. Solubilization is also an important aspect of de-tergency (see Section 4.7). Dirt is removed and held in solution by solubi-lization when surfactant molecules are adsorbed in a film around a grease droplet. However, these are often better viewed as surfactant-stabilized particles rather than micelles. Solubilization of monomer in micelles in an aqueous solution is believed to provide the environment for polymer-ization during emulsion polymerization. Because it corresponds to the addition of more hydrophobic material to the solution, solubilization tends to reduce the CMC.

A good example of the biological relevance of solubilization in micelles is provided by the mechanism by which fats are digested by animals. This is achieved using bile salts, which act as surfactants in the stomach and intestine. Examples of cholesterol derivatives that are bile salts are illus-trated in Fig. 4.21. Cholesterol itself is weakly amphiphilic due to the presence of a terminal -OH group (in fact, it is an example of a lipid

Cholate

Glycocholate
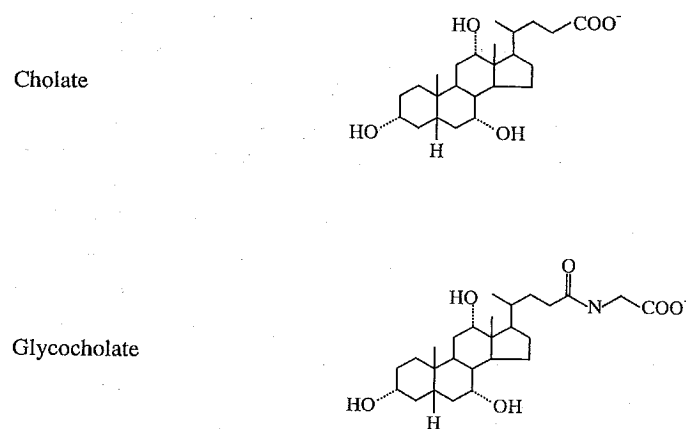
Figure 4.21   Typical bile salts

lipids and surface-active material

Pancreatic lipase
bile salts

1. Emulsification

2. Hydrolysis of fats

3. Micellization

4. Transport of mixed micelle to intestine wall

5. Adsorption of fatty acids and lipids

6. Movement of bile salt micelle down intestine

7. Adsorption of bile salts
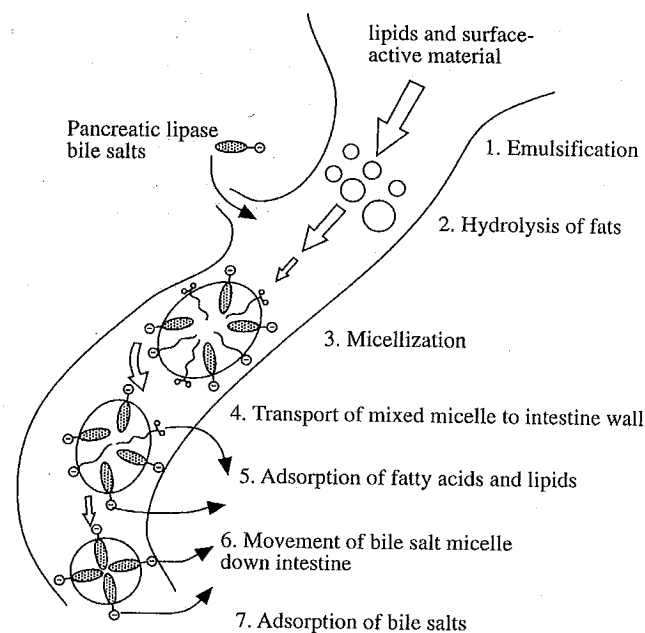
Figure 4.22   Schematic showing solubilization and digestion of fats in the stom-ach and upper intestine. [Reproduced from D. F. Evans and H. Wennerström, *The Colloidal Domain*, 1st Edition, Wiley–VCH, New York (1999)]

steroid). The mechanism of fat digestion involves a number of steps, summarized in Fig. 4.22. First, ingested fats pass into the duodenum (the upper part of the small intestine) and are emulsified by mechanical action. Pancreatic enzymes then break the triglyceride fats into fatty acids and 2-monoglycerides. Simultaneously bile salts are released from the gall-bladder. The fatty acids are insoluble in water at low pH; therefore they combine with bile salts and 2-monoglyceride lipids to form mixed micelles. These mixed micelles are then transported to the intestine walls. Here, the lipids and fatty acids are adsorbed on to the membrane of the intestine wall and both are re-esterified by enzymes to form triglycerides. Bile salts, being more polar, are not adsorbed until lower in the intestine, where they flow into the liver prior to being recycled. Thus, the solubilization of fats occurs through the formation of mixed micelles of fatty acids, lipids and bile salts.

Vesicles and liposomes (vesicles formed by lipids) are also important in solubilization applications, as discussed further in Section 4.11.4.

4.9 INTERFACIAL CURVATURE AND ITS RELATIONSHIP TO MOLECULAR STRUCTURE

The phase behaviour of surfactants at high concentration is described by two types of model. The first is based on the curvature of a surfactant film at an interface. The second is based on the shape of the surfactant molecules themselves. We now consider each of these approaches in turn.

In the model for interfacial curvature of a continuous surfactant film, we use results from the differential geometry of surfaces. A surface can be described by two fundamental types of curvature at each point P in it: mean and Gaussian curvatures. Both can be defined in terms of the principal curvatures $c_1 = 1/R_1$ and $c_2 = 1/R_2$, where R_1 and R_2 are the radii of curvature. The mean curvature is

$$H = \frac{c_1 + c_2}{2} \qquad (4.46)$$

whilst the Gaussian curvature is defined as

$$K = c_1 c_2 \qquad (4.47)$$

Radii of curvature for a portion of a so-called saddle surface (a portion of a surfactant film in a bicontinuous cubic structure) are shown in Fig. 4.23, although they can equally well be defined for other types of surface, such as convex or concave surfaces found in micellar phases. To define the signs
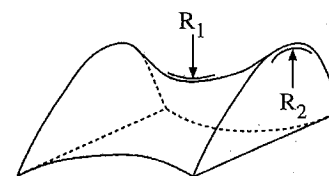
Figure 4.23   Principal radii of curvature of a saddle surface

of the radii of curvature, the normal direction to the surface at a given point P must be specified. This is conventionally defined to be positive if the surface points outwards at point P. In Fig. 4.23, c_1 is negative and c_2 is positive. The mean and Gaussian curvatures of various surfactant aggregates are listed in Table 4.2.

It should be noted that in this table the 'end effects' in elongated micelles due to capping by surfactant molecules which leads to an ellipsoidal or spherocylindrical (cylinder capped by hemispheres) structure are neglected. This will, however, change both mean and Gaussian curvatures, to an extent that depends on the relative surface area of 'cap' and 'tubular' parts.

The elastic free energy density associated with curvature of a surface contains, for small deformations, the sum of contributions from mean and Gaussian curvature. It is given approximately by

$$F_{el} = F_{mean} + F_{Gauss} = \frac{1}{2}\kappa(c_1 + c_2 - c_0)^2 + \bar{\kappa}(c_1 c_2) \qquad (4.48)$$

Here c_0 is the spontaneous curvature, i.e. twice the equilibrium mean curvature for the case of zero Gaussian curvature, $c_0 = c_1 = 2H_{eq}$, $c_2 = 0$.

Table 4.2   Mean and Gaussian interfacial curvature for common aggregate shapes. Here $R = R_1 = R_2$ denotes a radius of curvature

Structure/phase	Mean curvature $H = (c_1 + c_2)/2$	Gaussian curvature $K = c_1 c_2$
Spherical micelles or vesicles (outer layer)	$+1/R$	$+1/R^2$
Cylindrical micelles	$1/(2R)$	0
Bicontinuous cubic phases	0 to $1/(2R)$	$-1/R^2$ to 0
Lamellae (planar bilayers)	0	0
Inverse bicontinuous cubic phases	$-1/(2R)$ to 0	$-1/R^2$ to 0
Inverse cylindrical micelles	$-1/(2R)$	0
Inverse spherical micelles or inner layer of vesicles	$1/R$	$1/R^2$

As the term suggests, the spontaneous curvature is that adopted by a surfactant membrane in the absence of constraints, to reduce the curvature elastic free energy, which in Eq. (4.48) is defined with respect to the flat membrane. The quantities κ and $\bar{\kappa}$ are the elastic moduli for mean and Gaussian curvatures respectively, and have units of energy. Other things being equal, κ for a bilayer (for example in a vesicle) is twice that of a monolayer. The interfacial curvature model is thus useful because it defines these elastic moduli, which can be measured (by light scattering, for example) and characterize the flexibility of surfactant films. Uncharged surfactant films typically have elastic energies $F_{el} \leq k_B T$, i.e. they are quite flexible.

An alternative approach to the description of lyotropic mesophases in concentrated solution is based on the packing of molecules. The effective area of the head group, a, with respect to the length of the hydrophobic tail for a given molecular volume controls the interfacial curvature, as sketched in Fig. 4.14. The effective area of the head group (an effective molecular cross-sectional area) is governed by a balance between the hydrophobic force between surfactant tails which drives the association of molecules (and hence reduces a) and the tendency of the head groups to maximize their contact with water (and thus increase a). The balance between these opposing forces leads to the optimal area per head group, a, for which the interaction energy is minimum.

Simple geometrical arguments can be used to define a packing parameter, the magnitude of which controls the preferred aggregate shape. Consider, for example, a spherical micelle. The association number is given by the ratio of the micelle volume to the volume per molecule, V

$$p = \frac{\frac{4}{3}\pi R_{\mathrm{mic}}^3}{V} \tag{4.49}$$

where R_{mic} is the micelle radius. The association number is also given by the ratio of the micellar area to the crosssectional area per surfactant molecule, a:

$$p = \frac{4\pi R_{\mathrm{mic}}^2}{a} \tag{4.50}$$

Equating Eqs. (4.49) and (4.50), it follows that

$$\frac{V}{a R_{\mathrm{mic}}} = \frac{1}{3} \tag{4.51}$$

Since R_{mic} cannot exceed the length of a fully extended chain, l, the condition for stability of a normal spherical micelle is simply

$$\frac{V}{al} \leq \frac{1}{3} \tag{4.52}$$

The term

$$N_s = \frac{V}{al} \tag{4.53}$$

is called the *surfactant packing parameter*, or critical packing parameter. The surfactant parameter can be used to estimate the effective head group area, a, or vice versa. The surfactant packing parameter is concentration dependent, reflecting changes primarily in a (but to a lesser extent in V) upon varying the amount of solvent. We can make use of the following relationship for the extended length of an alkyl chain containing n_C carbon atoms:

$$l/\mathrm{nm} = 0.154 + 0.127 n_C \tag{4.54}$$

Here 0.154 nm is a C—C bond length and 0.127 nm is the projection of this distance on to the chain axis in the case of an all-*trans* conformation. For the volume of the hydrocarbon chain it has been found that

$$V/\mathrm{nm}^3 = 0.027(n_C + n_{\mathrm{Me}}) \tag{4.55}$$

where the n_{Me} term accounts for the fact that methyl groups occupy twice the volume of a CH_2 group (for single chain amphiphiles $n_{\mathrm{Me}} = 1$, but for double tail amphiphiles $n_{\mathrm{Me}} = 2$).

Just as spherical micelles can be considered to be built from the packing of cones, corresponding to effective molecular volumes, other aggregate shapes can be considered to result from packing of truncated cones, or cylinders. Thus, by arguments analogous to those for spherical micelles, Table 4.3 can be assembled, which shows the range of surfactant packing parameters for different aggregate shapes. A complication for elongated micelles, such as ellipsoids, is that the ends of the micelle are 'capped' by molecules. These caps can be approximated as hemispheres, where the head group area is larger than it is in the cylindrical regions of the micelles.

The surfactant packing model and the interfacial curvature description are related. Comparison of Tables 4.2 and 4.3 shows that a decrease in the surfactant parameter corresponds to an increase in mean curvature. The packing parameter approach has also been used to account for the

Table 4.3   Surfactant packing parameter range for various surfactant aggregates

Spherical micelles	$V/al < 1/3$	
Cylindrical micelles	$1/3 < V/al < 1/2$	
Vesicles, flexible bilayers	$1/2 < V/al < 1$	
Lamellae, planar bilayers	$V/al \approx 1$	
Inverse micelles	$V/al > 1$	

packing stabilities of more complex structures, such as the bicontinuous cubic phases. Here the packing unit is a wedge, which is an approximation to an element of a surface with a saddle-type curvature (Fig. 4.23). Then it is possible to allow for differences in the Gaussian curvature different structures, as well as the mean curvature.

4.10   LIQUID CRYSTAL PHASES AT HIGH CONCENTRATIONS

4.10.1   The Phase Rule

The Gibbs phase rule is useful to relate the number of phases, P, that can exist in amphiphile solutions with two (solvent plus amphiphile) or more components, C, to the number of degrees of freedom, F, of the system. The degrees of freedom are the independent intensive variables that describe the thermodynamic state of the system, i.e. for surfactant solutions these are temperature, pressure and composition. The phase rule states that

$$P + F = C + 2 \qquad (4.56)$$

For a binary surfactant/solvent mixture, we must have $P + F = 4$. Thus, a one-phase region of the phase diagram is specified by three degrees of

freedom: temperature, pressure and composition. In a two-phase region, it is only necessary to specify temperature and composition, for example. Three- and four-phase regions are also possible in a two-component system. A good example of the former is a eutectic line, which occurs at a fixed composition, depending on either temperature or pressure. A four-phase region would then result when the pressure is adjusted to the vapour pressure of the mixture at a temperature on the eutectic line.

Usually phase diagrams for binary systems are presented at constant pressure in the temperature–composition plane. For ternary mixtures (for example surfactant with oil and water in a microemulsion section), $P + F = 5$. The number of degrees of freedom that specify regions with different numbers of phases can be counted following similar arguments to those for binary systems, although there are now two composition variables. Ternary phase diagrams are usually presented at constant pressure in a phase triangle, with the pure components represented by the corners, the composition varying along the edges of the triangle. A schematic of a phase triangle for a microemulsion is shown in Fig. 3.17. This representation is also convenient for mixtures of surfactant + cosurfactant + solvent.

4.10.2   Phase Diagrams

At high concentrations, amphiphiles tend to self-assemble into ordered structures called lyotropic liquid crystal phases. The prefix *lyo-* (from the Greek for solvent) indicates that concentration is a controlling variable in the phase behaviour, as well as temperature. Temperature alone controls the self-assembly of thermotropic liquid crystals, which is the subject of the next chapter. Lyotropic liquid crystal phases can be formed in non-aqueous solvents. However, here we shall consider lyotropic liquid crystal phases formed in water, since these are by far the most important and widely studied.

The nature of the lyotropic liquid crystal phase formed by amphiphiles in solution is described at a molecular level by the surfactant packing parameter model, introduced in Section 4.9. Consider the situation where the head group has a larger effective cross-sectional area than the chain. This is the usual situation, and the resulting structures are termed *normal* structures. If there is a large difference in cross-sectional area between the head group and chain ($N_s < \frac{1}{3}$), spherical micelles are formed (Fig. 4.24a). For molecules with less of a mismatch between the effective head and tail cross-sectional areas, rod-like micelles provide a more
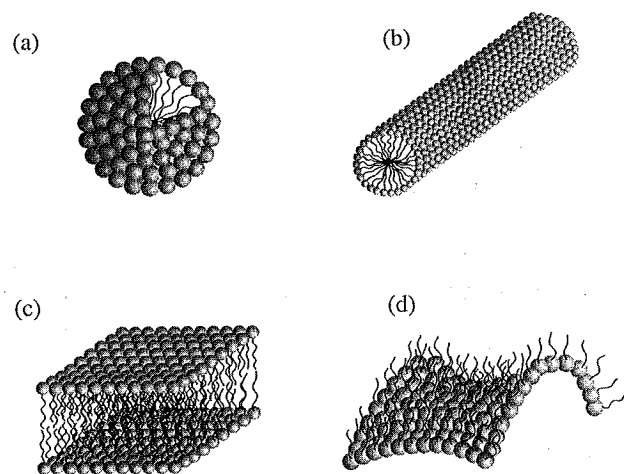
Figure 4.24　Normal aggregate structures and an amphiphillic bilayer: (a) spherical micelle, (b) cylindrical micelle, (c) bilayer, (d) saddle surface, one half of the bilayer of a bicontinuous cubic structure

efficient packing (Fig. 4.24b). If the head group and hydrophobe are nearly matched in effective cross-sectional area, a planar interface is preferred; i.e. a layer structure is expected to be stable (Fig. 4.24c). At certain concentrations it is sometimes observed that the packing of amphiphiles with an asymmetry in the head versus tail cross-sectional area is most efficiently achieved in a saddle-splay surface, as shown in Fig. 4.24d.

The asymmetry in cross-sectional area between the two parts of an amphiphilic molecule leads to interfacial curvature, which can be characterized by mean and Gaussian values (Section 4.9). The interfacial curvature picture is preferable when considering the structure of the lyotropic phase at a mesoscopic, rather than molecular, level. Changes in curvature for a given amphiphile are induced by variation of concentration, just as the effective cross-sectional area of the head group changes in the surfactant packing parameter. Micelles have a large mean (and Gaussian) curvature. At low concentrations, micelles are arranged in a liquid structure, with no long-range translational order. The normal micellar structure is termed the L_1 phase. At higher concentrations, micelles can fill space efficiently by packing in a cubic array (I_1 phase), of which a number have been observed (for example the body-centred cubic structure shown in Fig. 4.25a). On the other hand, it is more usual on increasing concentration for the shape of the micelles to change from spherical to rod-like. Rod-like micelles then pack into hexagonal structures, the normal version
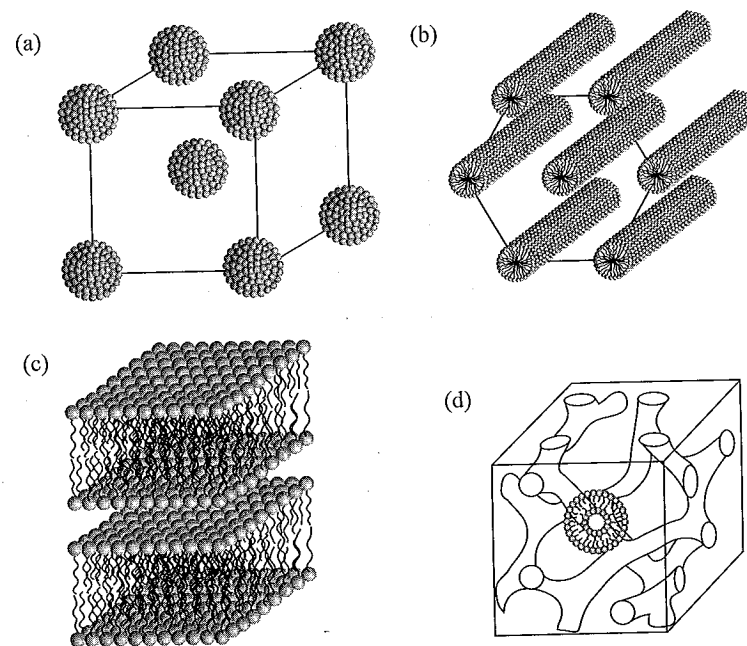
Figure 4.25　Normal structures and the lamellar phase: (a) normal micellar cubic structure (I_1), (b) normal hexagonal structure (H_1), (c) lamellar phase (L_x), (d) normal bicontinuous cubic structure (V_1). Here a portion of the 'gyroid' structure is sketched. The amphiphilic molecules form a bilayer film separating two continuous labyrinths of water. The amphiphilic film is a network with threefold node points, which defines the gyroid phase

of which is called the H_I phase (Fig. 4.25b). Bilayers tend to stack into a lamellar (L_α) structure (Fig. 4.25c). Structures based on saddle-splay surfaces are bicontinuous cubic phases characterized by non-zero mean curvature and negative Gaussian curvature. The most common bicontinuous cubic phase, the gyroid phase, is shown in Fig. 4.25d. A normal bicontinuous structure consists of two continuous channels of water, separated by a bilayer of surfactant molecules. In Fig. 4.25d, the surfactant bilayer is only shown in one region for clarity. In the gyroid phase, the two continuous channels are formed from labyrinths with threefold connection nodes. Bicontinuous cubic phases with four- and sixfold connectors are also known. Complex phases with tetragonal or rhombohedral symmetry that have been called 'mesh' phases, because of their connected structures, are also known.

The sequence of phases observed on increasing mean curvature is shown in the idealized phase diagram shown in Fig. 4.26. Here the
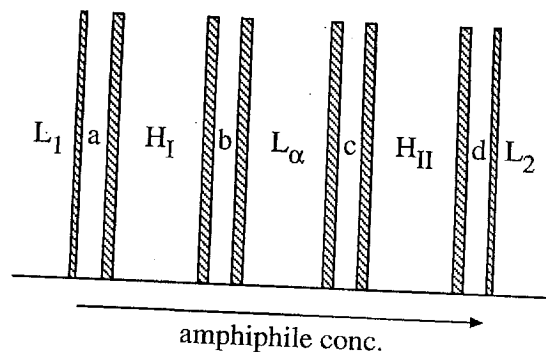
Figure 4.26 Sequence of phases observed on increasing solvent content, in a binary amphiphile–solvent system, representing a hypothetical phase diagram where phase transitions are controlled by solvent content only. Here a, b, c and d indicate intermediate phases (for example the bicontinuous cubic structure shown in Fig. 4.25d), L_2 denotes the inverse micellar solution, L_α is the lamellar phase, H_{II} is the inverse hexagonal phase, L_α is the lamellar phase, H_I is the normal hexagonal phase and L_1 is the normal micellar phase. In practice, the full sequence of phases is rarely observed, and in reality the phase transitions depend on temperature as well as concentration

Figure 4.27 Inverse aggregate structures: (a) spherical micelle, (b) cylindrical micelle and (c) saddle surface, one half of the bilayer of an inverse bicontinuous cubic structure

interfacial curvature and thus the phase behaviour is controlled by concentration alone. The shaded areas are biphasic regions. At low amphiphile concentrations, normal structures are observed, a progression from L_1 to H_1 to L_α being anticipated on increasing concentration. Sometimes *intermediate phases* are observed between L_1 and H_1 and between H_I and L_α phases (regions a and b respectively in Fig. 4.26). In region a, an intermediate phase is often a cubic-packed micellar structure, whereas in region b, it is often a bicontinuous cubic or mesh structure. When the solvent becomes the minority phase, *inverse structures* are favourable. The most common inverse structures are shown in Fig. 4.26, i.e. the inverse hexagonal phase, H_{II} (formed from rod-like water channels in an amphiphile matrix), and the inverse micellar liquid phase (L_2), with higher negative mean curvature. Region c is commonly an inverse bicontinuous phase (V_2) and d may be an inverse micellar cubic phase (I_2). In the surfactant packing parameter approach, inverse structures are characterized by $N_s > 1$. The packings of molecules in inverse structures are illustrated in Fig. 4.27 for spherical micelles (Fig. 4.27a), rod-like micelles (Fig. 4.27b) and a saddle-splay portion of the interface of a bicontinuous structure (Fig. 4.27c).

The hypothetical sequence of phases shown in Fig. 4.26 is never observed in its entirety and phase transition boundaries are rarely vertical. However, the predominant dependence of phase structure on concentration and the order with which phases are stable upon increasing

concentration provides a first approximation to the phase behaviour of many ionic surfactants, both cationic and anionic. A representative phase diagram for the latter class is provided by the well-studied sodium dodecyl sulphate (SDS)/water system. Many features of the binary phase diagram (Fig. 4.28) are in qualitative agreement with the 'roadmap' (Fig. 4.26). The phase transition boundaries are vertical and the sequence of phases on increasing surfactant content is L_1, H_I and L_α. A number of intermediate cubic and mesh phases are stable between the hexagonal and lamellar phases (space does not permit a full listing), although intermediate phases have not been identified between the hexagonal and micellar solution phases. The Krafft point for SDS in water solutions is quite high; hence there are large regions of hydrated crystal phases in the phase diagram of Fig. 4.28, which we do not differentiate here since we are concerned with the lyotropic liquid crystal structures.

For nonionic surfactants, temperature plays a role at least as important as that of concentration. For example, the solubility of poly(oxyethylene), which forms the hydrophilic group in many nonionics, decreases markedly as temperature is increased. The phase boundaries are then not vertical. In these cases, increasing temperature plays a qualitatively similar role to decreasing water content. Thus, the phase diagrams for these nonionics are complex, although some general features can be established. Representative phase diagrams for aqueous solutions of three
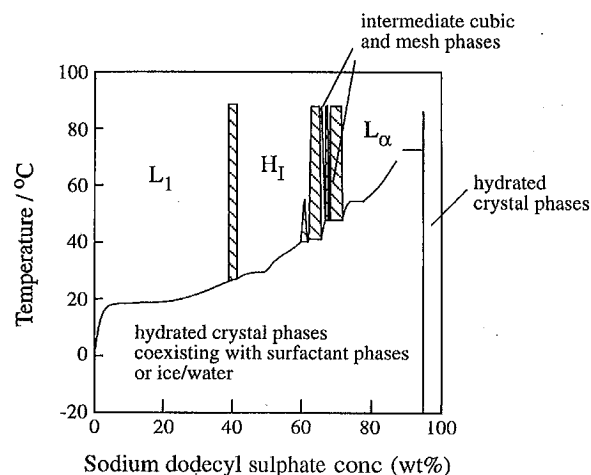
Figure 4.28 Phase diagram of the anionic surfactant sodium dodecyl sulphate in water. [Redrawn from P. Kékicheff and B. Cabane, *Acta Cryst. B*, 44, 395, Copyright (1988), with permission from IUCr. http://journals.iucr.org]

compounds from the best-known class of nonionic surfactant, poly-oxyethylene alkyl ethers, are shown in Fig. 4.29. In these phase diagrams, biphasic regions are not indicated when they are narrow. Diagrams are shown for surfactants with a constant hydrophobic chain length ($m = 12$) but increasing poly(oxyethylene) chain length, n. For short E chains
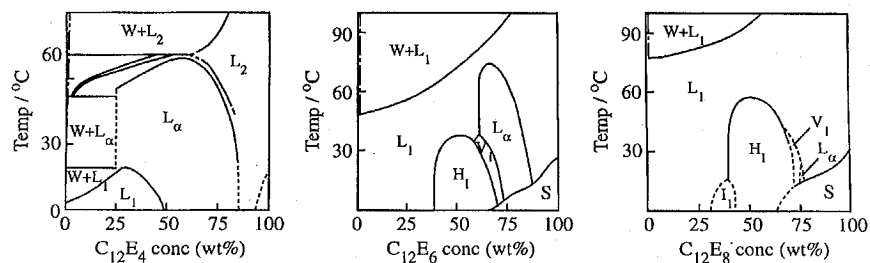
Figure 4.29 Phase diagrams of common nonionic surfactants, polyoxyethylene alkyl ethers C_mE_n with a fixed hydrophobic chain length ($m = 12$) and varying hydrophilic chain length, n. Here C denotes a methylene or methyl group and E denotes an oxyethylene group. Narrow biphasic regions are not shown. The notations for phases are as for Figs. 4.25 and 4.26. In addition, W denotes the water phase containing surfactant molecules, L_2 denotes an inverse micellar phase, V_1 denotes a normal bicontinuous structure and S denotes a solid phase. The dashed lines indicate approximate phase boundaries and dotdashed lines show the CMC. [Redrawn from D.J. Mitchell, G.J.T. Tiddy, L. Waring, T. Bostock and M.P. McDonald, *J. Chem. Soc., Faraday Trans. I*, 79, 975, Copyright (1983) – Reproduced by permission of the Royal Society of Chemistry]

(for example $C_{12}E_4$), the preferred mean interfacial curvature is near zero, and there is a tendency for formation of lamellar and inverse micellar phases. In the equivalent surfactant packing parameter picture, $N_s \geq 1$. In fact, for $C_{12}E_3$ (not shown) there are no normal micellar phase regions. Instead, directly above the CMC, a two-phase water + L_α region or a two-phase water + L_2 region are formed. As the hydrophilic segment length is increased from E_4, there is an increasing tendency for formation of normal micellar (L_1 and H_1) phases at the expense of the lamellar phase. This is exemplified by the phase diagrams for $C_{12}E_6$ and $C_{12}E_8$ in Fig. 4.29.

4.10.3 Identification of Lyotropic Liquid Crystal Phases

Lyotropic mesophases can, to a certain extent, be distinguished based on textures observed using polarized light microscopy. The lamellar and hexagonal phases are both birefringent and have different characteristic textures, whereas cubic phases are all optically isotropic and so cannot be distinguished from one another. The usual method of identifying lyotropic mesophases is to use small-angle scattering, either SAXS or SANS. The positions of observed Bragg peaks reflect the symmetry of the structure. Nuclear magnetic resonance (NMR) can also be used to identify lyotropic structures, using ^{2}H NMR on solutions in D_2O. Cubic, hexagonal and lamellar phases can be distinguished due to different averages of the quadrupolar interaction which result from differences in the curvature and symmetry of the amphiphile-water interface.

4.11 MEMBRANES

The two most important types of aggregate formed by amphiphiles are micelles and lamellae. We considered the former in detail in Section 4.6. Here we consider some aspects of structures based on bilayers of surfactant molecules, also known as membranes.

4.11.1 Formation of Layer Phases

The formation of layer phases in concentrated amphiphile solutions can be rationalized on the basis of the membrane interfacial curvature, which is related to the surfactant packing parameter. As detailed in Section 4.9, if the surfactant parameter $N_s \approx 1$, then a lamellar phase is favoured

based on the efficient packing of molecules. This corresponds to equality between the cross-sectional area of the head group and that of the hydrophobic tail. This leads to a mean curvature $H = 0$ (the Gaussian curvature $K = 0$ also). The tendency to form a lamellar phase can usually be enhanced by increasing the hydrophobic chain cross-sectional area, for instance by using a double-tailed amphiphile. Alternatively, the head group area can be reduced; for example, for the nonionic amphiphiles $C_{12}E_n$, the lamellar region of the phase diagram expands as n decreases from 8 to 4 (Fig. 4.29). Double-chain lipids (with $N_s \approx 1$) often form lamellar phases directly upon increasing concentration at the CMC. In contrast, single-chain surfactants tend to form micelles at the CMC. By increasing concentration, a lamellar phase can be formed from such molecules if interaggregate interactions favour it energetically. In this case, rod-like or disc micelles are often formed above the CMC, which ultimately transform into lamellae at higher concentrations.

4.11.2   Elastic Properties of Layered Phases

In the lamellar (L_α) phase of amphiphiles, thermal fluctuations are appreciable at ambient temperatures, and the layers are characterized by undulations. If the surfactant film is very flexible, thermal fluctuations can even lead to the formation of the L_3 sponge phase. As its name suggests, this phase is a random network of membranes separating water channels. It is a two-component analogue of the three-component bicontinuous microemulsion structure (Fig. 3.16). Electrostatic interactions between charged amphiphiles can lead to films that are stiffer than those that result from hydrophobic self-assembly alone; thus $F_{el} > k_B T$, and the sponge phase is not observed. For flexible membranes, thermal fluctuations lead to the deformation modes shown in Fig. 4.30. These fluctuations are confined to occur within the volume defined between successive layers (characterized by a spacing d); thus they give rise to an entropic force, an effective repulsion between surfactant membranes (bilayers). If the layers are brought closer, for the undulation mode (Fig. 4.30a) the force decreases as d^{-3} whereas for the peristaltic or squeezing mode the decrease is proportional to d^{-5}. The undulation force is long range; i.e. there is an effective repulsion between layers even at large separation. When layers are brought close together, other repulsive forces become important, especially forces arising from protrusion of molecules from lamellae and overlap of head groups (Fig. 4.30c).
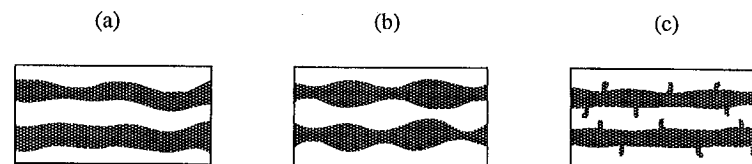
Figure 4.30   Deformation of amphiphilic membranes: (a), (b) thermal fluctuation deformation modes and (c) local steric deformation due to protrusion of molecules, where (a) is termed the 'undulation' mode and (b) the 'peristaltic' mode. [Adapted from J. N. Israelachvili, *Intermolecular and Surface Forces*, 2nd Edition, Academic Press, London (1991)]

4.11.3   Cell Membranes

Cell membranes are discussed further in Section 6.2.1.

4.11.4   Vesicles

A vesicle is a hollow aggregate with a shell made from one or more amphiphilic bilayers. A vesicle formed from a single bilayer is termed a unilamellar vesicle, while one with a shell of several bilayers is known as a multilayer vesicle, or sometimes an onion vesicle. A unilamellar vesicle is sketched in Fig. 4.31.

Vesicles formed by lipids are termed *liposomes*. These are of great interest since they are simple models for cells, although without their chemical functionality. In addition, vesicle formation and fusion are believed to be important in many physiological processes such as cell division and fusion. Liposomes are also technologically important in cosmetics and for drug delivery. In both cases, the liposome acts as a delivery agent for material contained inside. The liposomes are formed from lipid molecules
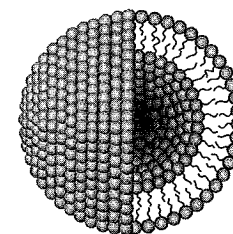
Figure 4.31   A unilamellar vesicle, cut open to show the shell-like structure

in the presence of the compound to be encapsulated. In the case of drug delivery, the liposome solution is injected into the bloodstream where they carry the drug to the target, whilst protecting it from unwanted release. Because liposomes bind to cell walls, they are particularly effective in delivering drugs directly to cells rather than dispersing them in the bloodstream. However, at present this targeting is unselective. It is likely that, in the future, vesicles will be made which incorporate membrane proteins to enable recognition and binding on certain target cells, thus ensuring highly specific delivery of the vesicle contents. Already, the use of liposomes incorporating the protein biotin (functionalized with hydrophobic chains so that it binds to the cell membrane) to make artificial tissue has been investigated. Here, biotin-functionalized liposomes stick together to form the tissue. Liposomes offer the advantage that they are biocompatible. A prime disadvantage in their use in drug delivery systems is that the release rate is not controlled, whereas often it is desirable for the drug to be released slowly, ensuring a dose to the target cells for a long period.

Vesicles are usually not in thermodynamic equilibrium. However, they can be kinetically stable for quite long periods. There are many methods to prepare them, which result in different types of vesicles and size distributions. They are often formed by sonication (exposure to ultrasound) of dilute lamellar phases. Lamellae are broken up by the action of the high-frequency sound waves and can reassemble as vesicles. This leads to small vesicles with rather a broad size distribution since the mechanical action is very uneven. Sometimes multilamellar vesicles form spontaneously by dissolving dry phospholipids in water. An alternative method is to disperse a lamellar phase formed at high concentration in a large excess of solvent. Another procedure involves dispersing the amphiphile in an organic solvent and injecting this into an excess of water. Large unilamellar vesicles form as the organic solvent evaporates or is dissolved in water. Dialysis against water of a solution of amphiphile in detergent is also used to prepare quite uniform vesicles. All of these methods are somewhat hit-and-miss in their ability to deliver the technologically desirable goal of uniform vesicles with a large encapsulation ratio (i.e. the ratio of solvent inside the vesicle to that outside). Application of steady shear to a lamellar phase is a useful means of preparing multilamellar vesicles with a narrow size distribution. Here the mechanical deformation is more uniform than with sonication. Varying the shear rate enables the average size to be controlled. Vesicles that are formed in a metastable state by such methods eventually break up. In rare cases,

specifically in mixtures of lamellar-forming amphiphiles, it is thought that spontaneous curvature of the bilayer can lead to thermodynamically stable vesicles.

4.12   TEMPLATED STRUCTURES

The self-assembly of surfactants can be exploited to template inorganic minerals, such as silica, alumina and titania. The resulting structures resemble those of zeolites, except that the pore size is larger for the surfactant-templated materials than those that result from channels between atoms in classical zeolite structures. In conventional zeolites, the pore size is typically up to 1 nm, whereas using amphiphile solutions it is possible to prepare an inorganic material with pores up to several tens of nanometres. Such materials are thus said to be mesoporous. They are of immense interest due to their potential applications as catalysts and molecular sieves. Thus, just as the channels in conventional zeolites have the correct size for the catalytic conversion of methanol to petroleum, the pore size in surfactant-templated materials could catalyse reactions involving larger molecules. The cooperative ordering of inorganic materials by organic matter also sheds light on the process of biomineralization, for example the formation of bones, shells and corals.

It was initially believed that the templating process simply consisted of the formation of an inorganic 'cast' of a lyotropic liquid crystal phase. In other words, pre-formed surfactant aggregates were envisaged to act as nucleation and growth sites for the inorganic material. However, it now appears that the inorganic material plays an important role and that the structuring usually occurs via a cooperative organization of inorganic and organic material. Considering, for example, the templating of silica, a common method is to mix a tetraalkoxy silane and surfactant in an aqueous solution. Both ionic and nonionic surfactants have been successively used to template structures, as have amphiphilic block copolymers (these behave as giant surfactants and enable larger pore sizes). The cooperative self-assembly process leads to a structure in which the silica forms a shell around amphiphilic aggregates, the latter being removed by calcination. Figure 4.32 shows a hexagonal honeycomb pattern where the silica has been templated from the hexagonalpacked cylinder (H_1) phase. Layered structures have been prepared in a similar manner, by templating the lamellar (L_α) phase. Highly monodisperse silica beads
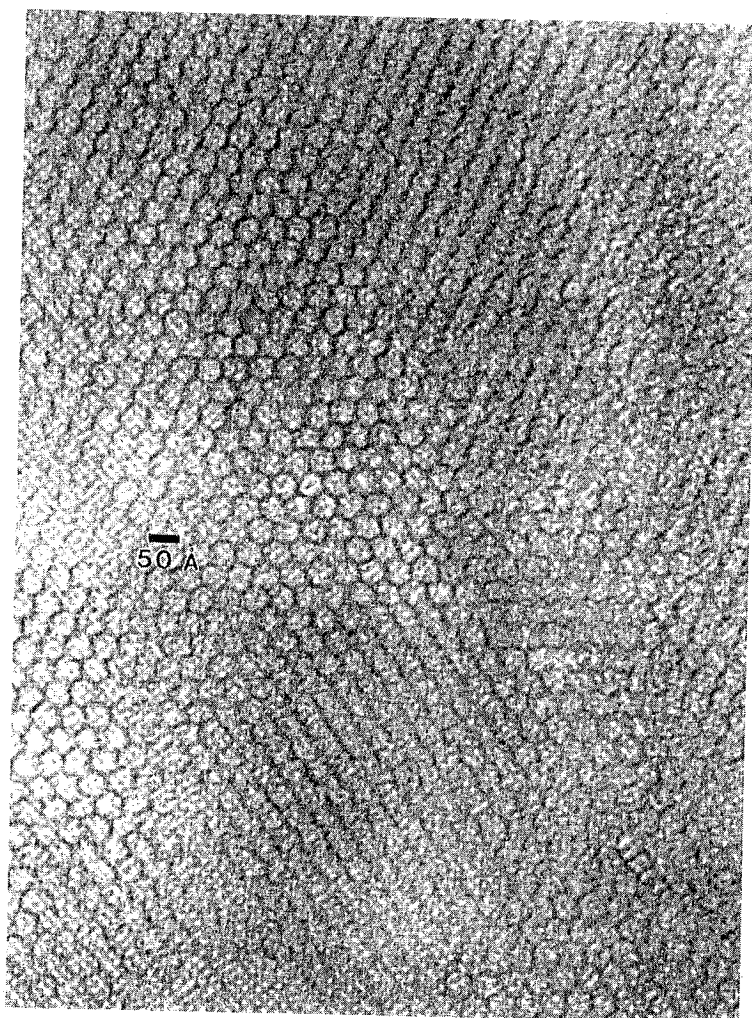
Figure 4.32   Silica templated by a cationic surfactant in aqueous solution. The hexagonal structure resembles that of conventional zeolites, but the pore size is 10 times larger. [Photograph reproduced by permission of C. Kresge, Mobil Central Research Laboratories, Princeton. New Jersey]

have been made by templating spherical micelles. A series of intricate structures formed by templating an aluminophosphate mineral is shown in Fig. 4.33. These structures are believed to result from the templating of vesicles in which there is additional separation of the organic and inorganic material within the vesicle walls. For comparison, Fig. 4.33 also includes micrographs of the shells of microscopic marine organisms
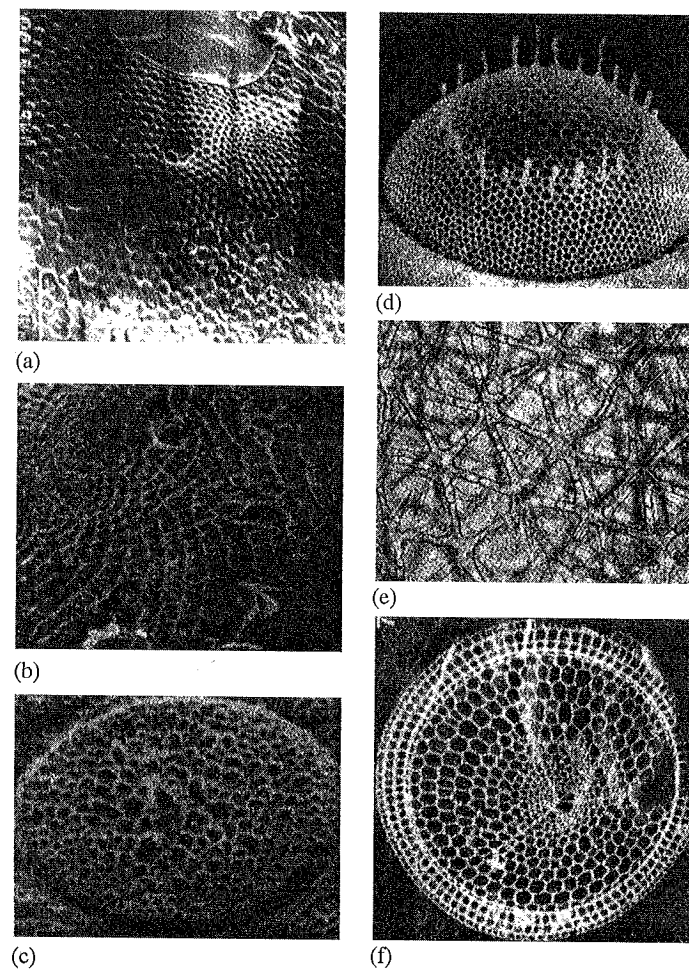
Figure 4.33   Templating an aluminophosphate mineral produces structures (a–c) that resemble the shells of microscopic marine creatures called radiolarians and diatoms (d–f). The synthetic materials are prepared from a mixture of phosphoric acid and aluminium hydroxide in solution in tetraethylene glycol with an alkylamine surfactant. The similarity of the structures suggests that biomineraiization in this case may result from the templating of vesicles. [From P. Ball, *Made to Measure*, Princeton University Press, Princeton (1997), based on work by G. Ozin and colleagues at the University of Toronto]

called radiolarians and diatoms. The resemblance between the synthetic and natural minerals is striking and suggests a mechanism for biomineralization in this system that is based on the formation of mineralized casts of vesicles.

FURTHER READING

Adamson, A. W. and A. P. Gast, *Physical Chemistry of Surfaces*, 6th Edition, Wiley, New York (1997).

Attwood, D. and A. T. Florence, *Surfactant Systems*, Chapman and Hall, London (1983).

Ball, P., *Made to Measure*, Princeton University Press, Princeton (1997).

Evans, D. F. and H. Wennerström, *The Colloidal Domain. Where Physics, Chemistry, Biology and Technology Meet*, 2nd Edition, Wiley–VCH, New York (1999).

Hunter, R. J., *Foundations of Colloid Science*, Vol. I, Oxford University Press, Oxford (1987).

Jönsson, B., B. Lindman, K. Holmberg and B. Kronberg, *Surfactants and Polymers in Aqueous Solution*, Wiley, Chichester (1998).

Larson, R. G., *The Structure and Rheology of Complex Fluids*, Oxford University Press, New York (1999).

Mann, S., *Biomineralization: Principles and Concepts in Bioinorganic Materials Chemistry*. Oxford University Press, Oxford (2001).

Petty, M. C., *Langmuir–Blodgett Films. An Introduction*, Cambridge University Press, Cambridge (1996).

Seddon, J. M., *Biochim. Biophys. Acta*, 1031, 1 (1990).

Shaw, D. J., *Introduction to Colloid and Surface Chemistry*, 4th Edition, Butterworth–Heinemann, Oxford (1992).

Voet, D. and J. G. *Voet, Biochemistry*, 2nd Edition, John Wiley, New York (1995).

QUESTIONS

4.1 Describe what happens when a little *n*-hexanol is dropped on to a clean water surface at 20° C, given that

$$\gamma_{wa} = 72.8 \text{ mN m}^{-1}$$
$$\gamma_{oa} = 24.8 \text{ mN m}^{-1}$$
$$\gamma_{ow} = 6.8 \text{ mN m}^{-1}$$

and that for a saturated solution of *n*-hexanol in water $\gamma_{wa} = 28.5 \text{ mN m}^{-1}$.

4.2 The concentration and corresponding surface tension of aqueous solution of butanol were measured at 20 °C with the following results:

c/mol dm^{-3}	0.0264	0.0536	0.1050	0.2110	0.4330
γ/mN m^{-1}	68.00	63.14	56.31	48.08	38.87

Determine the area occupied per molecule.

4.3 The surface tensions of aqueous solutions of sodium dodecyl sulphate at 20 °C were measured and the following values obtained:

$10^3 c$/mol dm^{-3}	0	2	4	5	6	7	8	9	10	12
γ/mN m^{-1}	72.0	62.3	52.4	48.5	45.2	42.0	40.0	39.8	39.6	39.5

Determine the critical micelle concentration. Use the Gibbs adsorption equation to evaluate the area occupied by each adsorbed dodecyl sulphate ion at this concentration.

4.4 (a) Calculate values of the thermodynamic parameters ($\Delta G_m^{\ominus}$, $\Delta H_m^{\ominus}$, $\Delta S_m^{\ominus}$) for micellization of the following surfactants from the information below for $T = 298$ K:

Surfactant	c_{CMC}(mol dm^{-3})	d ln c_{CMC}/dT (K^{-1})
$C_6H_{13}S(CH_3)O$	0.437	−0.01436
$C_8H_{17}S(CH_3)O$	0.0281	−0.01056
$C_{10}H_{21}S(CH_3)O$	0.00188	−0.007314

   (b) Show that in $\log c_{CMC} = A - Bn_c$, where A and B are constants and n_C is the number of carbon atoms. Evaluate A and B.

   (c) Comment on the significance of your results.

4.5 Describe briefly two reasons why surfactants are useful as detergents.

4.6 The surface tension of the nonionic surfactant $E_{24}B_{10}$ (E = oxyethylene, B = oxybutylene) was measured at 25 °C as a function of concentration with the following results:

$10^3 c$/ g dm^{-3}	0.583	1.77	5.40	13.8	29.9	54.4	108.0	233.4	651.8	1534
γ/mN m^{-1}	61.1	50.2	43.2	35.3	32.1	31.6	31.7	31.6	32.1	31.6

Estimate the critical micelle concentration and the average area per surfactant molecule adsorbed at the air–water interface.

4.7   Obtain a general expression for the molar Gibbs energy of micelliza-
      tion in the phase separation model for an ionic surfactant given that
      $(1 - \alpha)$ moles of counterion are transferred from their standard state
      in solution to the micelle. Also give the appropriate equation at the
      CMC.
4.8   At low concentration, monolayers of amphiphiles behave as two-
      dimensional ideal gases. Describe how Eq. (4.33) for this sys-
      tem may be modified to give the two-dimensional van der Waals
      equation.
4.9   The closed association model of micellization can be used to obtain
      the fraction of molecules in micelles as a function of total amphiphile
      concentration. Using concepts from Section 6.4.5 derive expressions
      for the fractions of associated and unassociated molecules and hence
      obtain plots similar to those in Fig. 4.18.
4.10 Derive Eq. (4.40) within the phase separation model.
4.11 Estimate the largest association number for micelles of sodium tetrade-
      cyl sulphate in water.

5
Liquid Crystals

5.1   INTRODUCTION

We are all familiar with gases, liquids and crystals. However, in the nineteenth
century a new state of matter was discovered called the liquid crystal state.
It can be considered as the fourth state of matter (although plasmas are also
candidates for this accolade). The essential features and properties of liquid
crystal phases and their relation to molecular structure are discussed in this
chapter. Specifically, the focus is on thermotropic liquid crystals (defined
in the next section). These are exploited in liquid crystal displays (LCDs)
in digital watches and other electronic equipment. Such applications are
outlined later in this chapter. Surfactants and lipids form various types of
liquid crystal phase but this was discussed separately in Chapter 4. Finally,
this chapter focuses on low molecular weight liquid crystals, liquid crystalline
polymers being touched upon in Section 2.10.

The term 'liquid crystal' seems to be a contradiction in terms. How can a
crystal be liquid? What it really refers to is a phase formed between a crystal
and a liquid, with a degree of order intermediate between the molecular
disorder of a liquid and the regular structure of a crystal. What we mean
by order here needs to be defined carefully. The most important property
of liquid crystal phases is that the molecules have long-range orientational
order. For this to be possible the molecules must be anisotropic, whether this
results from a rod-like or a disc-like shape.

Molecules that are capable of forming liquid crystal phases are called
mesogens and have properties that are mesogenic. From the same root, the
term *mesophase* can be used instead of liquid crystal phase. A substance in

Introduction to Soft Matter

Synthetic and Biological Self-Assembling Materials

REVISED EDITION

Ian W. Hamley

WILEY

Contents